AN EXAMINATION OF THE CAUSES OF HEADING BIAS IN COMPUTER SIMULATED SELF-MOTION

A thesis

submitted in fulfilment

of the requirements for the degree

of

Doctor of Philosophy

at the

University of Waikato

by

RUTH SUSAN KIM

University of Waikato

2003

ABSTRACT

A series of experiments were devised in order to examine aspects of human visual performance during simulated self-motion. The experimental stimuli were computer simulations of observer translational motion through a 3-D random dot cloud. Experiments were specifically designed to obtain data regarding the problem of bias in judgments of heading, and to determine the influence of various experimental factors upon the bias. A secondary aim was to use these results to develop a workable computer model to predict such bias in heading estimation.

Heading bias has been known for many years, but it is generally assumed only to be a problem for complex observer motion. However, the current work involved simple observer translation, and found a significant amount of heading bias. A wide variety of experimental factors were examined, and it was found that scene depth and speed had the greatest effect upon the accuracy of heading estimates, with a faster speed or smaller depth reducing bias.

It was proposed that yaw eye movements, driven by the rotational component of radial flow, were responsible for the bias. An adaptation of the Perrone (1992) model of heading was used to model this, and a highly significant correlation was obtained between the experimental data and the predictions of the model.

ACKNOWLEDGMENTS

Several people have made significant contributions to this thesis. Grateful acknowledgments are due to the following: firstly, of course, my principal supervisor, Dr. John Perrone needs special acknowledgment for his advice and assistance, and most definitely for programming the various incarnations of the heading model used in section B of this thesis.

I should also like to thank Dr. Robert Isler, my second supervisor, for helping with eye-tracking methodology and equipment.

Without the participants there would have been no thesis, so I would like to thank all of the students who took part in these experiments for their generosity in giving their time and sharing their ideas with me.

I would also like to thank the computer programmers, Ross Oliver and Andrew Malcolm, for getting the basic stimuli up and running, modifying the programme whenever I needed, and keeping it working. And thanks also to technical expert, Rob Bakker, for designing and making some extremely practical (and unique) pieces of equipment.

Thanks also to the University of Waikato and FRST for the Waikato Doctoral and Bright Futures Scholarships that supported this work during the past three years.

And finally, my family: Nick, Rebekah, Jonathan and Catherine, who helped me with pilot-testing some of the experiments, offered advice and moral support as needed, and put up with me through the entire process. This thesis is dedicated to you.

CONTENTS

LIST OF TABLES

LIST OF FIGURES

LIST OF APPENDICES

Appendix Page

E Experiment Six – Fixation Direction

SECTION A

AN EXAMINATION OF THE CAUSES OF BIAS IN HEADING ESTIMATION

CHAPTER 1

Overview

In order to move about in the world with any amount of accuracy, the human visual system must solve a variety of problems regarding the layout of the environment and the observer's own motion. One such problem of importance in human navigation is that of estimating the current direction of motion, or *heading*.

The various cues and methods that the visual system may use to extract heading direction have been topics for research and speculation for many years. In the mid 20th century, Gibson (Gibson, 1950; Gibson, 1966; Gibson, Olum, & Rosenblatt, 1955) created the basis for modern studies of heading perception when he described the visual input for heading as being composed of more than a just a succession of static images. Whenever a person moves through the world, or when objects in the world move relative to the observer, a temporal change in the structure of the optic array, or layout of objects in the visual environment, will occur. Gibson named this temporal change *optic flow*, and demonstrated that it could potentially be used to guide estimates of heading as follows. Simple *translation* (moving in a straight line without head or eye movements) of an observer through a stationary environment generates a radial pattern of optical flow on the retina, in which 2-D image motion radiates outwards from the focus of outflow, also known as the *focus of expansion* (FOE). This singularity in the visual field corresponds to the direction of heading, and is specified by the radial directions of all elements throughout the visual field. This effect is best demonstrated by considering the view through the front windscreen of a car travelling along a long straight road. The images of objects in the scene will appear to expand away from direction of motion, or FOE.

Since that time, a large quantity of empirical research has been carried out, mostly using computer-based displays consisting of moving dots showing optic flow, which has supported the idea that heading can be solved using just visual motion information (e.g. Cutting, 1986; Rieger & Toet, 1985; Stone & Perrone, 1997; W.H. Warren & Hannon, 1990). However, one problem with reliance upon using optic flow for heading estimation is that the FOE is only present when the motion is purely translational. This is rarely the case in the real world, and observer rotations shift or eliminate the focus of expansion, meaning that this source of information can no longer be directly used for heading estimation (e.g. Regan & Beverley, 1982; van den Berg, 1992; Royden, 1994; W.H. Warren & Hannon, 1988, 1990). This situation is known as the *rotation problem* (e.g. Regan & Beverly, 1982; van den Berg, 1999) and it is a major challenge for all computational models of heading. Because rotational motion is such a problem, most of the empirical research in this field has used combinations of translation and rotation in an effort to understand the mechanisms controlling heading estimation.

An underlying assumption of such work has been that, in situations where there is no rotation (pure translation), heading estimation is done with a high degree of accuracy. Despite this belief, however, it is not entirely clear that human observers can judge heading accurately, even in the case of pure translation. In fact, it has been repeatedly observed that the perceived heading is biased towards the centre of the display screen (e.g. Gibson, 1947; Johnston, White and Cumming, 1973; Llewellyn, 1971; W.H. Warren & Saunders, 1995a). This phenomenon could provide a vital clue to the processes behind the neural extraction of heading in the same way that visual illusions such as motion aftereffects provide insights into the workings of the visual system. However insufficient research has been carried out to allow us to decide whether this is a simple response bias or if it is a genuine perceptual effect.

A problem with the existing research emphasis upon the rotation problem in the self-motion perception field is that it adds a much greater level of complexity to the interpretation of the results. It makes sense to believe that whatever extraction methods are at work in the case of pure translation will also underlie the processes controlling estimation with rotation. Therefore we should first aim to develop a good understanding of the mechanisms controlling heading estimation in this, the simplest condition, prior to concentrating upon the more complex system.

This thesis aims to address the gaps in the current level of understanding of heading estimation, by examining the heading bias evoked by pure translational motion, and the factors that help to control this bias. The data so gained will then be used in an attempt to understand and model the neural mechanisms controlling this bias.

The following sections of this introduction will examine the current level of understanding regarding the estimation of heading, and will be broadly divided into two sections. The first of these is an overview of the current state of heading research theory, in which the mathematical analysis of the optic flow field and the main classes of computational model will be introduced. The second section covers some empirical aspects of heading perception first by examining the brain physiology that is believed to underlie such judgments, and then by looking at some empirical studies of heading bias.

Theoretical Aspects

Current theorizing regarding the calculation of heading is based upon the concept of optic flow, as already discussed. Mathematical analyses have been developed to formally define the geometrical relationships among objects in the visual field, and these have in turn been used as the basis for various models of heading perception. In order to properly understand the implications of the various empirical findings on heading estimation, it is important to have a reasonable level of understanding of these theoretical aspects.

Mathematical Analyses

The question of how humans estimate their direction of self-motion has been the subject of many mathematical analyses (Cutting, 1986; Hanada & Ejima, 2000a; Heeger & Jepson, 1992; Hildreth, 1992; Koenderink & van Doorn, 1975; Lee, 1980; Longuet-Higgins & Prazdny, 1980; Nakayama & Loomis, 1974; Rieger & Lawton, 1985; Royden, 1997; Tsai & Huang, 1981; Zacharias, Caglayan, & Sinacori, 1985). All of these analyses, regardless of their wider aim, rely upon the fact, first described by Gibson (Gibson, 1950; Gibson, 1966; Gibson, Olum, & Rosenblatt, 1955), that the 3-D motion of points in the environment can be reduced to a 2-D vector flow field on a surface, such as the retina.

First it is important to understand the simple 3-D coordinate system for specifying the principal planes and axes of the human body. For this system three coordinate axes are fixed relative to the observer in 3-D space; X gives the horizontal component, Y the vertical component and Z the depth component of motion. In the discussion that follows, the standard convention of referring to angles in the XZ plane as degrees of azimuth and angles in the YZ (vertical) dimension as degrees of elevation will be used. Any movement of the observer in the world can thus be expressed in terms of translation components along the

three (X, Y, Z) axes, and these are denoted by the vector term $T= (T_x , T_y , T_z)^T$. Rotation can likewise be expressed in terms of rotation around each of these axes, denoted by the vector $R= (R_x, R_y, R_z)^T$. That is, any motion of a person through a 3-D environment may be expressed in terms of a combination of translations and rotations around the three coordinate axes.

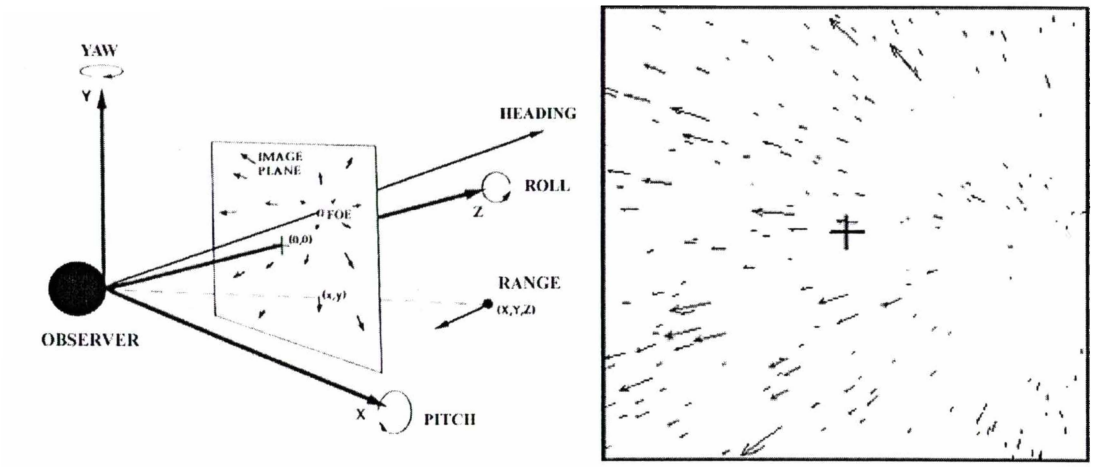

Figure 1.1. (a) Two-dimensional information on an image plane is used to extract the observer's heading direction. Rotation about the three coordinate axes and relative distances between objects can also be derived from the image motion. (b) The 2-D velocity vector field for 800 ms of translational motion at 2 $m.s^{-1}$ through a 3-D cloud of points with a depth of 100 m and a heading direction of 15° to the right.

Although this 3-D description of observer motion is useful for characterizing the observer motion, a transformation of the 3-D motion field to a 2-D vector flow field, as on the retina, is required for understanding the computation of heading because this is the input used by the visual system of humans and many animal species. This requires the position and motion of each point in the world to be represented on a flat surface, and is illustrated in Figure 1.1.

This 3-D to 2-D transformation permits the use of simple geometric relationships to describe the motion of the objects in the world relative to the 2-D retinal coordinate system of the observer. This transformation is described below, and is based on the work of Hildreth (1992).

Where:

Translation is $T = (Tx, Ty, Tz)^T$ in $m.s^{-1}$ ..... (1)

Rotation is $R = (Rx, Ry, Rz)^T$ in $rad.s^{-1}$ ..... (2)

If the position of a point in 3-D space is given by the coordinate vector $P = (X, Y, Z)^T$, then the 3-D velocity of P in the observer's coordinate frame is given by

$$V = \left(\dot{X}, \dot{Y}, \dot{Z}\right)^T = -T - R \times P \quad \text{..... (3)}$$

Where:

$$\dot{X} = -T_x - R_yZ + R_zY \quad \text{..... (4)}$$

$$\dot{Y} = -T_y - R_zZ + R_xY \quad \text{.....(5)}$$

$$\dot{Z} = -T_z - R_xZ + R_yY \quad \text{.....(6)}$$

Assuming a perspective projection of velocity V onto the 2-D surface, with a focal length of 1.0, the projection of P onto the image (x, y) will be given by $x = X/Z$ and $y = Y/Z$. The 2-D projected velocities of P along the x and y coordinates in the 2-D surface (v_x, v_y) are then given by Equations 7 and 8:

$$v_x = (- T_x + xT_z) /Z + R_xxy - R_y (x^2 + 1) + R_zy \quad \text{.....(7)}$$

$$v_y = (- T_y + yT_z) /Z + R_x (y^2 + 1) + R_zxy - R_zx \quad \text{.....(8)}$$

The first term in equations 7 and 8 equates to the component of image velocity due to the translation of the observer, and it can be seen that this depends on the depth, Z, to each point. The remainder of each equation equates to the component of image velocity due to the observer's rotation, and is independent of depth. Thus the translatory component of an object's perceived motion will depend upon its depth relative to the observer, but the rotational component is independent of depth. This finding has important implications for the recovery of heading from retinal flow.

Another implication of these equations is that each object on the 2-D plane will have both a direction and magnitude of motion, as it is now represented in vector form. The exact direction of this retinal motion will depend upon the movements of the observer, but during simple translation through a rigid environment there will always be pure radial 2-D motion away from the FOE. The magnitude of the vectors will depend upon the distance of the object from the observer, the observer's speed, and the point's location on the image plane, and equates to the image speed. The retinal images of closer objects will move faster, and the images of further objects will move more slowly.

The self-motion estimation problem reduces to the need to solve for 3-D parameters (Tx, Rx, etc.) on the right side of equations 7 and 8, from 2-D image velocities (Vx, Vy) derived from some small (normally 5) number of image flow vectors (e.g., see Koenderink & van Doorn, 1976; Longuet-Higgens & Prazdny, 1980).

From this mathematical description, it can be seen that, in theory, the instantaneous retinal flow contains enough information for the recovery of the instantaneous direction of translation, rotation, and the relative depth of objects in the 3-D world.

Computational Models

A range of computational models of human heading estimation have been developed on the basis of the mathematical considerations given above (e.g. Hanada & Ejima, 2000a; Heeger & Jepson, 1992; Hildreth, 1992; Koenderink & Doorn, 1976; Lappe & Rauschecker, 1993; Loomis & Beall, 1998; Longuet-Higgins & Prazdny, 1980; Perrone, 1992; Perrone and Stone 1994; Prazdny, 1980; Rieger & Lawton, 1985; Zacharias et al., 1985).

In order to understand the differences between these models it is important to remember that in most real world situations, eye-movements, or movement along a curved path, will produce a complex rotational flow which shifts and disrupts the FOE (i.e. the rotation problem). There are three major classes of model: decomposition, motion parallax and error minimization, each with various subclasses. The major difference between these models is how they deal with the presence of rotation in these more complex flows. Some models fit into more than one grouping, and in such cases we have placed them into the category best suited to that approach according to Hildreth and Royden (1998).

Vector-based Decomposition Models.

Decomposition models form the major group of heading models currently in use. These models assume that velocity vectors are derived from retinal input, and that the resultant complex vector flow is then separated into its individual rotational and translational components using a variety of different algorithms (e.g. Koenderink & van Doorn, 1975; Rieger & Lawton, 1985; Heeger & Jepson, 1992; Hildreth, 1992; Lappe, Bremmer, Pekel, Thiele & Hoffmann, 1996; Lappe & Duffy, 1999; Lappe & Rauschecker, 1993, 1994; Royden, 1997; Waxman & Ullman, 1985). This process relies on the fact that when two

image points lie close together on the 2-D plane, but the actual objects are located at different depths in the world, the rotational component of their 2-D motion is independent of depth. In theory the rotational component can therefore be subtracted, leaving only the translational component common to both vectors. The point of origin of these difference vectors can then be taken as being the direction of heading (Longuet-Higgins & Prazdny, 1980; Rieger & Lawton, 1985). Vector decomposition is a very attractive solution to heading estimation, because heading can be obtained from the flow field regardless of observer rotation.

Discrete models. These models are essentially a static form of the decomposition approach. A group of single image features are tracked across a period of time. Changes in the positions of these features form the input for a series of equations that solve for 3-D structure and motion. Many of these models concentrate on determining the minimum number of motion measurements required for a unique solution of these problems (Longuet-Higgins, 1981; Nagel, 1981; Prazdny, 1980; Tsai & Huang, 1981, 1982, 1984a, 1984b; Weng, Huang & Ahuja, 1989). It has been found that 2 or 3 views of 4 to 7 points in motion are sufficient under most conditions.

Differential models. Another approach to decomposition uses first or second-order derivations of the flow field to recover observer motion and the 3-D structure of the environment (e.g. Crowell, Banks and Royden 1989; Hanada and Ejima, 2000a; 2000b; Hildreth, 1992; Longuet-Higgins & Pradzny, 1980; Poggio, Verre, & Torre, 1991; Reiger & Lawton, 1985; Royden, Banks, & Crowell, 1992; Royden, 1997; Subbarao & Waxman, 1986; Waxman & Ullmann, 1985).

One such system uses the differential invariants of the flow field (Koenderink & van Doorn, 1975; Longuet-Higgins & Pradzny, 1980; Subbarao & Waxman, 1986; Waxman & Wohn, 1988). Each point in a locally smooth flow field can be described as

being the sum of the divergence, curl, deformation and translation. Some properties of the flow field, such as divergence and deformation, depend only on the observer's translation and the surface slant, and are therefore invariant under rotation and can in theory be used to determine the direction of heading.

Dynamical Models. Verri, Girosi, and Torre (1989) have used the theory of planar dynamical systems to model the evolution of the optical flow field over time. The FOE is structurally stable over time, and in principle estimates of heading derived from this region are less vulnerable to measurement errors.

Motion Parallax Models

The second major class of heading models is based on motion parallax, the relative motion between objects at different depths (e.g. Cutting, 1986; Cutting et al., 1992; Eriksson, 1974). One such model proposes an invariant property of global retinal flow – differential motion parallax (DMP) – as the basis for perceived direction of heading (Cutting et al., 1992). Under polar projection, when an observer fixates on and pursues an object located somewhere in the middle of a cluttered environment, the retinal velocity vectors of nearer objects are greater than, and in a direction opposite to the velocity vectors of more distant objects. Also, the direction of nearer objects is away from heading while further objects appear to move towards the heading direction. The heading direction of the observer can therefore be easily determined as being in the direction opposite to that of the object with the greatest retinal velocity. Consequently, it can be hypothesized that in order to navigate through the environment successfully, observers simply needs to shift their gaze focus continuously in the direction opposite to that of the most rapid object, and fixate on a new position. The proponents of these models argue that provided the retinal flow is rich

enough to provide the information for any perceptual task without decomposition, then the decomposition of the retinal flow into the respective translation and rotation components (a non-trivial task) can be avoided.

Error-Minimization Models

The third class of models computes a set of motion and 3-D structure parameters to provide the best fit for the measured optical flow (e.g. Bruss & Horn, 1983; Adiv, 1985; Ballard & Kimball, 1983). They do this by selecting one particular error criterion. One example of such a model is that of Bruss and Horn (1983), who developed a set of three algorithms that assume pure translation, pure rotation, or a combination of the two. An iterative method is used to find the optimal solution combining image motion measurements over the entire image. Many modern heading models incorporate some form of error minimization (e.g. Heeger & Jepson, 1992; Hildreth, 1992). One such group is represented by the Template models, and this will be discussed in more detail below.

Template Models. A template based approach for primate vision has been proposed as an alternative to decomposition models of heading (e.g. Beintema & van den Berg, 1998a,1998b; Beintema & van den Berg, 2001; van den Berg & Beintema, 1997; Hatsopoulos & W.H. Warren, 1991; Perrone, 1992; Perrone & Stone, 1994; Saito, Yukie, Tanaka, Hikosaka, Fukada, & Iwai, 1986; Tanaka, Hikosaka, Saito, Yukie, Fukada, & Iwai, 1986; Tanaka & Saito, 1989). These models are based on direction and speed-tuned neurons similar to those found in the middle temporal (MT) and medial superior temporal (MST) regions of the brain.

Image motion is initially processed by MT-like sensors that produce a certain level of activity depending on the direction and speed of the stimulus. A number of these sensors

feed into each MST-like detector, which is in turn tuned to a specific FOE location. These detectors integrate information across a large portion of the field by summing the activities of the most active sensors at each location.

A number of heading models have been produced that build on the basic template concept and provide specific neural connectivity rules (e.g. Perrone, 1987, 1992). The early template models (e.g. Glünder, 1990; Hatsopoulos & W.H. Warren, 1991, Perrone, 1987) could not cope with complex combined motions of translation and rotation, and were not as versatile as the decomposition models in solving heading. However, later models overcame this deficit by using rotation detector networks to detect the rotational component visually, and to allow the heading templates to be modified (Perrone, 1992). Note that the rotational and translational components are not separated out as in decomposition models. More complex models incorporating eye movement signals have recently been proposed (Beintema & van den Berg, 1998 a).

Summary

There are a wide variety of heading models currently in existence. The majority of these are decompositional vector flow models, which seek to remove rotational components from the optic flow leaving only the translational components for heading analysis. However motion parallax models, based on the relative motion of points in the world, and template models, based on the known physiology of MT and MST neurons, have also been developed.

Both the physiology of the brain and the results of psychophysical experiments support the idea of MST neurons being connected into radially organized networks forming specialized heading detectors (e.g. Perrone, 1992; Perrone & Stone, 1994). This system is

not specific to template models, as many decomposition models also include a stage after the removal of rotation in which heading is determined from the remaining translational field using a network. Thus the idea that the brain computes heading from the radial pattern of image motion is fundamental to many theoretical approaches. In theory it should be a trivial task to compute the FOE by finding the point of intersection of two or more non-collinear vectors, however it appears that humans find this a difficult task, and bias in heading estimation is commonly observed in heading research (e.g. D'Avossa & Kersten, 1996; Johnson, White, & Cumming, 1973; Llewellyn, 1971; R. Warren, 1976).

Note that for all models, factors such as sparse or discontinuous flow, a narrow field of view, or image noise can provide a challenge to their ability to provide an accurate estimate of heading. Specific models may also exhibit vulnerability to other aspects of the flow field. One example of this is the aperture problem, in which the true direction of image motion is hard to obtain when edges are present in the scene (for a review of this issue see Perrone, 2001). Any model that aims to provide a good representation of the processing of heading direction by the human visual system needs to be robust enough to deal with these problems.

Empirical Research

A large body of empirical work has been carried out concomitant with the theoretical research into heading estimation. This basically falls into two major divisions: physiological and psychophysical. Each of these branches of research is important in developing our understanding of the neurological mechanisms underlying heading perception, and I will examine each in turn.

Physiological Structures and Motion Perception

Our understanding of the physiology underlying our perception of self-motion has been increased in recent times by electrophysiological studies of primate brains, and by neuro-imaging studies using Positron Emission Tomography (PET) and functional Magnetic Resonance Imaging (fMRI) of humans.

Visual information from the retina reaches the Primary Visual Cortex (V1), via the Lateral Geniculate Nucleus. From V1, two major cortical pathways for the processing of visual information have been distinguished. One is a ventral stream, which leads to the temporal area, and is believed to be involved in processing colour and form. The other is a dorsal stream, which leads to the parietal area, and is thought to be involved in the perception of motion and spatial relations. This latter pathway is believed to be the one most directly involved in the perception of heading, and therefore this review will be limited to the consideration of this pathway alone.

Middle Temporal Area (MT)

Neurons in area MT of the primate brain are specialized for visual motion extraction (Dubner & Zeki, 1971; Maunsell & Newsome, 1987). The visual fields of cells in areas MT are typically small in the central region of the retina, but become larger as the eccentricity from the fovea increases (Albright & Desimone, 1987).

The most important characteristic of neurons in area MT is that they are both direction and speed tuned. Direction selectivity is not unique to neurons in MT, and other neurons projecting to it along the pathway also show directional sensitivity to moving stimuli (Tanaka, 1998). However it is only at area MT that neurons become selective for motion with a specific speed and direction. This means that when a dot moves across the

receptive field with the preferred direction and/or speed, the cell will respond with a strong burst of activity. However, when the same dot moves across the receptive field with a non-preferred direction or speed, the neuron will respond only weakly, or not at all. On average, a deviation from the optimal direction of approximately 30° will halve the magnitude of the response (Albright, 1984; Maunsell & Van Essen, 1983a; Newsome, Wurtz, Dursteler, & Mikami, 1985; Stoner & Albright, 1992).

The visual speed signals from area MT are implicated in a number of important behavioural tasks, such as the pursuit of moving targets with our eyes (Lisberger & Movshon, 1999; Newsome et al., 1985) and the determination of self-motion. Perrone and Thiele (2001) have shown that many MT neurons respond to particular stimulus speeds and have properties that are closely matched to those required for the detection of moving edges.

The speed tuning of MT cells has been assessed using moving bars or random dot patterns over a range of speeds (Lagae, Raiguel, & Orban, 1993; Maunsell & Van Essen, 1983a; Perrone & Thiele, 2001) and the resulting tuning curves are often quite peaked (Maunsell & Van Essen, 1983a, 1983b).

While MT cells are sensitive to both direction and speed, they are generally insensitive to the shape, colour, luminosity and texture of moving stimuli (Albright, 1992; Dobkins & Albright, 1994; Saito, Tanaka, Isono, Yasuda & Mikami, 1989; Zeki, 1974). However, many of them preferentially respond to stimuli smaller than the size of the receptive field (Cheng, Hasegawa, Saleem & Tanaka, 1994).

Middle Superior Temporal Region (MST)

Most of the physiological research regarding self-motion has focused upon the MST region, as this is the first area in the cortical motion pathway to display genuine optic flow selectivity (Duffy & Wurtz, 1991a,1991b). These neurons are selective for the location of the focus of expansion (Duffy & Wurtz, 1995), and neuronal responses during combined optic flow and eye movements suggest that area MST can apparently deal with the problem of rotation (Bradley, Maxwell, Andersen, Banks, & Shenoy, 1996; Page & Duffy, 1999; Erickson & Their, 1991).

Area MST is broadly divided into two sections, the dorsal region (MSTd), and the ventral region (MSTv), each of which exhibits direction and speed tuning, and plays a role in the processing of motion information. However, while neurons in MSTd are broadly tuned to a wide field of motion and the retinal location of the expanding flow, MSTv neurons prefer the movements of a single small stimulus (Duffy & Wurtz, 1995a). Area MSTd is therefore more suited for the determination of the direction of self-motion (Tanaka, 1998).

Optic flow can theoretically be locally decomposed into several basic components such as radial, circular, translation, and sheer motion (Koenderink, 1986; Koenderink & Doorn, 1987), although Orban et al, (1992) have shown that MST neurons do not do this. Neurons in MSTd have been shown to respond to translational, radial, and circular motion, with one third being exclusively activated by one of these forms of motion, and the remaining two-thirds by fronto-parallel translation in some direction. In addition, there are known to be MSTd neurons that respond more strongly to combinations of rotation, translation and expansion or contraction than to pure forms of these (Duffy & Wurtz,

1991a,1991b; Graziano, Andersen, & Snowden, 1994; Orban, Lagae, Raiguel, Xiao, Maes, & Torre, 1992; Saito et al., 1986; Tanaka, Fukada, & Saito, 1989; Tanaka & Saito, 1989).

The directionally sensitive MSTd neurons have large receptive fields, 10-100° in diameter, many of which extend over both visual hemifields. They also respond best to large stimuli, indicating that extensive spatial summation occurs in this region (Burr, Morrone, & Vaina, 1998; Duffy & Wurtz, 1991a; Steinmetz, Motter, Duffy, & Mountcastle, 1987; Tanaka et al., 1986; Tanaka & Saito, 1989). The response of these neurons is insensitive to dot density, image speed, and often also to stimulus position (Duffy & Wurtz, 1991a,1991b). They also do not distinguish local object motion from global object motion, even when clear boundary information is available (Ungerleider & Desimone, 1986). These combined properties show MSTd to be the ideal candidate for the computation of optic flow information. Direct evidence for MSTd having a role in heading perception has been provided by Britten and van Wezel (1998), who showed that the electrical stimulation of MSTd neurons lead to systematic shifts in the heading response of trained monkeys. Perrone and Stone (1998) have also shown that MST neuron properties are compatible with heading estimation, based on their template model.

Psychophysical experiments in humans suggest that a similar process occurs in which neural units integrate local motion signals along complex motion trajectories (Morrone, Burr, & Vaina, 1995; Regan & Beverley, 1979). In agreement with neurophysiological studies of MT and MST, these units have large receptive fields and sum information over one or two seconds (Burr et al, 1998). There is also some evidence that there is selectivity in humans for optic flow along 'cardinal directions' (circular and radial) but this claim is controversial (Morrone, Burr, DiPietro, & Stefanelli, 1999; Snowden & Milne, 1996).

Summary

There is evidence that the MT and MSTd regions of the primate brain are jointly involved in the extraction of heading from the optic flow field. It is believed that MT neurons perform an initial coding of motion in the optic flow field, responding maximally to a particular speed and direction of motion at each point. Filtered signals then feed into the MSTd region where motion activity across the entire field is integrated, allowing the extraction of heading direction. The MSTd neurons respond to patterns of motion across large areas of the visual field, making them ideal candidates for involvement in the extraction of self-motion.

Bias in Heading Estimation

There is a considerable body of research suggesting that human heading estimation is not done with great accuracy (e.g. Johnson, White & Cumming, 1973; Llewellyn, 1971; Warren, 1976). In this section we will examine those studies most directly applicable to the current work..

Historical Bias Research

Since Gibson's early work (Gibson, 1950; Gibson, 1966; Gibson et al., 1955), researchers have been interested in the ability of people to estimate their current direction of heading. Results from the initial experiments were not very accurate, and a substantial amount of bias was found. Llewellyn (1971) was one of the first to examine accuracy in heading estimation using translational motion towards a fronto-parallel plane created using a shadow caster. Participants were asked to indicate heading using a cursor at the end of

each trial. He found a bias that ranged from 4.8° to 9.3° towards screen centre, with bias increasing as the true heading became further off-screen.

Johnson, White, and Cumming (1973) performed the next experiment looking at the ability of humans to determine heading. They also used approaches towards a random-dot plane, however this experiment varied time-to-contact using large-field film displays in a projection dome with constant size elements. Participants were again asked to indicate the point to which they were travelling with a cursor at the end of each trial. Bias was found to range from 7.7° to 13.3° toward the screen centre.

R. Warren (1976) used the more natural case of translation parallel to a ground plane. He presented films of planar random-dot ground surfaces simulating a fast walking speed of 2 $m.s^{-1}$ and varied heading angle between 0° and 90° to the right from the centre of the screen, meaning that the FOE was not always visible. Observers had to indicate their direction of heading using a metal-rod pointer. He found that observers tended to have a constant bias in their heading estimates of about 5.6° off-screen to the right. This contrasted with the strong centre screen bias found by Johnson et al., (1973) and Llewellyn (1971).

This early work showed definite constant error biases in heading perception. In theory it should be a trivial task to extract the direction of heading from the flow field, and it is not obvious why such large errors should be found. However two of these studies found a central bias, and one found a bias to the outside of the true heading direction. It is not known how this difference came about, but we now know that motion towards a fronto-parallel plane forms a specific case that leads to increased amounts of bias (W.H. Warren, Morris, & Kalish, 1988). Any explanation of bias in heading perception needs to be robust enough to be able to explain such differences in performance under various conditions.

Modern Bias Research

The general field of heading estimation research is now very large. However, the majority of studies are not directly relevant to this work. To be directly relevant, research in the field of heading estimation needs to meet the following criteria. First, the paper must use pure translational heading, as any rotation adds unwanted complexity to the flow field; second, the work must involve a direct measure of heading estimation, as some studies use only heading difference thresholds and it is difficult to relate these to absolute error; and third, the experimental design must involve a fixed direction of gaze as free fixation leads to rotation being added to the flow field. Although a lot of work has been carried out to look at accuracy in heading, only one study meets all three of these criteria, and this is the work of D'Avossa and Kersten (1996).

D'Avossa and Kersten (1996) carried out the only series of experiments to explicitly examine the accuracy of heading estimation with observer translation. Optic flow through a random-dot cloud was generated using 3-D points distributed throughout a 45° cone with its vertex at the viewpoint, with speed of translation and scene depth being unspecified by the authors. Heading was estimated using a cursor and heading direction was varied across the scene, also in an unspecified manner, and this changed in both azimuthal and elevational dimensions, enabling the independent analysis of the variable error generated by each. It was found that all of the observers could perform the task with varying degrees of accuracy. A consistent central bias was found for all observers for both the azimuthal and elevational dimensions, but the bias was larger for elevation than for azimuth. Thus it seems that heading bias does occur with translational displays, and that it can cause varying amounts of difficulty for individuals. However, there is clearly a need for further work is this fundamental area.

Summary

An investigation of heading bias during translation may help us to better understand the perceptual mechanisms underlying heading perception. It stands to reason that whatever part of the visual system is responsible for the extraction of heading in the complex case of rotation it is most likely also at work for translation.

The results of the D'Avossa and Kersten (1996) study suggest that heading is not as accurately estimated with pure translation as is usually believed. However as only the one experiment using simple translation through a 3-D cloud with a pointer task has been conducted, and that was not specifically designed to examine bias, it is difficult to know the extent of the heading bias that can be expected under various conditions. Our present level of understanding of the causes and extent of bias in heading estimation is extremely small, and the need for a systematic examination of accuracy in heading estimation is required.

Aims and Structure of this Thesis

Aims

The first purpose of this thesis was to obtain data relating to the amount of bias found in estimations of heading from computer-simulations of self-motion through a 3-D random-dot cloud, and to ascertain the influence of various experimental factors upon the size and direction of this bias.

The second aim was to use the results of these experiments to develop and test a computer model to predict bias in heading estimation. This model was developed from the Perrone (1992) model of heading estimation.

Structure

This thesis is divided into two sections, which shall be detailed in turn. A further examination of the literature for each sub-area is provided as an introduction to each experimental chapter. The first section is composed of a series of experiments, each of which is laid out as a complete chapter. The aim of the first group of experiments was to achieve a basic level of understanding of the size and source of any heading bias. An investigation of the role of phosphor streaking and a comparison of static and motion techniques of heading estimation is presented in Chapter 2. This is continued in Chapter 3 with an experiment examining the potential sources of the error found in the earlier experiments.

The second group of experiments examined the role of perspective cues: Chapter 4 looks at the role of the perspective cues of changing object size and shape. An investigation into the relative merits of having objects remain on the screen or disappear during response is detailed in Chapter 5. The third group of experiments looked at the role of proprioceptive cues in heading estimation: Chapter 6 details an experiment examining the influence of fixation direction upon heading accuracy, while Chapter 7 details an experiment looking at the relative contributions of head and body directions.

The largest group of experiments concerns the relative contribution of various aspects of the visual flow field: Chapter 8 contains an experiment looking at the effects of the number of dots upon heading estimation. Chapter 9 examines the role of scene depth, and Chapter 10 looks at speed of translation. Chapter 11 considers the influence of viewing time upon estimates of heading. A summary of all experiments is provided in Chapter 12.

The second section of the thesis attempts to gain a greater understanding into the factors controlling accuracy in heading estimation: Chapter 13 reviews our existing level of

knowledge about eye movements elicited by optic flow. Chapter 14 describes an existing heading model by Perrone (1992), including some modifications to that model, and compares the predicted output of this new model with the experimental heading data.

CHAPTER 2

Experiment 1: Bias in Heading Estimation

Our current understanding of the size and nature of heading bias during computer-simulated observer translation through a random dot cloud is extremely small. Consequently it was decided to run a simple preliminary heading experiment to confirm earlier reports of heading bias, and to determine the extent of the problem prior to attempting to determine the factors controlling bias during heading estimation.

Method

Participants

Ten students from the University of Waikato, 8 female and 2 male, aged between 19 and 24 years, participated in this experiment. All were first year psychology students who received partial course credit for taking part. All participants had visual acuity of 20:25 or better. None had previously taken part in any heading experiments.

Apparatus

The experiments were run on a Dell PC with 26 x 33 cm SVGA colour monitor with a screen resolution of 1280 x 1024 and a refresh rate of 80 Hz. Custom software, developed using Borland C++, showed translation through a random-dot cloud of non-growing white dots. The random dots-clouds were created by first allocating the dots a position on the screen, and then randomly assigning each a depth of somewhere between 1 m and the total scene depth of 100m. Each individual dot was 0.25° visual angle in diameter.

A red fixation cross of 1.33° of visual angle was shown in the middle of the screen throughout the session. Participants were instructed to look at this cross continuously, both during the trials and when responding. After each trial a white cross, controlled by the computer mouse, would appear over the top of the red fixation cross. Participants were required to move the white cross to the perceived direction of heading, and to left-click the mouse to record the response. They were required to maintain fixation on the centre of the screen at all times. The white cross was also 1.33° of visual angle, so as to be fully visible even in peripheral vision.

Participants sat with their head supported by a chin-rest, which kept their eyes a

constant 46 cm from the centre of the screen. The sides of the monitor were screened to exclude light. Thirty cm in front of the screen was a piece of black Plexiglas large enough to mask the computer monitor from the front, with an aperture 10 cm by 10 cm cut into the centre giving a square field of view subtending 34.5° of visual angle horizontally and vertically. The chin-rest was located 16 cm in front of the aperture, and had a flap of black card placed so as to occlude the left eye. Participants were not given the choice of using their preferred eye, as is normally the case, because I wanted to check for bias effects caused by the blind spot and the nose. At the beginning of each session participants adjusted their position until they had properly aligned their right eye so as to occlude the screen edges and to centralise a fixation cross.

Each trial lasted 800 ms, after which the dots would disappear from the screen, and the screen would remain black for 500 ms prior to the response cross appearing. Participants could take as much time as they required to respond to each trial, but once the mouse button was pressed, the next trial would appear. The viewing time of 800 ms was chosen because the limit of temporal integration in such experiments had previously been found to be around 300 ms (Crowell, Royden, Banks, Swenson, & Sekuler, 1990), and this was safely above the limit.

Procedure

The procedures used in this study were approved by the University of Waikato Ethics Committee.

Visual pre-screening of near visual acuity was carried out using a vision screen apparatus (Keystone Vs-II, model 1135A). Those who required prescription lenses for reading were asked to wear them both for this test and for the experimental session.

Prior to the experiment, each participant was read a standardized description of the requirements and ethical considerations. They then signed a consent form agreeing to take part in the experiment (Appendix A). Ten minutes of dark adaptation then occurred, followed by a practice session of 10 trials using the basic experimental design of a black screen and a motion approach. At no time was feedback given. The self-paced experimental trials were run in a darkened laboratory with only the experimental participant and the experimenter present.

All trials showed forward translation at 2 $m.s^{-1}$ through a random-dot cloud of 200 non-growing dots, with a scene depth of 100 m. Eleven azimuthal headings (-15, -12, -9, -6, -3, 0, 3, 6, 9, 12, 15° of visual angle) were used, with each heading being presented 10 times, giving a total of 110 trials overall. The entire experimental session took approximately 20 min to complete.

The resulting experimental data were analysed using SPSS and MATLAB software programs.

Results

The results of the experiment are shown in Figure 2.1, with the mean estimated heading plotted against the actual direction of heading. The means, mean biases, and standard deviations of these estimates are shown in Table 2.1. The bias in each case was calculated by subtracting the absolute value of the actual heading from the absolute value of the heading estimate value. Under this scheme, a negative bias term indicates a mean estimate lying closer to the centre of the screen than the actual heading, while a positive term indicates that it lay to the outside of the actual heading direction. This can be seen in Figure 2.1. If negative bias has occurred, the slope of the line will be less than one.

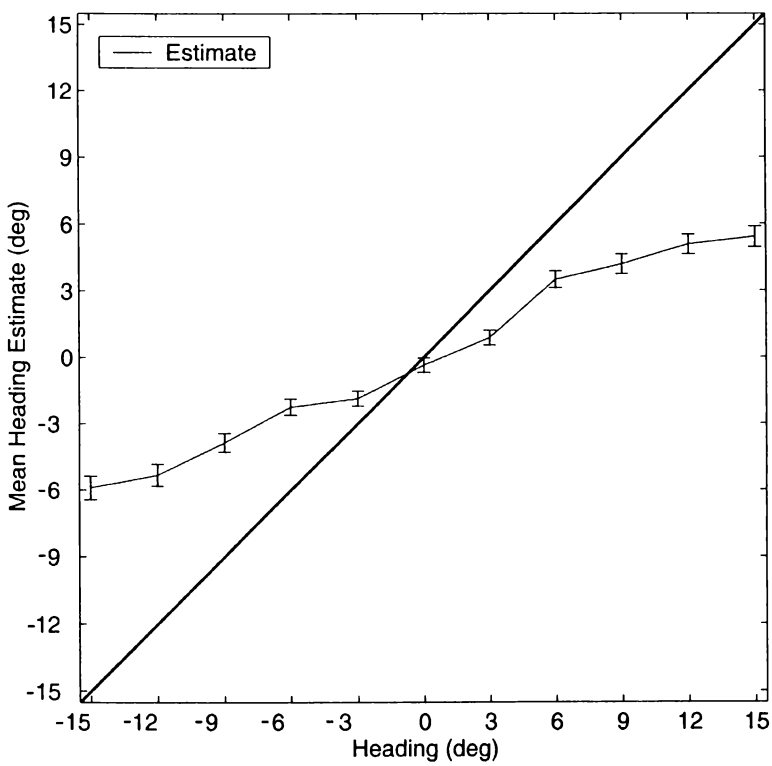

Figure 2.1. Mean heading estimates as a function of heading direction (±2 SE). Veridical performance is shown by the 45° line.

The data, summarised in Figure 2.1, shows that all headings, there was bias to the centre. The standard errors for the mean estimates are quite small, around 1 to 2°, showing the responses to have been reasonably consistent across participants and trials.

In Table 2.1, the mean biases for the various heading directions show a consistent tendency for participants to judge their heading direction as lying closer to the centre of the screen than was actually the case.

Table 2.1.

Mean heading estimates, mean bias and standard deviations N=100 (10 participants x 10 trials).

Heading	Mean	Mean Bias	Std. Dev. of Mean
-15	-5.90	-9.10	5.30
-12	-5.33	-6.67	4.94
-9	-3.86	-5.14	4.26
-6	-2.25	-3.75	3.66
-3	-1.87	-1.13	3.40
0	-0.36	-0.36	3.23
3	0.87	-2.13	3.26
6	3.50	-2.50	3.81
9	4.19	-4.81	4.45
12	5.08	-6.92	4.48
15	5.42	-9.58	4.62

In order to characterise the trends in the data, a regression analysis was carried out on the actual heading estimates. Curve fitting was carried out using the SPSS program, and this showed a linear fit to be significant ($p < .0001$). Therefore linear regression was used for the following analysis. The same method of curve fitting is used throughout this thesis. The full details of the regression equation are given in Table 2.2, while the scatterplot is shown in Figure 2.2.

The p values for the slope reach significance for the regression, meaning that the slope is significantly greater than zero. However, the 95% confidence interval for the slope does not include 1.0, therefore a significant bias to the screen centre occurred.

Table 2.2.

Linear regression statistics for estimated headings.

Slope	95% C.I.	Intercept	95% C.I.	R	p
0.414	0.388 to 0.440	-0.214	-0.295 to 0.201	0.967	<.0001

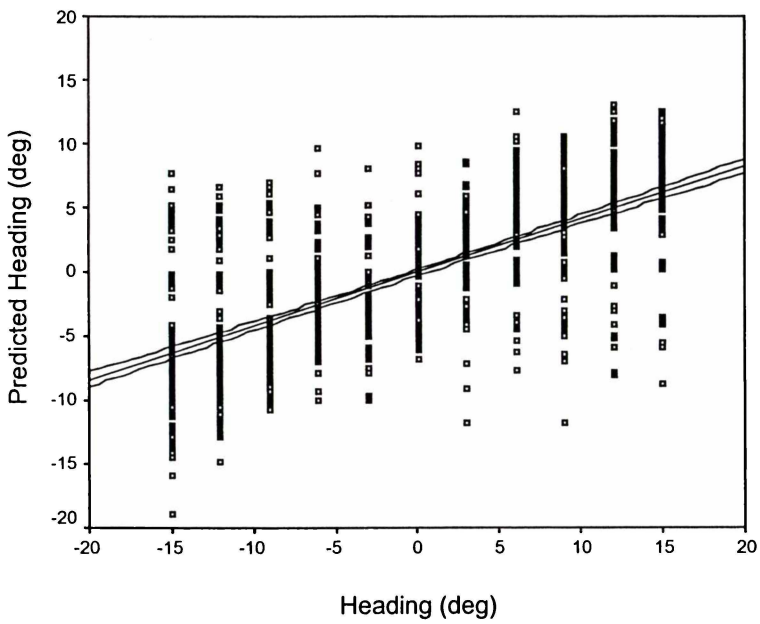

Figure 2.2. Scatterplot, regression line and 95% confidence interval for estimates of heading direction.

Discussion

The major finding of this experiment is that, humans appear to be unable to properly estimate their direction of heading when presented with displays using naturalistic scene depths and observer translation speeds. Mean heading estimates are biased towards the screen centre by a significant amount, and the size of this bias increased with the eccentricity of the actual heading direction.

In theory, the FOE should be easily obtained from the intersection of two or more non-collinear vectors, and the fact that participants were unable to locate the FOE with any accuracy suggests that the mechanisms underlying the apparently simple case of translation are not properly understood. More research in this area is needed in order to properly describe the various factors that may be at work here.

CHAPTER 3

Experiment Two: Static versus Motion-Based Methods of Heading Estimation

Experiment 1 demonstrated that human observers show a significant central bias when estimating the direction of heading with simple translation. However, an unanswered question in heading research concerns whether, when faced with a computer display simulating motion through an environment, humans do in fact calculate heading using motion inputs (optic flow), or whether they instead use some 'static' method of calculation based on the pattern of radial lines on the screen.

A static cue as to heading direction could arise from an artefact of computer-based displays - phosphor trails. When a spot of light moves across the black background of a computer screen, it leaves behind it a glowing trail, which lingers on the screen for a short time. This phosphor lingering can be visually detected at levels too low for instruments to pick up, and is a potential problem for computer-based experimental designs (Groner, Groner, Muller, Bischof, & DiLollo, 1993). In heading experiments such as Experiment 1, the phosphor trails all originate from the focus of expansion, and participants could potentially use them to find the heading direction without having to compute heading based on motion. Pilot testing indicated that the phosphor trails were indeed visible and easily accessible on the screen for quite some time after the dots had disappeared in each trial. Figure 1.1 demonstrates the way in which phosphor trails could indicate the direction of heading, as an image of each radial line remains on the screen following a trial. The impact of phosphor trails was tested in this experiment by comparing estimates of heading using a black response screen, on which phosphor trails linger, with that using a grey response screen, designed to mask the phosphor trails. If phosphor trails are being used in standard

heading experiments, we expect the black display screen to produce less bias than the grey because the grey screen should remove the trails.

A second set of conditions was used as another way of establishing whether static or motion cues are used for heading estimation. This compared static displays of radial lines (as would occur with phosphor traces) with the usual motion displays of dots. If static methods are being used to estimate heading, we would expect the motion and static displays to lead to equivalent levels of performance for the black screen, but to different levels of performance for the grey, where the phosphor trails will be obscured in the motion condition.

A second question to be addressed in this experiment concerns the amount of heading bias that occurs across the visual field. There is reason to suspect that there will be differences in the amount of bias in the azimuthal and elevational components of heading. In a series of heading experiments D'Avossa & Kersten (1996) found a consistent pattern of bias to the centre of the visual display, with 3 – 45 % more variance for elevation than for azimuth. The authors suggest that the results of this experiment point to an independent coding of azimuth and elevation. However the pattern of heading bias across the visual field was not reported. This issue requires further examination, and therefore the present work seeks to determine the pattern of heading bias across the visual field. In order to compare accuracy of estimation across the visual field, a grid system of heading directions was used. I expect heading bias to occur across the visual field, and that this bias will be directed towards the centre of the screen. I also expect that there will be more heading bias for the elevational component than for the azimuthal.

Method

Participants

Fifteen students from the University of Waikato, 9 female and 6 male, aged between 18 and 42 years, participated in this experiment. All were first year psychology students recruited by an advertisement on the departmental notice board (see Appendix A), and received partial course credit for taking part. All participants had a visual acuity of 20:25 or better (corrected if necessary). None had previously taken part in a heading experiment.

Apparatus

The apparatus for this experiment was the same as that used in Experiment 1.

Procedure

The procedure was as for Experiment 1, with the following changes. Twenty-five heading directions were arranged in a grid pattern across the field of view by crossing five steps of azimuth (-10, -5, 0, +5, +10° of visual angle), with five steps of elevation (-10, -5, 0, +5, +10° of visual angle). This allowed an examination of performance across the entire visual field, as well as for azimuth and elevation alone. Each heading direction was presented 5 times during an experimental condition, to give a total of 125 trials for each.

Two types of display were used for this experiment. In the first, participants saw motion in depth through the random dot cloud (motion condition). In the second, they saw a display consisting of lines showing the distance and direction of the motion that the dots would have described on the screen in the motion condition (line condition). The lines in the line condition were of the same width and brightness as the dots in the motion

condition.

Two response screen colours were also used: the first was a standard black screen, (black condition), while the other was a grey half way between the white and black screens in intensity (grey condition). Display types and response screens were crossed. The order of presentation of these four was randomly assigned to each participant, and within each condition the trials were also randomised. All conditions were run in the same session, with each taking about 10 minutes, the total session lasting approximately 50 minutes.

Results

The results of the experiment are shown below in Figures 3.1 and 3.2, with the mean estimated heading plotted against the actual direction of heading. Only zero elevation trials have been used for azimuth, and vice versa for elevation. Descriptive statistics for the same data are shown in Table 3.1, with mean bias being calculated by subtracting the mean heading estimate from the heading direction.

The data summarized in Figures 3.1 and 3.2 shows that for all conditions, there was a bias to the screen centre, with motion displays leading to more bias than the static line displays.

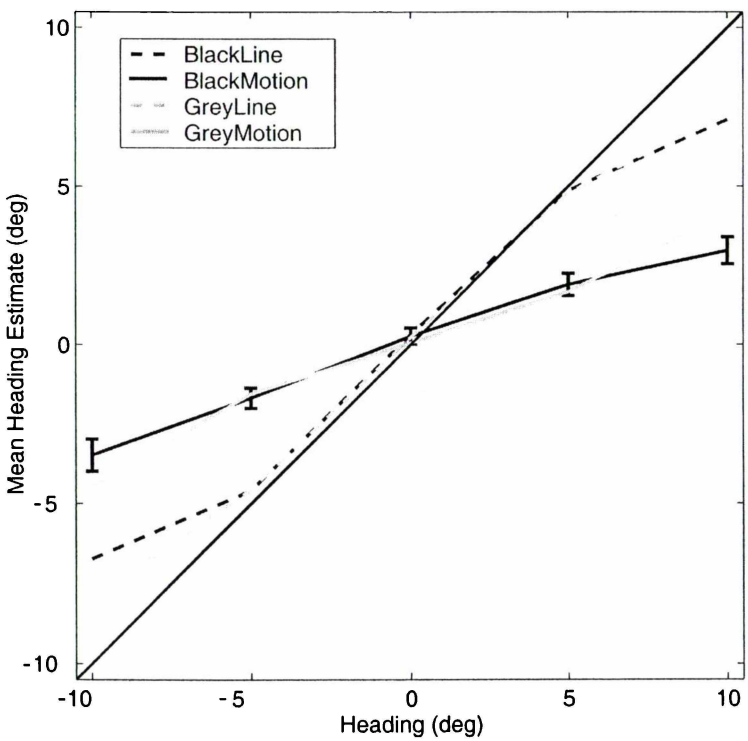

Figure 3.1. Mean heading estimates for azimuth as a function of heading direction for line and motion displays using grey and black response screens, ±2 SE for black-motion and black-line conditions. Veridical performance is shown by the 45° line.

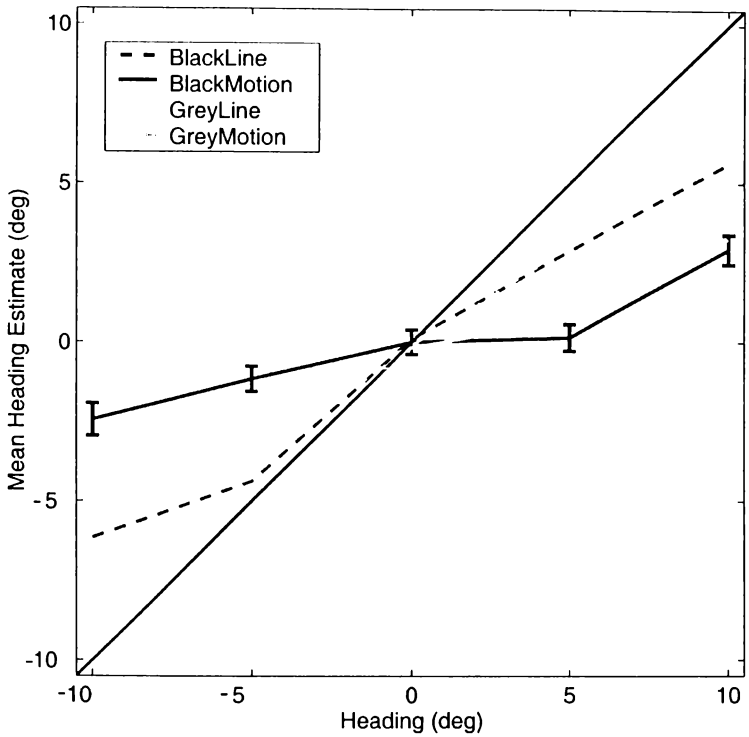

Figure 3.2. Mean heading estimates for elevation as a function of heading direction for line and motion displays using grey and black response screens, ±2 SE for black-motion and black-line conditions. Negative headings down, positive up. Veridical performance is shown by the 45° line.

Table 3.1

Mean heading estimates, mean bias and standard deviations for line and motion displays using grey and black response screens – azimuth only (N = 150)

Condition	Heading	Mean	Mean Bias	Std.Dev. of Mean
Black-Line	-10	-6.73	-3.27	2.19
	-5	-4.59	-0.41	2.00
	0	0.33	-0.33	2.39
	5	4.87	-0.13	2.57
	10	7.10	-2.90	2.57
Black-Motion	-10	-3.48	-6.53	4.38
	-5	-1.68	-3.32	2.77
	0	0.27	-0.27	2.22
	5	1.9	-3.10	3.03
	10	2.97	-7.03	3.67
Grey-Line	-10	-7.94	-2.06	3.31
	-5	-4.56	-0.44	2.80
	0	0.23	-0.23	2.92
	5	4.78	-0.22	2.51
	10	7.37	-2.63	3.92
Grey-Motion	-10	-4.49	-5.51	4.76
	-5	-1.55	-3.45	3.30
	0	0.05	-0.05	2.02
	5	1.67	-3.33	3.23
	10	4.14	-5.86	4.51

Table 3.2

Mean heading estimates, mean bias, and standard deviations for line and motion displays using grey and black response screens – elevation only (N = 150).

Condition	Heading	Mean	Mean Bias	Std.Dev. of Mean
Black-Line	-10	-614	-3.86	3.06
	-5	-4.38	-0.62	3.02
	0	0.10	-0.10	3.03
	5	2.87	-2.13	3.20
	10	5.63	-4.37	3.15
Black-Motion	-10	-2.44	-7.56	4.41
	-5	-1.16	-3.84	3.40
	0	0.01	-0.01	3.37
	5	0.15	-4.85	3.60
	10	2.92	-7.08	4.03
Grey-Line	-10	-6.93	-3.07	4.22
	-5	-3.79	-1.21	2.93
	0	-0.10	-0.10	3.32
	5	3.00	-2.00	3.67
	10	5.92	-4.08	3.64
Grey-Motion	-10	-3.10	-6.90	5.14
	-5	-1.83	-3.17	3.11
	0	-0.17	-0.017	2.34
	5	0.74	-4.26	3.39
	10	3.25	-6.75	4.54

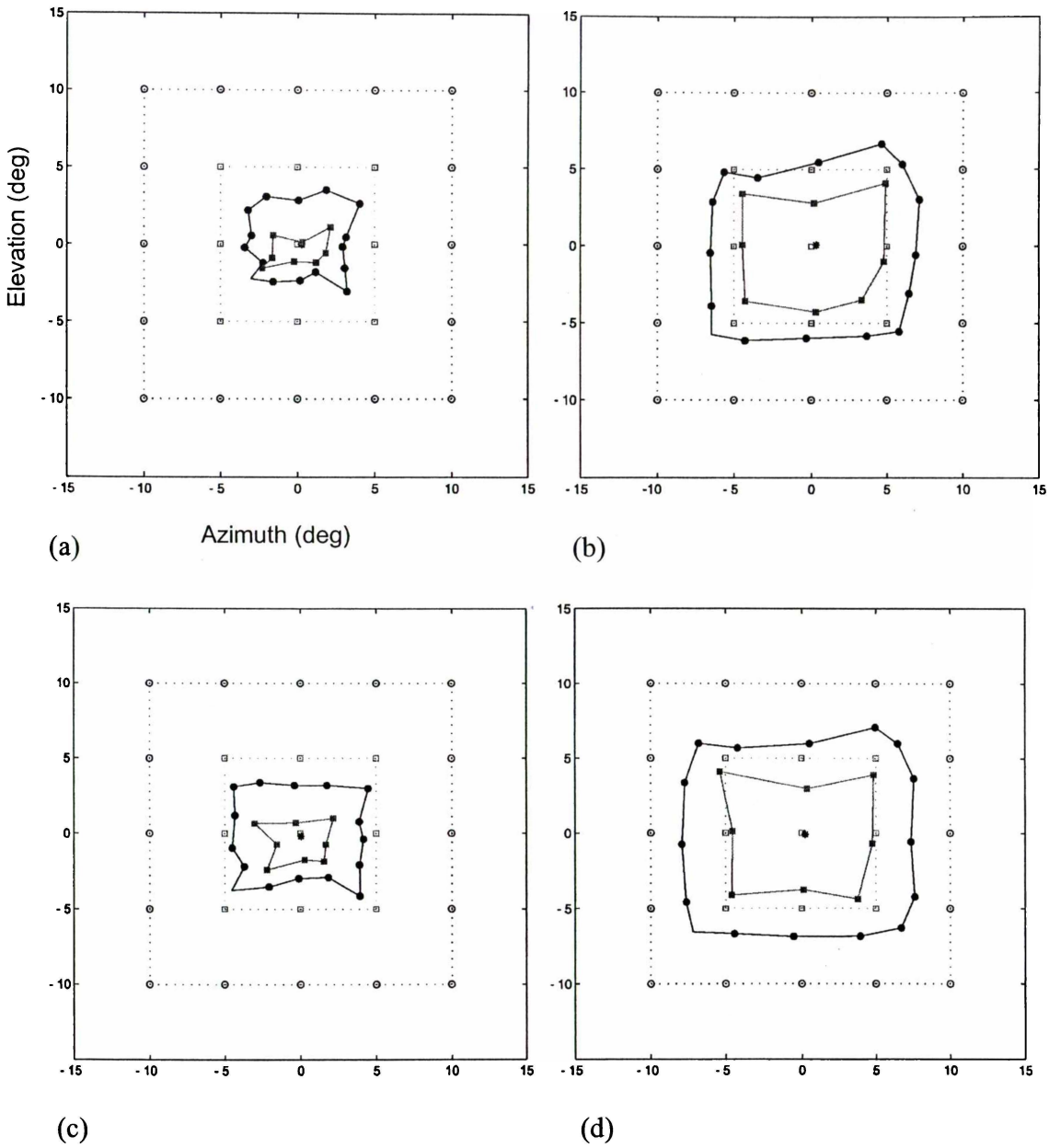

Figure 3.3. Mean estimates of heading showing azimuthal and elevational components for (a) Motion display with black screen, (b) Line display with black screen, (c) Motion display with grey screen and (d) Line display with grey screen. Open symbols = actual heading; filled symbols = mean estimated heading. Circles and squares = headings of 10° and 5° respectively. Unconnected central squares= 0°.

To enable us to examine the effect of display type and response screen colour across the visual field, mean estimates for each of the 25 headings have been graphed in Figure 3.3, with descriptive data given in Appendix B. Estimates for the different heading

eccentricities (5° and 10°) have been joined to permit a comparison between actual and perceived visual space. Central bias distorts perceived heading towards the middle of the visual field.

Figure 3.3 shows that bias to centre occurred for all headings, with the size of this bias depending upon the display type. For the motion conditions bias occurred at both 5° and 10° eccentricities, although the extent of this bias is greater at 10°. By contrast the line conditions show much less heading bias overall, and most of that is seen at 10° eccentricity. The black conditions do show somewhat more heading bias than the grey conditions, but again this is mainly at 10° eccentricity.

In order to characterise the trends in the data across the different conditions, regression analyses were carried out on the actual heading estimates for each condition for each dimension (azimuth and elevation) using only the zero condition of the other dimension. Curve fitting was carried out prior to regression to ensure that linear regression was appropriate, and a linear fit was found to be significant in all cases ($p < .0001$).

The full details of the regression equations are shown in Tables 3.3 and 3.4, while the scatter-plots for the black-line and black-motion azimuth conditions are shown in Figures 3.4 and 3.5. These two conditions have been selected as the grey and black conditions were not significantly different to one another as shown by the 95% confidence intervals.

Note that although the perceived scatter for these graphs is large as they contain many estimates, the 95% confidence intervals are small, showing a high level of response consistency in the underlying population.

Table 3.3

Linear regression statistics for estimated headings for azimuth for line and motion displays using black and grey response screens.

Condition	Slope	95% C.I.	Intercept	95% C.I.	R	P
Line-Black	0.723	0.707 to 0.728	0.209	-0.052 to 0.447	.906	<.0001
Motion-Black	0.325	0.281 to 0.376	-0.008	-0.343 to 0.326	.578	<.0001
Line-Grey	0.799	0.768 to 0.860	-0.024	-0.342 to 0.306	.875	<.0001
Motion-Grey	0.410	0.367 to 0.476	-0.035	-0.376 to 0.390	.621	<.0001

Table 3.4

Linear regression statistics for estimated headings for elevation for line and motion displays using black and grey response screens.

Condition	Slope	95% C.I.	Intercept	95% C.I.	R	P
Line-Black	0.581	0.571 to 0.661	-0.391	-0.702 to 0.068	.814	<.0001
Motion-Black	0.225	0.186 to 0.295	-0.064	-0.492 to 0.280	.942	<.0001
Line -Grey	0.648	0.598 to 0.701	-0.361	-0.743 to -0.018	.790	<.0001
Motion-Grey	0.255	0.251 to 0.361	-0.064	-0.610 to 0.169	.492	<.0001

The p values for the slope reach significance for the regression meaning that the slope is greater than zero. However, the 95% confidence interval for the slope does not include 1.0, therefore a significant bias to the screen centre occurred in all conditions.

For azimuth, the line-black and line-grey conditions are significantly different as shown by the fact that their slope values do not fall within the 95% C.I. for the other. The motion-black and motion-grey conditions are also significantly different to one another. Motion displays led to the most bias with both grey and black screens. Within a response screen colour, the motion and static conditions are significantly different with the line display leading to less error.

For elevation, the line-black and line-grey conditions do not differ significantly from one another, and neither do the motion-black and motion-grey conditions. However within a response screen colour the line and motion conditions are significantly different. with the motion conditions showing much more bias.

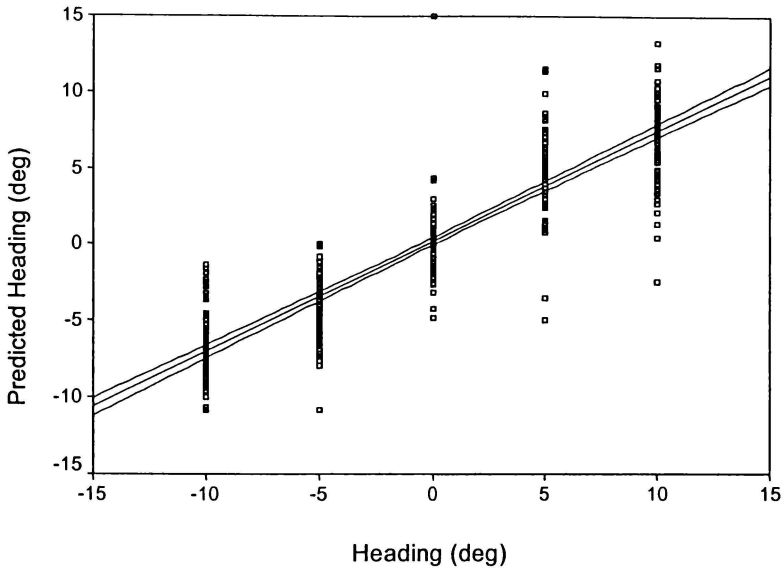

Figure 3.4. Scatterplot and regression line (± 95% C.I.) for the azimuthal component of heading estimates for the black-line condition.

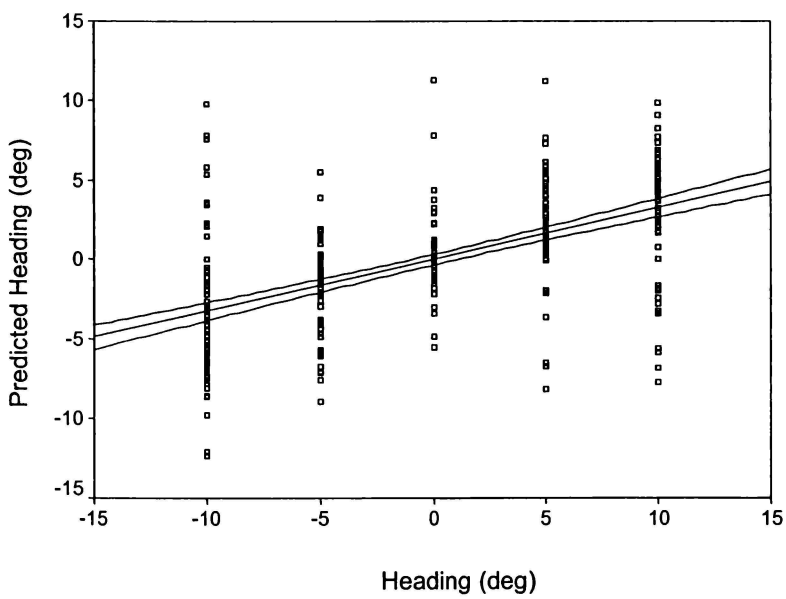

Figure 3.5. Scatterplot and regression line (± 95% C.I.) for the azimuthal component of heading estimates for the black-motion condition.

To ascertain which of the independent variables affected heading estimation, two three-way within-subjects analyses of variance were conducted for azimuth and elevation (with the other dimension collapsed). The dependent variable was Heading Error, a continuous variable calculated using the equation Mean Error = $\sqrt{(\delta_X^2 + \delta_Y^2)}$, where δ_X is equal to the screen deviation of the estimate from the actual direction in the X direction, δ_Y is equal to the same in the Y direction. The within subjects factors were screen colour with two levels (black and grey), display type with two levels (motion and line) and heading with five levels (-10, -5, 0, +5, +10° of visual angle). Any violations of sphericity were corrected using Mauchly's Test of Sphericity.

For azimuth, there were significant main effects for display [$F(1,14) = 0.642$, $p = .006$, $\eta^2 = .432$] and heading [$F(1.513, 21.179) = 15.863$, $p < .0001$, $\eta^2 = .531$], and significant interaction effects for colour x heading [$F(2.048,28.668) = 4.008$, $p = .028$, $\eta^2 = .223$] and display x heading [$F(1.6,22.405) = 4.718$, $p = .026$, $\eta^2 = .252$]. There was no significant main effect for colour [$F(1,14) = 2.387$, $p = .145$, $\eta^2 = .146$], and no significant interaction effects for colour x display [$F(1,14) = .144$, $p = .710$, $\eta^2 = .010$], or for colour x display x heading [$F(4,56) = .638$, $p = .638$, $\eta^2 = .044$].

For elevation, there were significant main effects for display [$F(1,14) = 13.321$, $p = .003$, $\eta^2 = .488$, power $= .924$] and for heading [$F(2.067, 28.938) = 22.126$, $p < .0001$, $\eta^2 = .752$]. There was also a significant interaction effect for display x heading [$F(1.374,19.23) = 4.011$, $p = .048$, $\eta^2 = .223$]. There was no significant main effect for colour [$F(1,14) = 1.426$, $p = .252$, $\eta^2 = .092$, and no significant interaction effects for colour x display [$F(1,14) = 2.036$, $p = .176$, $\eta^2 = .127$], for colour x heading [$F(1.876,26.268) = .336$, $p = .704$, $\eta^2 = .023$] or for colour x display x heading [$F(3.282,45.941) = 1.353$, $p = .268$, $\eta^2 = .088$].

Discussion

The major finding of this experiment is the size of the heading bias, which is especially large in the motion condition, with estimates of approximately 5° heading being made at 10° actual heading eccentricity. However the line condition, while giving a smaller bias, still had errors of 2° to 3° at 10° eccentricity, indicating some degree of constant error. An ANOVA analysis of the results revealed that for both azimuth and elevation there was a significant interaction effect. As hypothesised, bias was significantly greater for elevational components than for azimuthal for all but the black-motion condition, thus offering support for the findings of D'Avossa and Kersten (1996).

The results of this experiment do not support the idea that heading estimation is normally carried out using static techniques, i.e., observers simply rely on the radial pattern of line traces that are left on the screen by the moving dots. If this had been the case, we would have expected the line and motion displays to lead to similar levels of accuracy for the black displays, and to differ for the grey, where phosphor streaks were less available because of masking by the grey response screen that appeared immediately after the dot motion. However, regression analyses showed that estimation for line conditions was more accurate than that for motion conditions, and that there were no significant differences between response screen colours. A within-subjects repeated measures ANOVA revealed that the difference between line and motion displays increased with heading eccentricity for both elevational and azimuthal components, revealing a fundamental difference in estimation strategy between the two forms of display.

This result means that although the traces were visible, they did not give an advantage in performance, and a black response screen may safely be used in any future heading experiments. This is an extremely interesting finding given the superior

performance found with line displays, as phosphor trails give an almost identical effect on the screen. All participants independently reported being able to see the phosphor trails, and all commented that they could use them to estimate the direction of heading, which makes it all the more revealing that they apparently failed to be able to do so.

The fact that estimates for the motion condition contained more bias than the line condition is counterintuitive. Under the motion condition there was both movement *and* the static radial pattern provided by the phosphor traces, yet for some reason the observers performed less accurately. It appears that the participants were not able to access the information provided by the phosphor traces despite their belief to the contrary.

One other finding of interest in this experiment was the two participants whose heading estimates appeared to be reversed with positive heading directions being perceived as negative and vice versa. The data for these individuals was included in the overall data, as we presume they are representative of the performance of some proportion of the general population. The azimuthal estimates for the black-motion condition for one of the individuals is shown below in Figure 3.6. The two individuals who inverted their responses did so to a serious extent, such that when they were shown a heading of 10° deg to the right, they judged it to be 5° to the left. This level of error would mean an inability to correctly navigate through the environment if carried over into the real world.

Interestingly, estimates for the line condition did not display this inversion in performance, as can be seen in Figure 3.7. Therefore, whatever caused the inversion was only present in the motion condition.

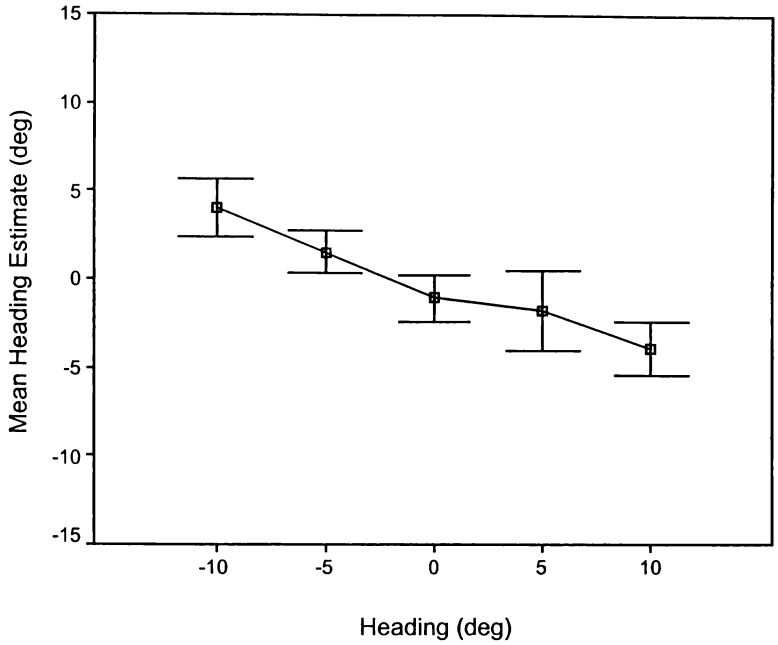

Figure 3.6 – Mean heading estimates (±2 SE) as a function of heading direction for the azimuthal component of heading estimates of one observer for the black-motion test condition.

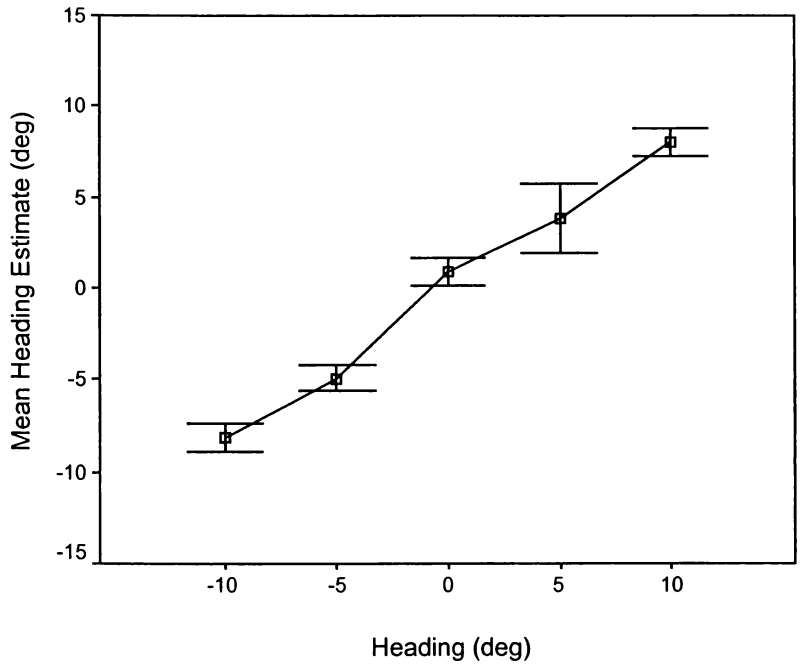

Figure 3.7 – Mean heading estimates (±2 SE) as a function of heading direction for the azimuthal component of heading estimates of one observer for the black-line test condition.

CHAPTER 4

Experiment Three: Sources of Bias in Heading Estimation

In Experiment 2 it was discovered that line and motion conditions led to different performance levels, with the line condition resulting in the more accurate estimates. However there was some bias observed even in the static condition and it would be useful to know at which stage this bias occurs in order to discover whether it is perceptually based, or some form of response error. The bias could potentially arise in any or all of three stages during the response cycle: (a) in the calculation of heading, (b) in the memory for the calculated heading, and (c) in moving the mouse correctly to the heading direction, i.e. some sort of motor response error. It was therefore decided to carry out another experiment to enable these to be examined separately.

From previous research it is known that pointing to remembered target positions can lead to bias in screen-based displays, a situation similar to the line displays in Experiment 2. No calculation of direction is required, but the task for the participant is simply to point to the remembered direction. For example, Gnadt, Bracewell, and Andersen (1991) ran an experiment in which monkeys moved their eyes to remembered targets. This resulted in a strong central bias at all eccentricities. When human observers are asked to point towards a stationary object on a screen, a central bias has been shown to occur. Of particular relevance to the present work is the series of experiments run by Sheth and Shimojo (2001), who used central fixation points and various object locations. They found that the eccentricity of vertical and horizontal targets was consistently underestimated, and that this bias increased with actual eccentricity of the target. Therefore it seems likely that at least some of the bias in Experiments 1 and 2 arose from errors in memory and motor response.

It is also probable that difficulties arising from the visual computation of heading had a role in some of the bias in these experiments, and that this had a greater role in the motion conditions of Experiment 2. This idea is supported by the findings of D'Avossa and Kersten (1996), who ran a control experiment in which participants were asked to point to a target that had been briefly displayed upon the screen. They found that overall the error for this task was significantly less than that for the full heading experiments.

The relative importance of memory, motor response, and computation bias will be tested in this experiment by reproducing the static and motion conditions of Experiment 2. However, instead of asking participants to estimate their direction of heading, a yellow spot was placed at the focus of expansion and they were simply asked to indicate the location of this spot.

No significant difference between the line and motion conditions (see Experiment 2) was expected in this experiment. However, there was a slight possibility that the movement of the dots in the motion condition of Experiment 2 disrupted the memory or response process, and therefore two speeds of observer translation (forward motion) were used in this experiment. If such disruption did occur, we would perhaps expect it to be greater with a faster speed of motion.

Method

Participants

Fifteen students from the University of Waikato, 8 female and 7 male, aged between 18 and 30 years, participated in this experiment. All were first year psychology students who received partial course credit for taking part. All participants had visual acuity of 20:25 or better. None had previously taken part in a heading experiment.

Apparatus

The apparatus was the same as that used in Experiment 1 (Chapter 2).

Procedure

The procedure used was the same as in Experiment 1, but with the following changes. Four experimental conditions were run crossing two translation speeds (2 $m.s^{-1}$ and 4 $m.s^{-1}$) with two displays (line and motion as in Experiment 2). A yellow spot subtending 0.65° of visual angle was placed at the FOE, and participants were asked to indicate where it had been located on the screen. Each heading was presented ten times for each of the 11 heading directions, during an experimental condition, giving a total of 110 per condition. Each condition took about 10 min to run, for a total session time of approximately 45 min.

Results

The results of the experiment are shown below in Figure 4.1, with the mean estimated heading plotted against the actual direction of heading for 2 $m.s^{-1}$ and 4 $m.s^{-1}$ speeds. Means and standard deviations for each condition are shown in Table 4.1.

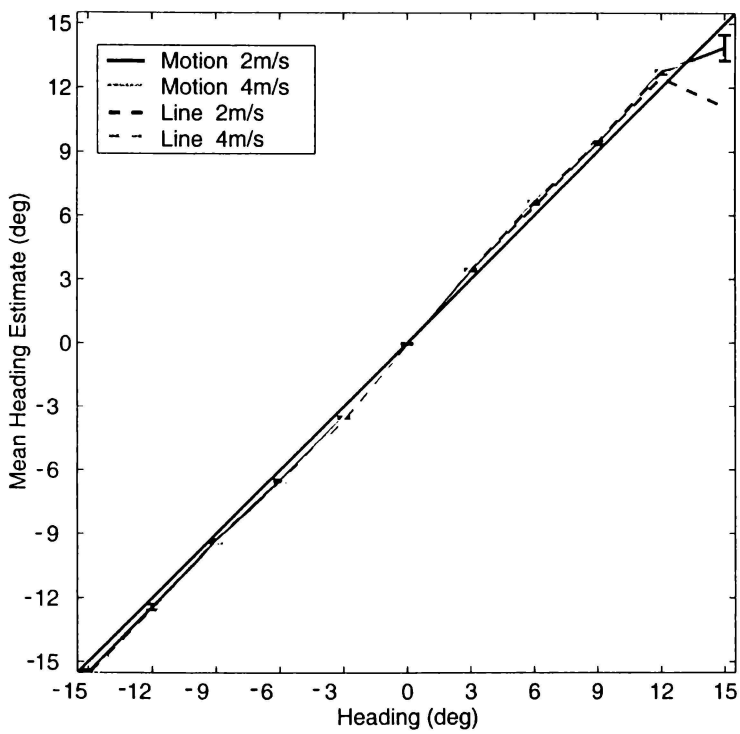

Figure 4.1. Mean heading estimates as a function of heading direction for line and motion displays with translation speeds of 2 $m.s^{-1}$ and 4 m.s-1, ±2 SE for the motion-2 $m.s^{-1}$ condition. Veridical performance is shown by the 45° line.

Table 4.1.

Mean heading estimates, mean bias, and standard deviations for line and motion displays at 2 m.s^{-1} and 4 m.s^{-1} when a spot is present at the FOE position. N = 150

Condition	Heading	Mean	Mean Bias	Std. Dev. of Mean
Motion - 2 m.s^{-1}	-15	-15.70	0.70	1.40
	-12	-12.46	0.46	3.25
	-9	-9.30	0.30	0.96
	-6	-6.50	0.50	0.81
	-3	-3.63	0.63	0.58
	0	0.01	0.01	0.04
	3	3.46	0.46	0.49
	6	6.42	0.42	0.94
	9	9.46	0.46	1.30
	12	12.47	0.47	1.18
	15	11.10	-3.90	9.34
Motion - 4 m.s^{-1}	-15	-15.49	0.49	1.3
	-12	-12.42	0.42	1.67
	-9	-9.35	0.35	0.91
	-6	-6.50	0.50	0.70
	-3	-3.50	0.50	0.46
	0	-0.03	0.03	0.28
	3	3.44	0.44	0.49
	6	6.61	0.61	0.78
	9	9.42	0.42	0.93
	12	12.74	0.74	1.05
	15	13.88	-1.12	7.49
Line - 2 m.s^{-1}	-15	-15.74	0.74	3.45
	-12	-12.65	0.65	1.16
	-9	-9.60	0.60	1.31
	-6	-6.60	0.60	0.71
	-3	-3.52	0.52	0.47
	0	0.06	0.06	0.50
	3	3.52	0.52	0.53
	6	6.60	0.60	0.68
	9	9.51	0.51	0.77
	12	12.69	0.69	0.84
	15	13.32	-1.68	7.07
Line - 4 m.s^{-1}	-15	-15.95	0.95	1.1
	-12	-12.91	0.91	1.19
	-9	-9.44	0.44	1.60
	-6	-6.77	0.77	1.62
	-3	-3.50	0.50	0.53
	0	0.01	0.01	0.05
	3	3.59	0.59	0.58
	6	6.81	0.81	0.76
	9	9.78	0.78	0.92
	12	12.91	0.91	0.92
	15	13.44	-1.56	6.76

The data summarized in Figure 4.1 shows that for both speeds and both display conditions, there was very little bias to the screen centre. As in previous experiments, the standard errors for these mean estimates are quite small, at around 1 to 2°, showing the responses to have been reasonably consistent across participants and trials. The small increase in bias seen at the 15° to the right for the 2 $m.s^{-1}$ motion condition is most likely caused by the blind spot, which lies in the region 12 to 15° in the temporal retina (Goldstein, 1989), and should not be taken to indicate an increase of bias for this condition. It is not known why the blind spot would make the estimate of position move inwards rather than outwards, but such an outcome is consistent with the overall trend towards central bias.

A linear fit was found to be significant ($p < .0001$) for the data, and regression analyses were carried out on the actual heading estimates. The full details of the regression equations are shown in Table 4.2, while the scatter-plots for the line-2 $m.s^{-1}$ condition and motion-2 $m.s^{-1}$ conditions are shown in Figures 4.3. These graphs were selected because the Static condition is not significantly different from the two 4 $m.s^{-1}$ conditions, as shown by the 95% confidence intervals.

Table 4.2

Linear regression statistics for estimated headings for line and motion displays using translation speeds of 2 $m.s^{-1}$ and 4 $m.s^{-1}$.

Condition	Slope	95% C.I.	Intercept	95% C.I.	R	p
Line-2 $m.s^{-1}$	1.022	1.006 to 1.03	-0.219	-0.371 to -0.067	0.967	<.0001
Motion-2 $m.s^{-1}$	0.979	0.958 to 0.999	-0.425	-0.621 to 0.230	0.942	<.0001
Line-4 $m.s^{-1}$	1.023	1.007 to 1.04	-0.302	-0.460 to -0.145	0.964	<.0001
Motion-4 $m.s^{-1}$	1.021	1.006 to 1.037	-0.110	-0.256 to 0.037	0.969	<.0001

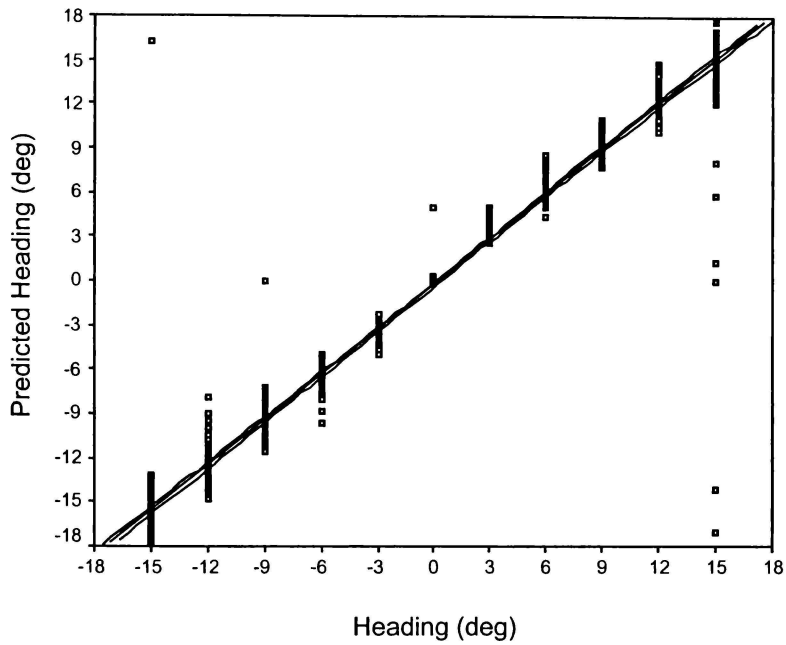

Figure 4.2. Scatterplot and regression line (± 95% C.I.) for heading estimates for the 2 $m.s^{-1}$-line condition.

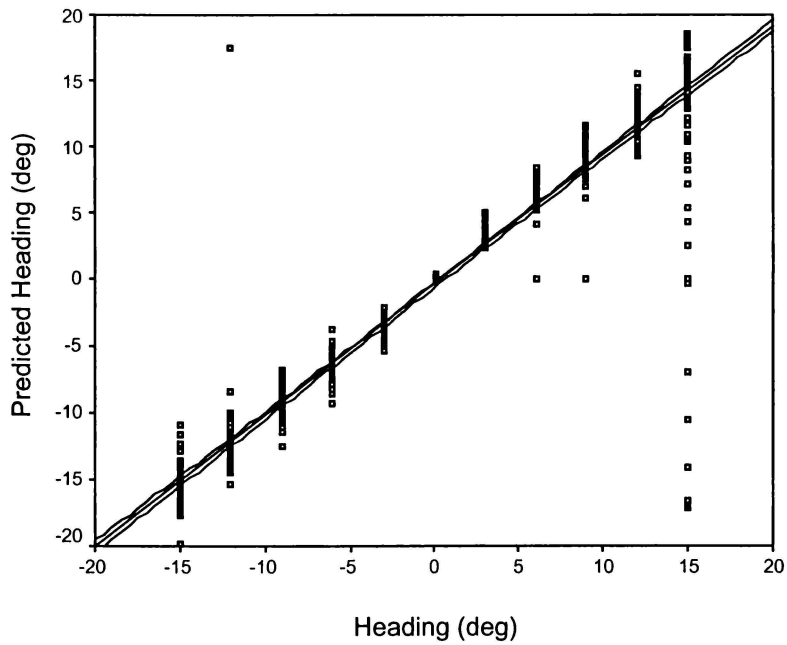

Figure 4.3. Scatterplot and regression line (± 95% C.I.) for heading estimates for the 4 $m.s^{-1}$-line condition.

The p values for the slope reach significance for the regression meaning that the slope is greater than zero. The 95% confidence interval for the slope does not include 1.0, therefore a slight bias occurred, however three of the conditions led to a slight positive bias and only the motion-2 $m.s^{-1}$ condition differed from this.

Looking at the scatterplot for the line-2 $m.s^{-1}$ condition, shown in Figure 4.3, it is easily seen that the two variables are linearly related such that as actual heading increases, the heading estimate also increases. The perceived scatter for these graphs is small although it does appear to increase somewhat with eccentricity. However, in no case is the error anywhere near as large as that seen in Experiments 1 and 2. Two two-way within-subjects analysis of variance were conducted to evaluate the effect of speed, display and heading upon estimates of heading. The dependent variable was the mean heading estimate. The within subjects factors were speed with two levels (2 $m.s^{-1}$ and 4 $m.s^{-1}$), display with two levels (motion and static) and heading with eleven levels (-15, -12, -9, -6, -3, 0, 3, 6, 9, 12, 15° of visual angle). Any violations of sphericity were corrected using Mauchly's Test of Sphericity.

There was a significant main effect for heading [$F(1.424, 12.812) = 8.226$, $p = .008$, $\eta^2 = .478$]. There were no significant main effects for speed [$F(1, 9) = 1.319$, $p = .280$, $\eta^2 = .128$] or for display [$F(1, 9) = .000$, $p = .983$, $\eta^2 = .000$], and no significant interaction effects for speed x heading [$F(2.147, 19.323) = .571$, $p = .586$, $\eta^2 = .060$], display x heading [$F(2.165, 19.489) = .210$, $p = .828$, $\eta^2 = .023$], speed x display [$F(1, 9) = 3.850$, $p = .081$, $\eta 2 = .300$] or speed x display x heading [$F(1.380, 12.424) = 1.246$, $p = .304$, $\eta^2 = .122$]. Because of the difference between static and motion conditions at 2 $m.s^{-1}$, paired t-tests were carried out for -15, -12, -9, -6, and -3° headings to test where the differences arose. These were chosen because the blind spot lies on the right, and this could have confused the results. Only the -9° heading was found to reach significance ($p<.035$).

Discussion

The bias in the current experiment equates to the amount of bias attributable to memory and response errors because a stationary target was present in the visual field during the trial, and we will therefore be able to be reasonably confident that any larger amount of bias found in earlier experiments will be mainly due to errors in the calculation of heading.

Consistent with the results of D'Avossa and Kersten (1996) and our initial hypothesis, this experiment showed that finding a point on a screen is performed with a much greater level of accuracy than is indicating heading, which involves estimation without a landmark feature such as a spot marking the FOE. The vast majority of the bias found for the motion conditions in Experiment 1 is therefore probably due to difficulty in calculating the direction of heading from optical flow rather than to memory or motor response errors.

Interestingly, Experiment 3 showed no central bias whatsoever for any of the conditions. In fact a slight overestimation of direction was the norm, especially with higher eccentricities. This stands in marked contrast to Experiment 2, in which a bias of 2-3° was seen with the larger 10° heading eccentricity even in the line condition. Presumably such bias is to be expected when the focus of expansion is not directly indicated.

This lack of central bias in this experiment is in direct contrast to the findings of Sheth and Shimojo (2001) and others who have found a central bias when people are asked to locate a spot on the screen. One possibility for this difference is the addition of line traces originating from the FOE in the current work, which may have served to 'fix' the point more securely on the screen.

Although the regression analysis revealed a significant difference between the motion and line conditions at 2 $m.s^{-1}$, a subsequent t–test showed this to only reach significance for +9° eccentricity. This lack of any significant difference between the four conditions shows that the increased amounts of bias found for motion in Experiment 2 was not due to the movement of the dots disturbing the memory for the spot location or the motor response.

On the basis of the results from this experiment, it appears that the large heading bias found in the motion conditions is not primarily due to difficulties in memory or response, and must therefore arise from the computation of heading. Determining the centre of perspective from a static display is a fairly simple task, presumably carried out by finding the point of convergence of the line traces. However calculating the direction of heading on the basis of motion cues can cause significant difficulties for human observers. On a superficial level, the two tasks seem very similar because they both involve the task of locating the point of intersection (of lines in the line condition and of motion directions in the motion condition). A deeper examination of the factors controlling these judgments is therefore in order.

CHAPTER 5

Experiment Four– Object Shape and Size

In this chapter, the effect of object shape and size on the heading bias is examined. The influence of object related perspective cues upon heading estimation has not been well studied, and such research as has been done has led to somewhat equivocal results. For example, Ehrlich, Beck, Crowell, Freeman, and Banks (1998) found that adding depth cues during simulated gaze rotations – binocular disparity, relative and changing size, occlusion, dynamic occlusion and linear perspective – did not improve the accuracy of heading estimates. A failure of background texture to aid performance has also been found in judgments of impact point during a simulated aircraft landing on a carrier (Kaufman, 1964).

However, Beusmans (1998) ran an experiment in which convex or concave edges were inserted into optic flow fields. Using this experimental design, he found that object shape did have an influence on heading judgments when simple translation was used. Similarly, van den Berg and Brenner (1994) examined the way in which humans combine optic flow with static depth cues to determine heading. On the basis of their results, they concluded that humans use additional information on depth and possibly shape that is independent of optic flow to extract heading. They suggest that depth order as specified by perspective, texture gradients, and nearness to horizon may be used to select the furthest points in the display and so estimate ego-rotation. They also propose that the higher amount of heading error seen with computer-simulated motion through a 3-D random dot cloud may be due to the absence of static depth cues.

Other researchers have examined the ability of perspective information to help in overcoming the rotation problem. Li and W.H. Warren (2000) performed an in-depth

analysis of the role of perspective cues in estimating heading. They used a dense texture-mapped display to compare random dots, textured ground planes, textured ground plane with posts, and textured ground plane with tombstone displays, each of which added another layer of perspective information to the overall scene. They found that, even under high rotation rates, heading could be perceived from retinal flow alone, provided that dense motion parallax and at least one reference object was present, and proposed that this is sufficient to overcome the rotation problem. There was a significant improvement in performance when dots were replaced with a textured ground plane. The addition of multiple objects on the ground yielded only small improvements. They also ran an experiment using a dense field of posts on a flat ground plane, and found that the path of self-motion could be determined just as accurately as with a continuous textured ground plane. As a result of these experiments, the authors proposed that two forms of optical information are required to determine the path of self-motion under rotation. Firstly, dense motion parallax, used to solve the rotation problem, and secondly, the presence of reference objects which are used to resolve path ambiguity. In other words, they propose that the path of self-motion is perceived relative to objects in the scene.

Although these experiments were concerned with translation *and* rotation, on the basis of these results, it is believed that the perspective cues of changing object shape and size may have a positive effect upon estimates of heading, by providing more information regarding the current direction of heading, and thereby reducing bias. To test this hypothesis, three types of dots were used in a standard heading experiment: 'non-growing dots' where the dots remain the same size on the screen throughout the trial (effectively shrinking in 3-D space as they get closer), 'growing dots' where the dots increase in screen size as they get closer to the observer (constant dot size in 3-D space), and 'growing cubes' (a constant cube size in 3-D space and increasing screen size). If object shape and size has

a positive influence on heading estimates, then less bias should be observed with the growing cubes and dots compared to the non-growing dots.

Method

Participants

Fifteen students from the University of Waikato, 12 female and 3 male, aged between 18 and 42 years, participated in this experiment. All were first year psychology students who received partial course credit for taking part. All participants had visual acuity of 20:25 or better. None had previously participated in a heading experiment.

Apparatus

The apparatus used in this experiment was the same as that used in Experiment 1.

Procedure

The procedure followed in this experiment was as for Experiment 2, with the following changes. For this experiment, the response screen was black for all trials, and only a motion display was used. Three dot types were tested in this experiment: fixed size dots, growing dots, and growing cubes. The fixed sized dots were identical to those shown in earlier experiments, growing dots appeared to grow in size as they approached, as did the cubes. The previous experiments reported in this thesis used just the fixed size dot condition. A grid of 25 heading directions was used as in Experiment 2, with 5 repeats per direction for each condition. This gave a total of 125 trials for each condition, and each took about 10 min to run, for a total session time of approximately 40 min.

Results

The results of the experiment are shown below in Figures 5.1 and 5.2. with the mean estimated heading plotted against the actual direction of heading for azimuth and elevation alone. For azimuth, only the zero elevation trials have been graphed, and vice versa for elevation. Descriptive statistics are provided in Table 5.1.

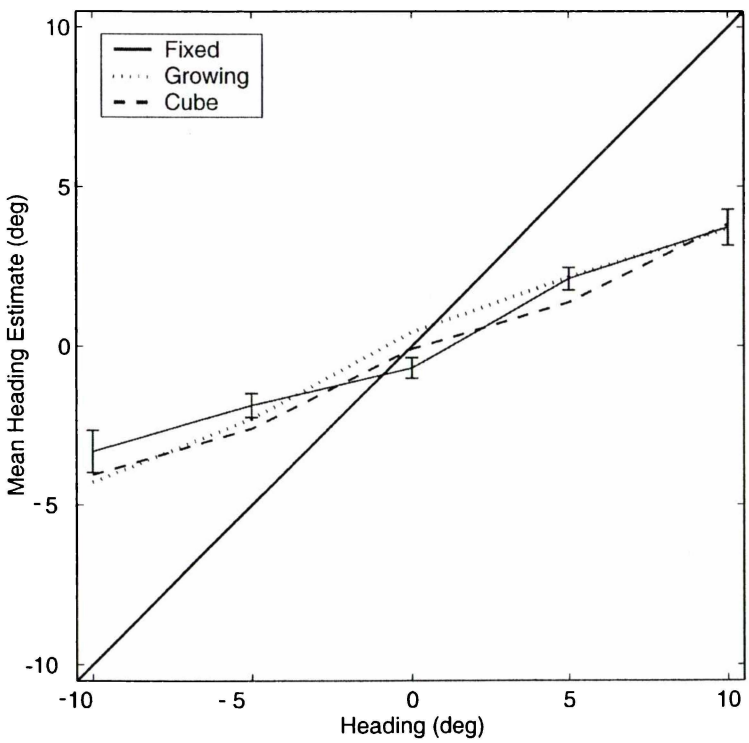

Figure 5.1. Mean heading estimates for azimuth as a function of heading direction for fixed size, growing and cube shaped dots, ±2 SE for fixed size condition. Veridical performance is shown by the 45° line.

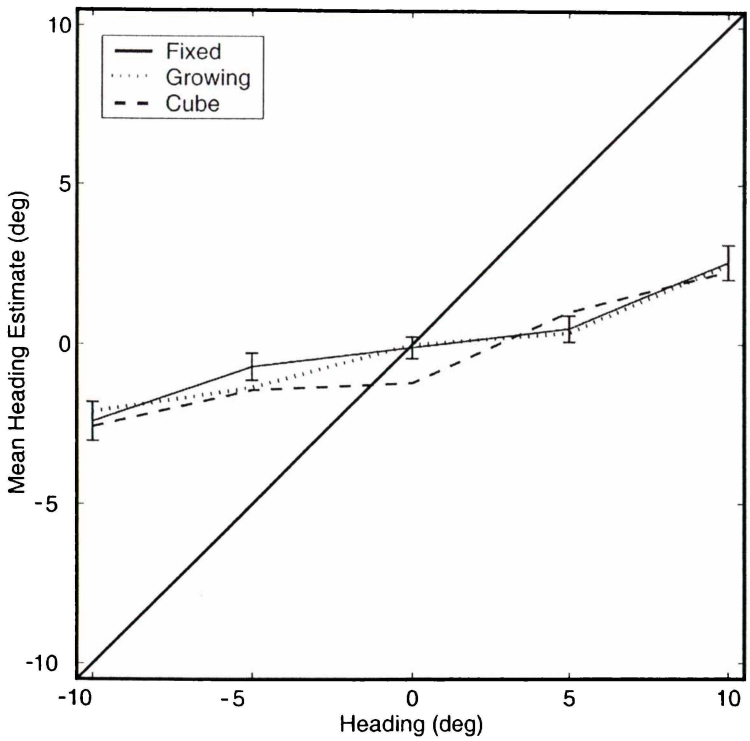

Figure 5.2. Mean heading estimates for elevation as a function of heading direction for fixed size, growing and cube shaped dots, ±2 SE for fixed size condition. Veridical performance is shown by the 45° line.

The data summarised in Figures 5.1 and 5.2 show that for all experimental conditions, there was a large bias to the screen centre. The standard errors for the mean estimates are quite small, at around 2° to 3° degrees, showing the responses to have been reasonably consistent across participants and trials.

In order to examine the effect of display type and response screen colour across the visual field, mean estimates for each of the 25 headings have been graphed together in Figures 5.3, and the descriptive data for these conditions are shown in Appendix C. These figures show that a significant bias to centre occurred for all headings.

Table 5.1

Mean heading estimates, mean bias and standard deviations for object type – azimuth only, N=75

Condition	Heading	Mean	Mean Bias	Std. Dev. of Mean
Dots	-10	-3.32	-6.68	5.76
	-5	-1.86	-3.14	3.23
	0	-0.69	-0.69	2.78
	5	2.11	-2.89	3.03
	10	3.72	-6.28	4.88
Growing Dots	-10	-4.06	-5.94	5.15
	-5	-2.60	-2.40	4.49
	0	-0.09	-0.09	3.52
	5	1.37	-3.63	3.41
	10	3.82	-6.18	4.34
Growing Cubes	-10	-4.29	-5.71	5.48
	-5	-2.29	-2.71	4.52
	0	0.44	-0.44	3.74
	5	2.16	-2.84	4.00
	10	3.67	-6.33	5.05

Table 5.2

Mean heading estimates, mean bias, and standard deviations for object type – elevation only, N=75.

Condition	Heading	Mean	Mean Bias	Std. Dev. of Mean
Dots	-10	-2.41	-7.59	5.24
	-5	-0.70	-4.30	3.65
	0	-0.09	-0.09	2.95
	5	0.49	-4.51	3.56
	10	2.58	-7.42	4.71
Growing Dots	-10	-2.57	-7.43	5.80
	-5	-1.43	-3.57	3.61
	0	-1.20	-1.20	2.37
	5	1.01	-3.99	4.75
	10	2.29	-7.71	4.99
Growing Cubes	-10	-2.10	-7.90	5.07
	-5	-1.35	-3.65	4.17
	0	0	0	3.37
	5	0.36	-4.64	3.80
	10	2.50	-8.50	4.60

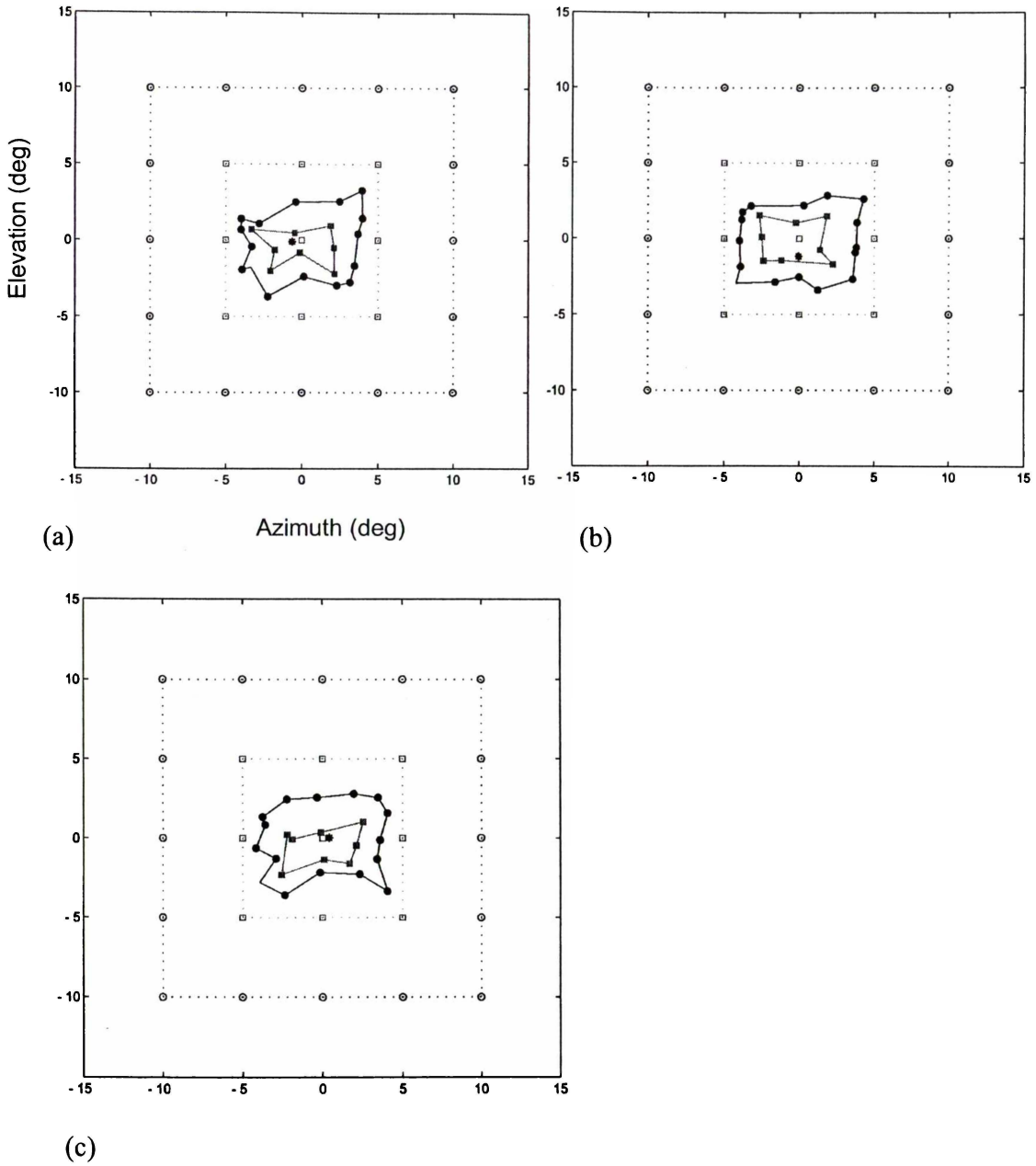

Figure 5.3. Mean estimates of heading showing azimuthal and elevational components for: (a) fixed sized dots, (b) growing dots and (c) growing cubes. Open symbols = actual heading; filled symbols = mean estimated heading. Circles and squares = headings of 10° and 5° respectively. Unconnected central squares = 0°.

Regression analyses were carried out on the actual heading estimates for each condition for each dimension (azimuth and elevation), using only the zero heading condition for the other dimension. Prior to carrying out the regression, curve fitting was done to ensure that linear regression was appropriate. A linear fit was found to be significant for all ($p < .0001$), and therefore linear regression was used for all conditions. Results of these regressions for azimuth and elevation respectively, are shown in Tables 5.3 and 5.4, and regression graphs for the fixed sized dots are shown in Figures 5.4 and 5.5.

Table 5.3

Linear regression statistics for estimated headings for azimuth for fixed size, growing and cube shaped dots.

Condition	Slope	95% C.I.	Intercept	95% C.I.	R	p
Fixed	0.357	0.301 to 0.412	0.015	-0.378 to 0.407	0.535	<.0001
Growing	0.387	0.330 to 0.444	-0.266	-0.670 to 0.138	0.556	<.0001
Cubes	0.396	0.334 to 0.458	-0.056	-0.495 to 0.383	0.532	<.0001

Table 5.4

Linear regression statistics for estimated headings for elevation for fixed size, growing and cube shaped dots.

Condition	Slope	95% C.I.	Intercept	95% C.I.	R	p
Fixed	0.222	0.166 to 0.277	-0.071	-0.464 to 0.322	0.365	<.0001
Growing	0.288	0.278 to 0.298	-0.383	-0.809 to 0.044	0.362	<.0001
Cubes	0.223	0.164 to 0.282	-0.112	-0.528 to 0.303	0.350	<.0001

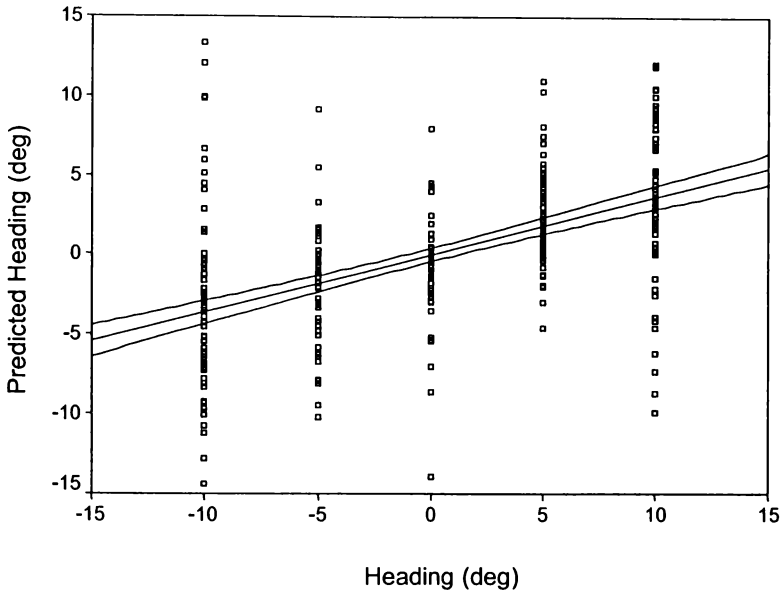

Figure 5.4. Scatterplot and regression line (± 95% C.I.) for the azimuthal component of heading estimates for the fixed size condition.

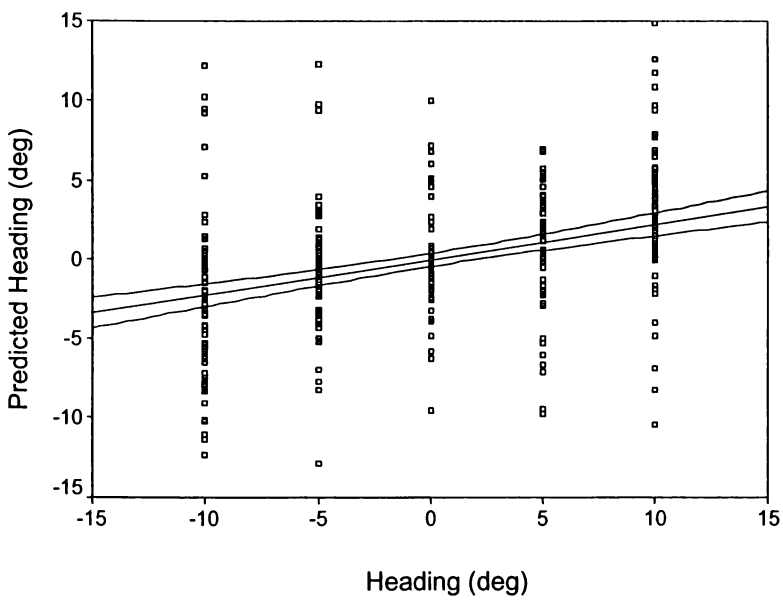

Figure 5.4. Scatterplot and regression line (± 95% C.I.) for the elevational component of heading estimates for the fixed size condition.

The p values for the slope reach significance for the regression meaning that the slope is greater than zero. However, the 95% confidence interval for the slope does not include 1.0, therefore a significant bias to the screen centre occurred for all conditions.

For azimuth, the slopes for the different conditions fall within the 95% confidence intervals for the other conditions, showing that there was no significant difference between the conditions. For elevation, both the fixed dots and growing cubes conditions have a slope that is significantly different to that of the growing dots condition.

Also, estimates for azimuth and elevation led to significantly different results, with the slopes for elevation being significantly less than for azimuth (as shown by the 95% C.I.s) meaning that more bias occurred. These trends can be seen in Figures 5.4 and 5.5.

Two two-way within-subjects analysis of variance were then conducted to evaluate the effect of object type and heading upon estimates of heading. As in Experiment 2 the mean error (the on-screen deviation of the mean estimate from the actual heading) was used as the dependent variable. Separate analyses were carried out for azimuth and elevation, with the other dimension collapsed. The dependent variable was the Heading Error, a continuous variable calculated as for Experiment 1. The within subjects factors were object type with three levels (fixed, growing and cubes), and heading with five headings (-10, -5, 0, +5, +10° of visual angle). Any violations of sphericity were corrected using Mauchly's Test of Sphericity.

For azimuth, there was a significant main effect for heading [$F(1.193, 16.702) = 1.655$, p =.07, $\eta^2 = .386$]. There was no significant main effect for object type [$F(2,28) = 1.655$, p =.209, $\eta^2 = .106$], and no significant interaction effect for object type x heading [$F(6.631,92.831) = 1.120$, p =.357, $\eta^2 = .074$].

For elevation, there were no significant main effects or interaction effects.

Heading [$F(1.004,14.053) = .939$, $p = .349$, $\eta^2 = .063$], object type [$F(1, 14) = .999$, $p = .381$, $\eta^2 = .067$] and object type x heading [$F(1,14.003) = .990$, $p = .337$, $\eta^2 = .066$] were all non-significant. The lack of main effect for heading means a flat plot for elevation.

Discussion

The results of this experiment show that, contrary to my original hypothesis, changing size and shape cues did not have a significant effect upon heading estimates. Although the experimental paradigms are different, this result is in agreement with that of Ehrlich et al (1998) who found that the addition of depth cues during simulated gaze rotations did not improve the accuracy of estimates.

The size of the bias in this experiment was very large, as shown by the flatness of the slopes in Figures 5.1 and 5.2. There were also significant differences in error between azimuth and elevation, with the regression slope being much lower for elevation. Although a significant difference was found between growing dots and the other two conditions for elevation in the regression analysis, a t-test showed that the difference only occurred at an eccentricity of 5°.

It is likely that estimating heading in azimuth and elevation dimensions simultaneously will create more difficulty than for any one dimension alone, therefore the increased bias in this experiment compared with Experiments 1 and 3 is expected. However the difference in the slope of the mean estimates between this and Experiment 2 is difficult to understand, as scene depth and translation speed were identical. In the earlier experiment, motion and static conditions were presented in random order, with half of the participants viewing a static condition first. It is possible that having seen these line traces gave participants a greater sensitivity to the direction of outflow.

As in Experiment 2, this experiment revealed two participants who responded in an inverse fashion to the given heading (these were different individuals from those in the earlier experiment). As in previous experiments, data from these individuals were included in the experimental data. While it is possible that these individuals simply misunderstood

the task, earlier data showing an ability to carry out heading estimation using a static display makes this unlikely. It is important not to overlook this data, as it may give an insight into the underlying cause of bias. These cases will be discussed again in Section B.

CHAPTER 6

Experiment Five– Objects Remain or Disappear

Previous experiments in this thesis have shown that observers could remember the location of a dot in space with high levels of accuracy. However when they were required to make judgments of heading direction, a significant bias to centre was found to occur.

One possible explanation for the bias is a perceptual distortion of space caused by the disappearance of the dots after each trial. In geometry, there are 2 ways to describe patterns of relationships: (a) Euclidean, using fixed coordinates with relationships specified in terms of them, and (b) coordinate free, with relationships defined in terms of internal relationships only. Humans appear to possess both kinds of coding systems (Howard, 1982). It is known that having a constant stimulus on the screen provides a coordinate free reference frame in terms of which other objects present may be judged, and the same may be true for heading estimation. In the real environment, objects do not disappear from view when we stop moving, and so the visual system may experience difficulties when this situation occurs in computer displays.

This possible negative influence of having the objects in the scene disappear will be tested by using two response screens: in the first, the dots will disappear from the screen following each trial, as for earlier experiments, while for the second they will remain onscreen during the response period.

Method

Participants

Fifteen students from the University of Waikato, 13 female and 2 male, aged between 18 and 33 years, participated in this experiment. All were first year psychology students who received partial course credit for taking part. All participants had visual acuity of 20:25 or better. None had previously been participants in a heading experiment.

Apparatus

The same apparatus as that used in Experiment 1 was used for this experiment.

Procedure

The same procedure as for Experiment 1 was used, with the following changes. Two experimental conditions were run: in one the dots remained in position on the screen after each trial, while for the other they disappeared, as in earlier experiments. Twenty-five heading directions were used in a grid pattern, as for Experiment 2. One hundred and twenty five trials were shown for each condition, with five repeats per heading, and each condition took about 10 min to run, for a total session time of approximately 30 min. The two dot levels were crossed with the 25 heading levels to give a 2 x 25 experiment.

Results

The results of the experiment are shown below in Figures 6.1 and 6.2, with the mean estimated heading plotted against the actual direction of heading for azimuth and elevation alone. For azimuth, only the zero elevation trials have been graphed, and vice versa for elevation. The descriptive data for azimuth and elevation for this experiment are given in Tables 6.1 and 6.2.

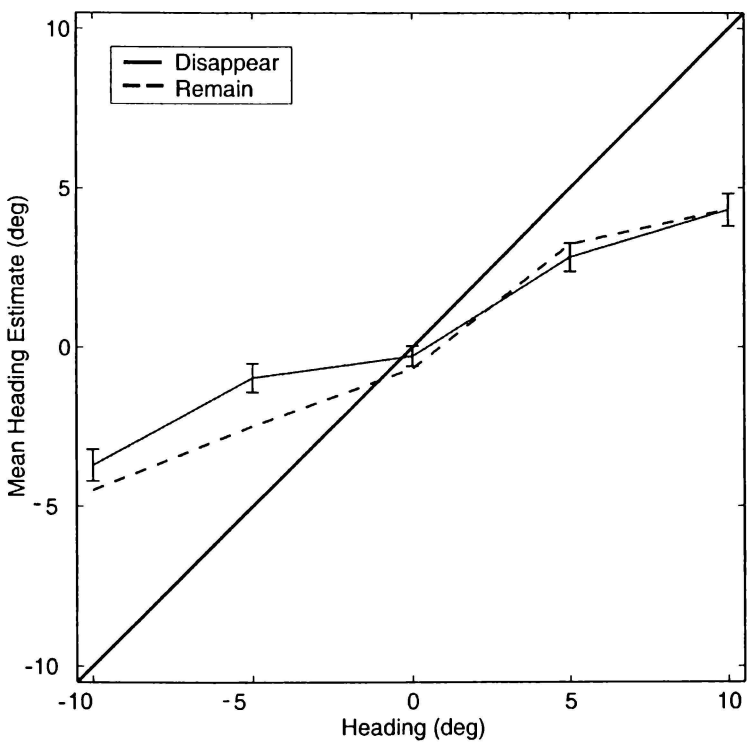

Figure 6.1. Mean heading estimates for azimuth as a function of heading direction for response screens with dots remaining or not, ±2 SE for dots not remaining. Veridical performance is shown by the 45° line.

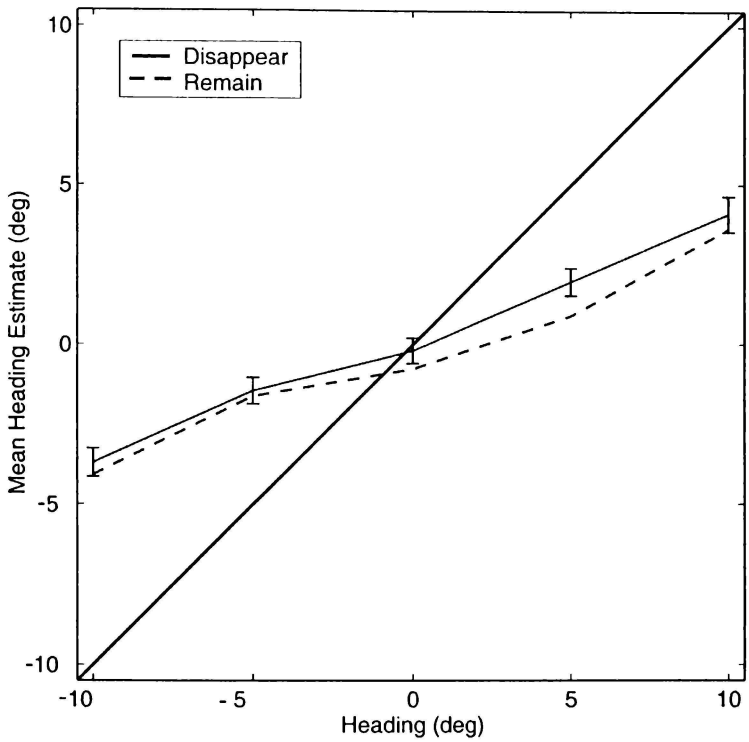

Figure 6.2. Mean heading estimates for elevation as a function of heading direction for response screens with dots remaining or not, ±2 SE for dots not remaining. Veridical performance is shown by the 45° line.

Table 6.1.

Mean heading estimates, mean bias, and standard deviations for dots disappearing or remaining onscreen – azimuth only, N=75

Condition	Heading	Mean	Mean Bias	Std. Dev. of Mean
Disappear	-10	-3.71	-6.29	4.32
	-5	-0.96	-4.04	3.90
	0	-0.28	-0.28	2.72
	+5	2.82	-2.18	3.84
	+10	4.30	-5.70	4.39
Remain	-10	-4.49	-5.51	4.64
	-5	-2.48	-2.52	3.48
	0	-0.67	-0.67	2.54
	5	3.23	-1.77	4.34
	10	4.31	-5.69	4.63

Table 6.2.

Mean heading estimates, mean bias, and standard deviations for dots disappearing or remaining onscreen– elevation only, N=75.

Condition	Heading	Mean	Mean Bias	Std. Dev. of Mean
Disappear	-10	-3.70	-6.30	3.86
	-5	-1.45	-3.55	3.56
	0	-0.19	-0.19	3.48
	5	1.97	-3.03	3.74
	10	4.09	-5.91	4.81
Remain	-10	-4.08	-5.92	3.91
	-5	-1.62	-3.38	3.66
	0	-0.76	-0.76	3.57
	5	0.90	-4.10	4.19
	10	3.61	-6.39	4.75

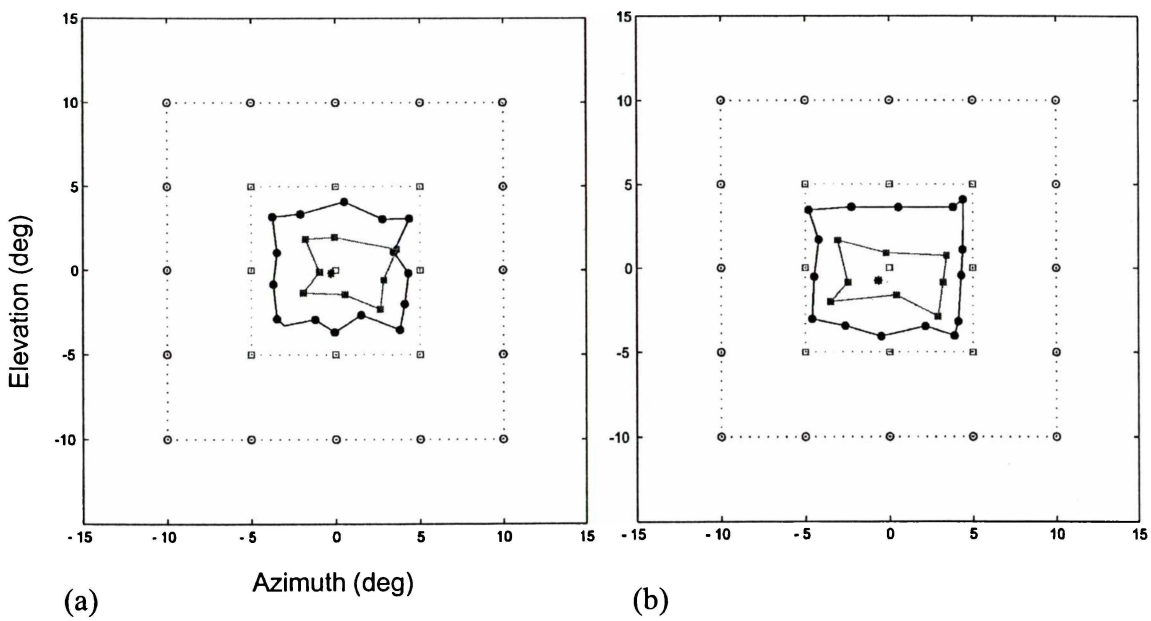

Figure 6.3. Mean estimates of heading showing azimuthal and elevational components for: (a) dots disappearing, and (b) dots remaining. Open symbols = actual heading; filled symbols = mean estimated heading. Circles and squares = headings of 10° and 5° respectively. Unconnected central squares = 0°.

The data summarised in Figures 6.1 and 6.2 show that for both conditions, there was a large bias to the screen centre.

Mean estimates for each of the 25 headings have been graphed together in Figure 6.3. These are constructed as for Experiment 1. Descriptive statistics for these graphs may be found in Appendix D. These figures show that a significant bias to centre occurred for all headings, and that there is not much difference between the two conditions. The greatest errors occurred for the 10° headings, but some error was also present for the 5° headings.

Regression analyses were carried out on the actual heading estimates for each condition and each dimension (azimuth and elevation) using only the zero condition of the other dimension. A linear fit was found to be significant in all ($p < .0001$) cases. The results are shown below in Table 6.3. Graphs of the dots remain condition are shown in Figures 6.4 and 6.5, these were chosen as there were no significant differences between the conditions as shown by the 95% confidence intervals in Table 6.3.

Table 6.3.

Linear regression statistics for estimated headings for azimuth and elevation for response screens with dots remaining or disappearing.

Condition	Slope	95% C.I.	Intercept	95% C.I.	R	p
Remain-Azimuth	0.466	0.408 to 0.524	-0.018	-0.427 to 0.391	0.634	<.0001
Disappear-Azimuth	0.396	0.340 to 0.452	0.432	0.037 to 0.827	0.585	<.0001
Remain-Elevation	0.358	0.300 to 0.416	-0.389	-0.800 to 0.022	0.531	<.0001
Disappear-Elevation	0.380	0.324 to 0.436	0.145	-0.252 to 0.542	0.568	<.0001

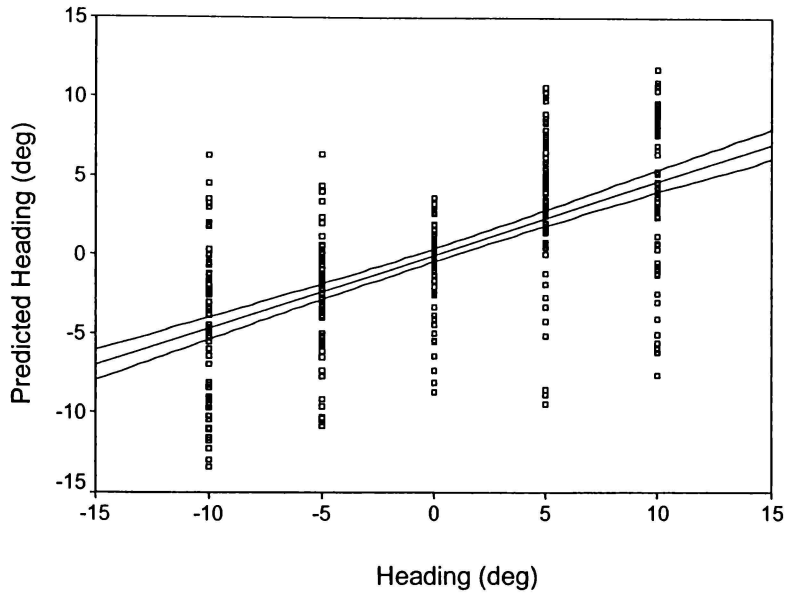

Figure 6.4. Scatterplot and regression line (± 95% C.I.) for the azimuthal component of heading estimates for the dots remaining condition.

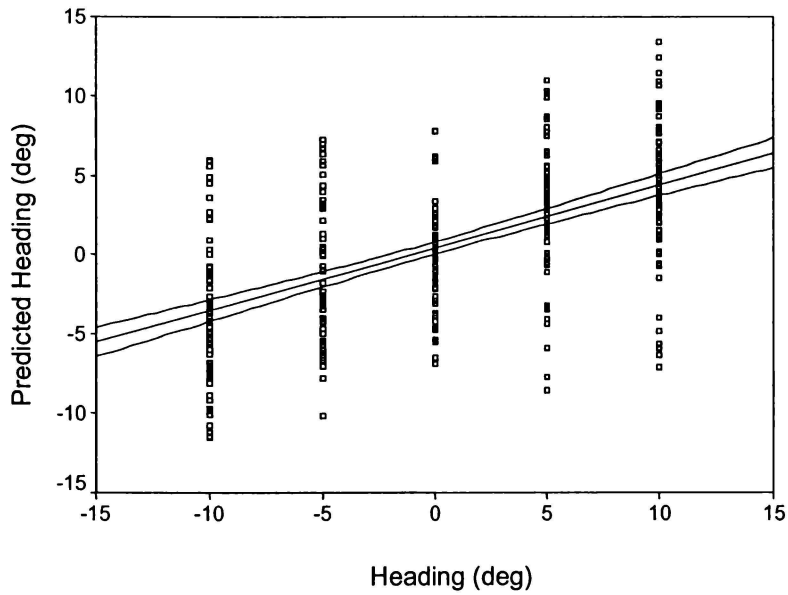

Figure 6.5. Scatterplot and regression line (± 95% C.I.) for the azimuthal component of heading estimates for the dots not remaining condition.

The p values for the slope reach significance for the regression meaning that the slope is greater than zero. However, the 95% confidence interval for the slopes do not include 1.0, therefore a significant bias to the screen centre occurred. For elevation, the dots remaining was not significantly different from having them disappear, although it does reach significance for azimuth (95% C.I.).

In order to test which of the experimental factors significantly affected estimates of heading, two two-way within-subjects analysis of variance were conducted to evaluate the effect of dots remaining and heading upon estimates of heading. Mean error was again used as the dependent variable. Separate analyses were carried out for azimuth and elevation, with the other dimension collapsed. The dependent variable was the heading error a continuous variable calculated as for Experiment1. The within subjects factors were dots remaining with two levels (remaining and not remaining), and heading with five headings (-10, -5, 0, +5, +10° of visual angle). Any violations of sphericity were corrected using Mauchly's Test of Sphericity.

For azimuth, there was a significant main effect for heading [$F(1.422, 19.912) = 14.237$, $p < .0001$, $\eta^2 = .504$]. There was no significant main effect for dots remaining [$F(1,14) = .262$, $p = .617$, $\eta^2 = .018$], and no significant interaction effect for dots remaining x heading [$F(2.056, 28.787) = .866$, $p = .434$, $\eta^2 = .058$].

For elevation, there was a significant main effect for heading [$F(2.057,28.804) = 25.039$, $p < .0001$, $\eta^2 = .641$]. There was no significant main effect for dots remaining [$F(1, 14) = .262$, $p = .617$, $\eta^2 = .018$], and no significant interaction effect for dots remaining x heading [$F(2.632, 36.846) = .737$, $p = .520$, $\eta^2 = .050$].

Discussion

Having the dots remain on the screen after each trial did not significantly improve estimates of heading, and our initial hypothesis is not supported. It is therefore unlikely that a distortion of perceived space due to a loss of reference frame is responsible for the central bias found in these experiments.

As in earlier experiments, one observer's responses were inverted relative to the actual heading direction. It appears that an inverted pattern of response is perfectly normal for a certain proportion of the population. The data for this individual were included in the overall data for this experiment.

CHAPTER 7

Experiment Six – Fixation Direction

Another unanswered question regarding bias in heading experiments concerns whether it is directed towards the center of the screen per-se, or whether it is towards the direction of fixation. W.H. Warren (1998) noted the general lack of research in this regard, and pointed out that in most cases the screen center and fixation direction are identical, which leads to a confounding of the two possibilities. These two factors need to be separated if the causes of bias in heading estimation are to be properly understood.

Only one experiment to date has directly examined the effect of fixation during a simulated heading task. Cutting, Vishton, Fluckiger, Baumberger & Gerndt (1997) used a pursuit task that required participants to fixate to the side while navigating through a cluttered naturalistic-style environment. These researchers found the best performance when looking directly ahead, and a general bias towards the direction of fixation.

If the bias is towards fixation rather than the screen centre, the retinal eccentricity of heading could play a part in heading bias. It is known that central and peripheral regions each have a role to play during visual navigation. When goggles are used to cover the peripheral visual field during a walking task, the decreased visual field causes performance disturbances, with more errors, and slower walking, while increases in peripheral vision leads to improved performance (Alfano & Michel, 1990). Various authors have examined the issue of which part of the visual field (if any) is the best suited to making judgments of heading. W.H. Warren and Kurtz (1992) compared the roles of central and peripheral vision during simple translation over a ground plane. They found that estimates were more accurate in central vision, and that errors increased with eccentricity. In addition Crowell and Banks (1993) found that human participants are more accurate with radial than lamellar

flow, regardless of part of retina stimulated, and that accuracy with radial flow increases near to the fovea. Atchley and Andersen (1999) examined whether the discrimination of heading from optical flow was retinally invariant. Their findings agree with those of W.H. Warren and Kurtz (1992), as heading sensitivity was again found to vary with retinal eccentricity, with more sensitivity in central than peripheral vision. The combined results of these experiments suggest that it is central rather than peripheral vision that is used to detect radial expansion, and that peripheral sensitivity is not as precise.

In this work, the possible effect of fixation is tested by using a variety of fixation directions with a grid of heading directions. It is expected that estimates will be more accurate when made close to fixation, and decrease in accuracy as eccentricity increases.

Method

Participants

Fifteen students from the University of Waikato, 10 female and 5 male, aged between 18 and 25 years, participated in this experiment. All were first year psychology students who received partial course credit for taking part. All participants had visual acuity of 20:25 or better. None had previously taken part in heading experiments.

Apparatus

The same apparatus is used in this experiment as was used in Experiment 1.

Procedure

The procedure is as for Experiment 1 with the following changes. Twenty-five heading directions were arranged as a grid pattern as in Experiment 2. This experiment used five different fixation points (central and 9° from the screen centre to the left, right, above and below) presented in random order. The flow stimuli remained the same as in previous experiments but instead of the observer fixating a cross only in the centre of the screen, their view direction was displaced towards the different fixation points. Therefore the heading direction (FOE) fell on different retinal locations relative to fixation. All trials for one fixation point were run before moving on to another fixation point. One hundred and twenty five trials were shown for each fixation, each took about 10 min to run, for a total session time of approximately 60 min.

Results

The results of the experiment are shown below in Figures 7.1 and 7.2, with the mean estimated heading plotted against the actual direction of heading for azimuth and elevation. For azimuth only the zero elevation trials have been used, and vice versa for elevation. Descriptive data for this experiment is shown in Tables 7.1 and 7.2, again with azimuth alone for central, left and right fixations, and elevation alone for central, upwards and downwards fixations.

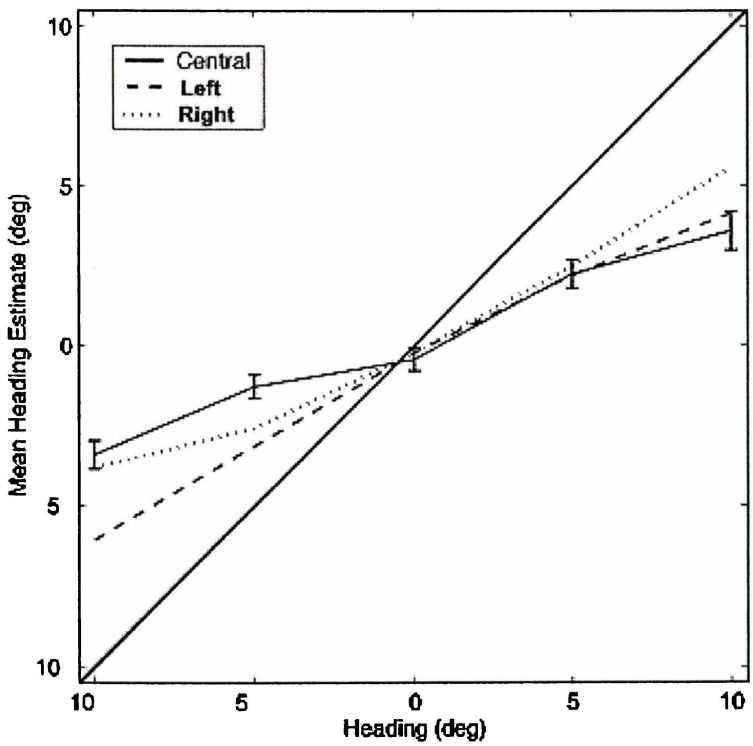

Figure 7.1. Mean heading estimates for azimuth as a function of heading direction for three fixation directions: central, left and right, ±2 SE for central fixation. Veridical performance is shown by the 45° line.

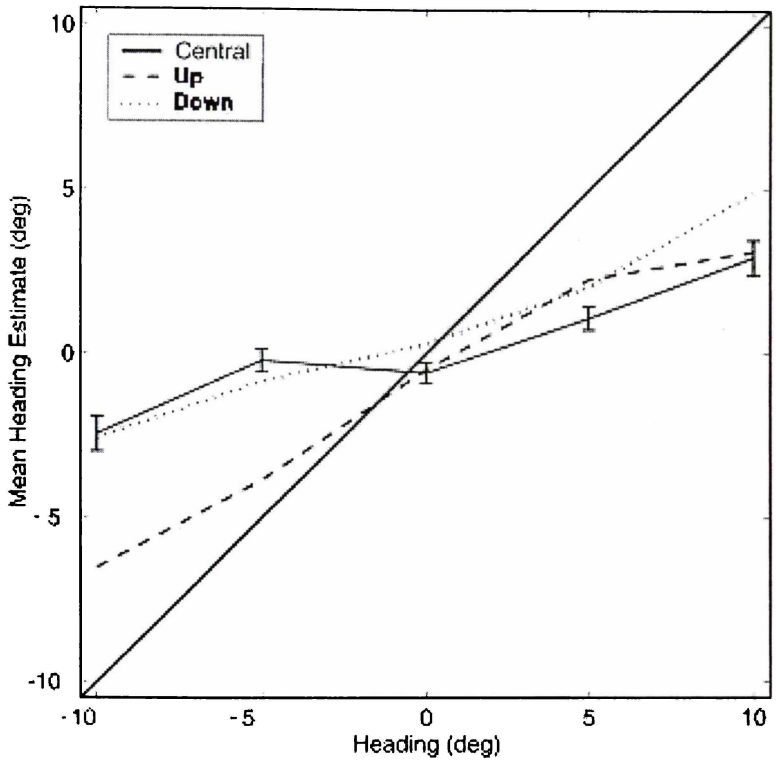

Figure 7.2. Mean heading estimates for elevation as a function of heading direction for three fixation directions: central, up and down, ±2 SE for central fixation. Veridical performance is shown by the 45° line.

The data summarised in Figures 7.1 and 7.2 show that for both azimuth and elevation there was a bias to the screen centre, with the central fixation condition leading to the greatest amount of bias overall, as is shown by the flatter slope of the line compared to the other conditions. There does appear to have been some increase in accuracy for heading estimation for those directions closest to a given fixation point, (as shown by a steeper curve at that point), but this was insufficient to overcome the overall central bias, and even estimates for those heading directions outside of the fixation point are biased so far towards the centre of the screen that they lie to the inside of the fixation point. For all fixation points the standard errors for the mean estimates are quite small, at around 2° to 3° showing the responses to have been reasonably consistent across participants and trials.

Table 7.1

Mean heading estimates, mean bias, and standard deviations for central, left and right fixation directions – azimuth only, N=75

Condition	Heading	Mean	Mean Bias	Std. Dev. of Mean
Central	-10	-3.42	-6.58	3.81
	-5	-1.28	-3.72	3.26
	0	-0.43	-0.43	3.11
	5	2.24	-2.76	3.84
	10	3.58	-6.42	5.24
Left	-10	-6.07	-3.93	5.72
	-5	-3.14	-1.86	4.73
	0	-0.23	-0.23	4.17
	5	2.19	-2.81	4.73
	10	4.14	-5.86	5.73
Right	-10	-3.82	-6.18	5.45
	-5	-2.59	-2.41	4.19
	0	-0.22	-0.22	3.39
	5	2.48	-2.52	4.21
	10	5.59	-4.41	6.21

Table 7.2

Mean heading estimates, mean bias, and standard deviations for central, upward and downward fixation directions – elevation only, N=75

Condition	Heading	Mean	Mean Bias	Std. Dev. of Mean
Central	-10	-2.44	-7.56	4.66
	-5	-0.21	-4.79	2.98
	0	-0.58	-0.58	2.74
	5	1.08	-3.92	3.06
	10	2.93	-7.07	4.68
Left	-10	-6.52	-3.48	6.05
	-5	-3.84	-1.16	3.66
	0	-0.48	-0.48	4.60
	5	2.26	-2.74	5.46
	10	3.12	-6.88	5.92
Right	-10	-2.57	-7.43	5.39
	-5	-0.84	-4.16	4.47
	0	0.31	-0.31	4.42
	5	2.03	-2.97	4.83
	10	4.92	-5.03	6.50

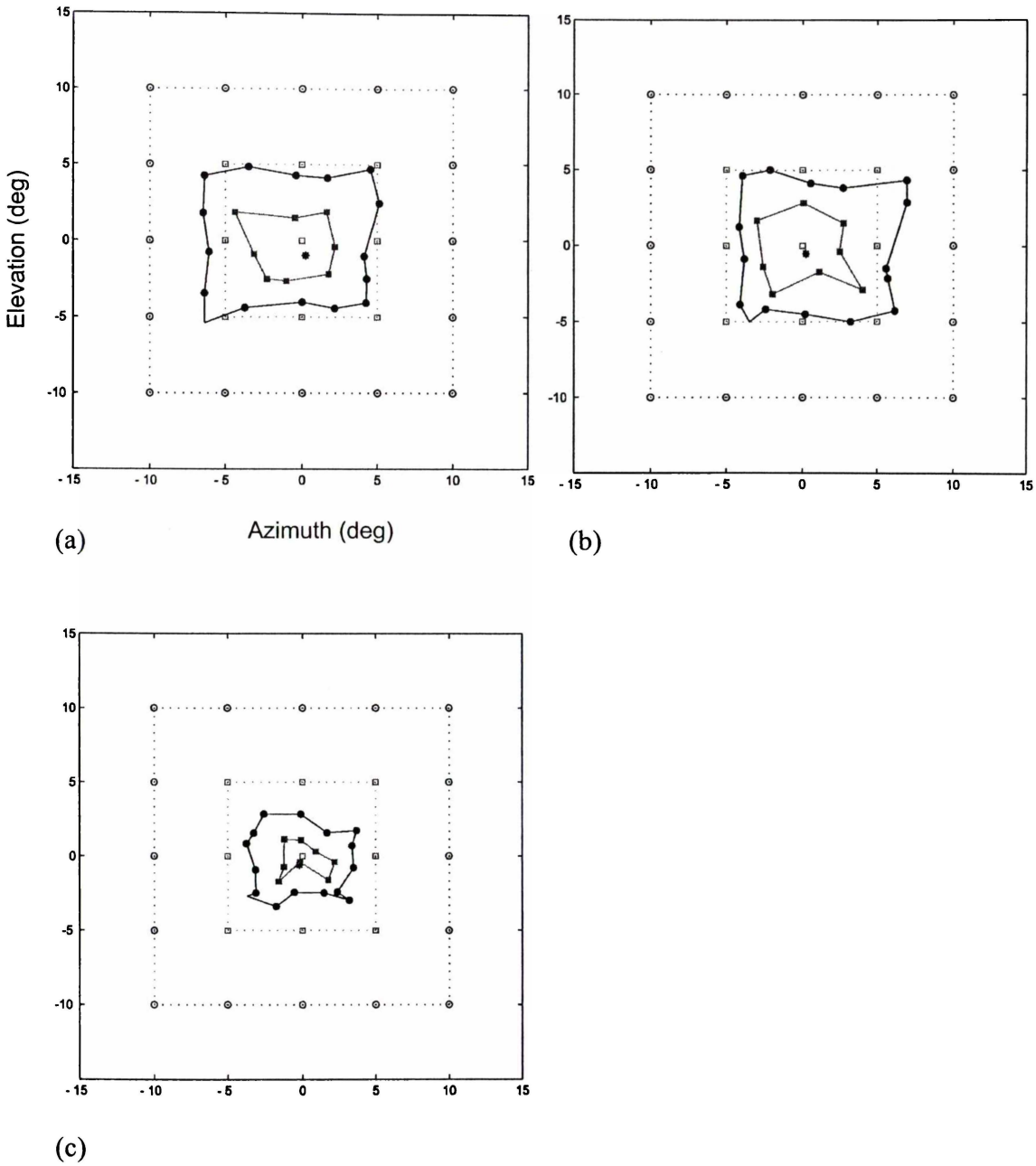

Figure 7.3. Mean estimates of heading showing azimuthal and elevational components for: (a) left fixation (b) right fixation and (c) central fixation. Open symbols = actual heading; filled symbols = mean estimated heading. Circles and squares = headings of 10° and 5° respectively. Unconnected central squares = 0°.

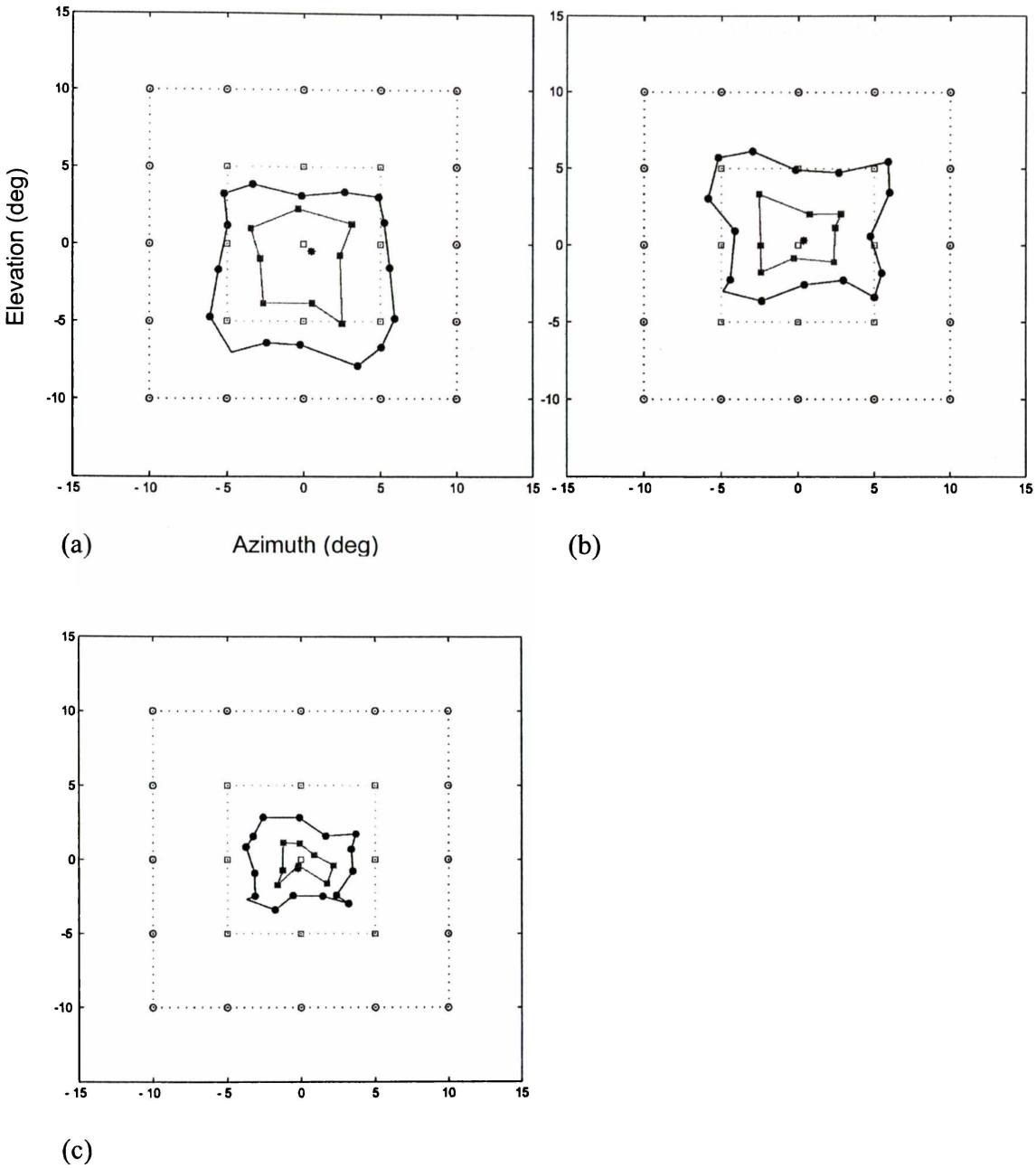

Figure 7.4. Mean estimates of heading showing azimuthal and elevational components for: (a) down fixation (b) up fixation and (c) central fixation. Open symbols = actual heading; filled symbols = mean estimated heading. Circles and squares = headings of 10° and 5° respectively. Unconnected central squares = 0°.

In order to examine the effect of fixation, mean estimates for each of the 25 headings for fixation directions in the azimuthal and elevational directions have been graphed in Figure 7.3 and 7.4. These are constructed as for Experiment 1. Descriptive statistics for these graphs may be found in Appendix E. Figures 7.3 and 7.4 show that a bias to centre occurred for all fixations, but that this bias appears to be strongest for the central fixation. For all fixations the greatest errors occurred for the 10° headings, but some error was also present at 5°.

In order to characterise the trends in the data across the different conditions, regression analyses were carried out on the actual heading estimates as in earlier experiments. A linear fit was found to be significant for all ($p < .0001$), and therefore linear regression was used for all conditions.

The full details of the regression equations for azimuth and elevation respectively are shown in Tables 7.3 and 7.4, while the scatter-plots for the central-azimuth and right-azimuth conditions are shown in Figures 7.4 and 7.5. These graphs have been chosen because all other fixations do not differ significantly from them.

Table 7.3

Linear regression statistics for estimated headings for azimuth for left, right and central fixation directions.

Condition	Slope	95% C.I.	Intercept	95% C.I.	R	p
Left	0.515	0.443 to 0.587	-0.531	-1.041 to -0.021	0.535	<.0001
Right	0.478	0.409 to 0.546	0.375	-0.109 to 0.859	0.556	<.0001
Centre	0.342	0.285 to 0.400	0.201	-0.205 to 0.607	0.532	<.0001

Table 7.4.

Linear regression statistics for estimated headings for elevation for upwards, downwards and central fixation directions.

Condition	Slope	95% C.I.	Intercept	95% C.I.	R	p
Up	0.357	0.283 to 0.431	0.769	0.245 to 1.293	0.440	<.0001
Down	0.507	0.432 to 0.582	-1.093	-1.623 to -0.563	0.567	<.0001
Centre	0.241	0.187 to 0.295	0.157	-0.223 to 0.537	0.414	<.0001

The p values for the slopes reach significance for all conditions, but the 95% confidence interval for the slopes do not include 1.0, indicating that a significant bias to centre occurred. The 95%C.I.s show that for azimuth, the central fixation condition was significantly different to the right and left conditions, however these did not differ from one another. For elevation, up and central were both different from down (only just in the case of up and down), but not to each other. That is, there appears to be a difference in the coding of heading direction across the visual field.

The scatter for these graphs is large as they contain many estimates, but the 95% confidence intervals are small showing that estimates were reasonably consistent.

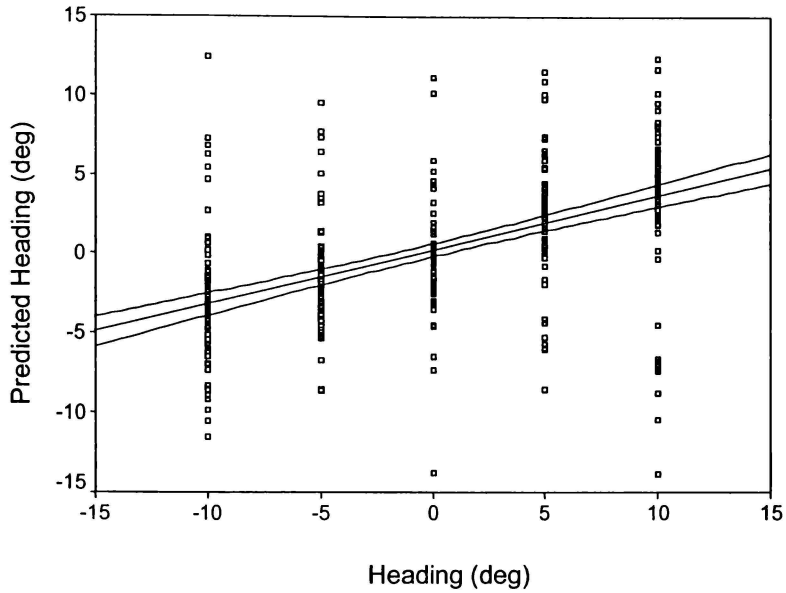

Figure 7.5. Scatterplot and regression line (± 95% C.I.) for the azimuthal component of heading estimates for the central fixation condition.

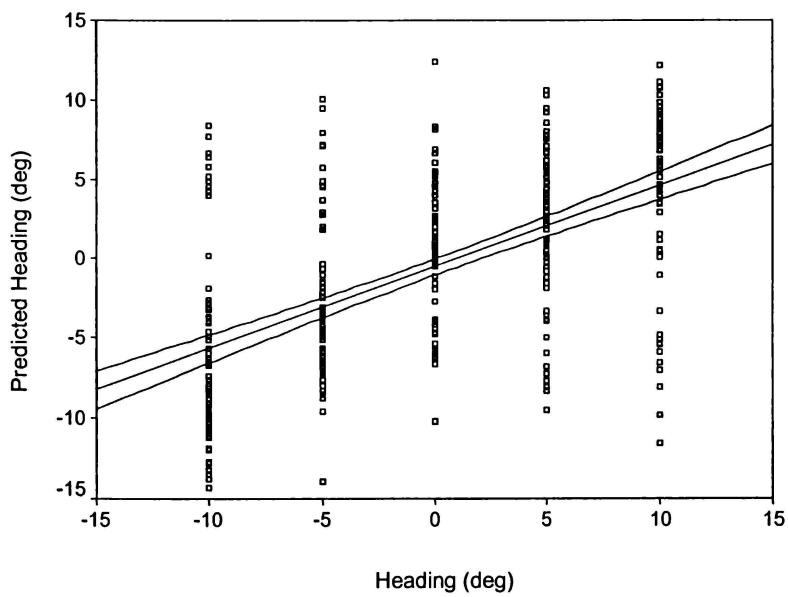

Figure 7.6. Scatterplot and regression line (± 95% C.I.) for the azimuthal component of heading estimates for the right fixation condition.

In order to further examine the impact of fixation direction upon the perceived heading, two two-way within-subjects analysis of variance were conducted to evaluate the effects of fixation and heading upon estimates of heading. Mean error was used as the dependent variable. Separate analyses were carried out for azimuth and elevation, with data for the opposite dimension collapsed. The dependent variable was the heading error a continuous variable calculated as for Experiment 1. The within subjects factors were fixation with three levels (either left, central and right, or up, central and down), and heading with five headings (-10, -5, 0, 5, 10° of visual angle). Any violations of sphericity were corrected using Mauchly's Test of Sphericity.

For azimuth, there were significant main effects for fixation [$F(1.37,19.181) = 4.079$, $p = .047$, $\eta^2 = .226$] and for heading [$F(1.028, 14.398) = 23.422$, $p < .0001$, $\eta^2 = .626$]. There was also a significant interaction effect for fixation x heading [$F(2.552, 35.732) = 4.008$, $p = .028$, $\eta^2 = .307$].

For elevation, there were significant main effects for fixation [$F(1.345,18.836) = 8.660$, $p = .005$, $\eta^2 = .382$] and for heading [$F(1.040, 14.567) = 36.514$, $p < .0001$, $\eta^2 = .723$]. There was also a significant interaction effect for fixation x heading [$F(2.634,36.876) = 7.174$, $p = .001$, $\eta^2 = .339$].

Discussion

The results of this experiment are somewhat equivocal, as they do not fully support the hypothesis that the direction of bias is towards fixation. When observers fixated a point lying 9° from the centre, headings lying to the outside of the fixation point were still reported as occurring to the inside of fixation, towards the centre of the screen. Thus it appears as though the main direction of the bias is towards screen centre.

However, heading estimates were found to be the most accurate when made close to fixation, regardless of its location, and accuracy decreased with increases in eccentricity from fixation. This finding is in agreement with the results of W.H. Warren and Kurtz (1992), Crowell and Banks (1993), and Atchley and Andersen (1999). Interestingly, with a non-central fixation, even when the offset of the heading direction from the fixation-point was at its most extreme, the amount of bias was no greater than that for a central fixation (see Figs 7.3 and 7.4). That is, a central fixation point appears to be the least efficient for the estimation of heading across the entire visual field, while a non-central fixation point improves estimates in the direction of fixation. Figures 7.1 and 7.2 shows this trend in more detail. This was a somewhat unexpected result in light of the findings of Cutting, Vishton, Fluckiger, Baumberger and Gerndt (1997) who found the best heading estimation performance occurred when observers were looking straight ahead. It is not immediately apparent how to explain the difference between these two sets of results, and further research into this area is needed.

Another interesting result in this experiment relates to the difference between azimuth and elevation revealed in the regression analysis. For azimuth, the centre fixation position led to the most error overall, while the left and right fixation positions showed no significant difference to one another. However for elevation, the centre and upwards

fixation positions led to more bias than did the downwards fixation. That is, there appears to be a difference in the way heading information is dealt with in the upper and lower visual fields, but no difference between the left and right, with a downward fixation direction being the most useful for estimates of elevation. This result supports that of Kersten and D'Avossa, (1999) who also found that for estimates of elevation, the variance was smaller in the lower visual field, while estimates of azimuth showed less variance in the upper visual field.

Overall the results of this experiment do not support the idea that heading is biased towards fixation. Instead the bias appears to be directed towards screen centre.

CHAPTER 8

Experiment Seven – Head Direction

Although Experiment 6 (Chapter 7) showed that the direction of bias was not towards the direction of fixation, there is also a possibility that the bias may not be towards the centre of the screen per-se, but rather towards the centre of the body's reference co-ordinate system as participants sit facing the screen.

Only a small body of research has been directed at finding the relative contributions of the different coordinate systems in heading, and all of these have involved active observer motion of some form. Telford and Howard (1996) looked at the role of optical flow field asymmetry in heading. They used a passive trolley task in which participants were propelled down a corridor and were required to point in the perceived direction of motion. They found that when observers were allowed to move their heads to look in the direction of self-motion, heading was accurately estimated. However, when heads were constrained so that the median plane of the head was oriented perpendicular to the direction of heading, a large underestimation of heading occurred in the absence of visual cues, while overestimation occurred when they were present. Later, Crowell, Banks, Shenoy, and Andersen (1997) examined heading perception during active head turns. They found that heading perception is mediated by information from the ears, neck, and an efference copy of the motor command to turn the neck.

In this experiment the aim was to examine whether the orientation of the head can have an impact on the heading estimates. This was tested by using two different head directions: straight ahead, and at 15° to the body orientation.

Method

Participants

Fifteen students from the University of Waikato, 6 female and 4 male, aged between 17 and 24 years, participated in this experiment. All were first year psychology students who received partial course credit for taking part. All participants had visual acuity of 20:25 or better. None had previously taken part in heading experiments.

Apparatus

The apparatus used was the same as that for Experiment 1.

Procedure

The procedure was as for Experiment 1, with the following changes. Two experimental conditions were run. In one, the participant viewed the screen as for previous experiments. In the second, the screen was rotated so that the normal from the screen to the neck position was oriented 15° to the right of the medial plane of the viewer's body and the eye looked straight ahead, while the body remained facing forwards. Eleven heading directions (-15, -12, -9, -6, -3, 0, 3, 6, 9, 12, 15°) were shown for each condition with 10 repeats of each. Each condition took about 10 min to run, for a total session time of approximately 30 min.

Results

The results of the experiment are shown below in Figure 8.1, with the mean estimated heading plotted against the actual direction of heading. Descriptive statistics are given in Table 8.1.

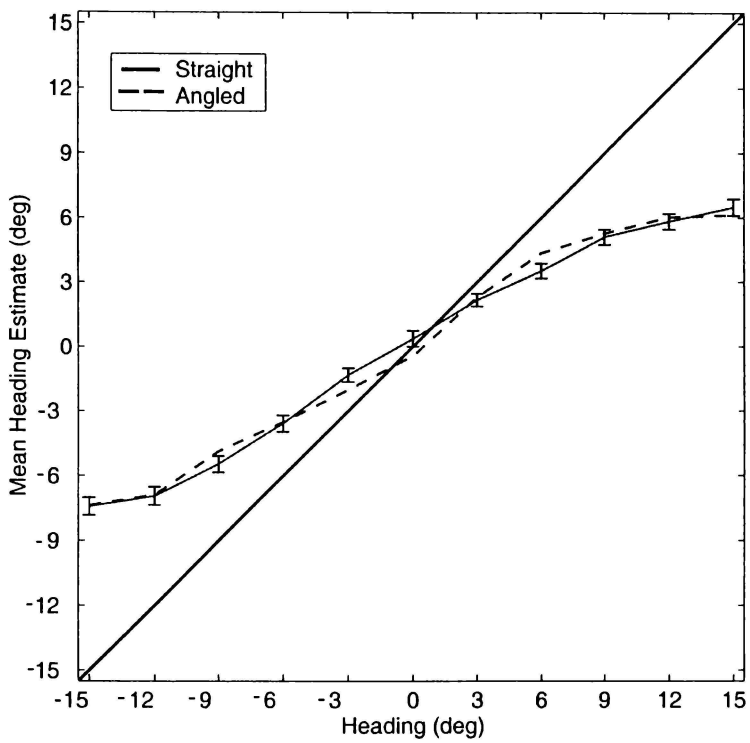

Figure 8.1. Mean heading estimates as a function of heading direction for head straight ahead and head angled test conditions ±2 SE for head straight condition. Veridical performance is shown by the 45° line.

The data summarised in Figure 8.1 shows that for both conditions, there was once again a large bias to the screen centre. The standard errors for the mean estimates are quite small, at around 2 to 3°, showing the responses to have been reasonably consistent across participants and trials. These figures show that a significant bias to centre occurred for all headings, and that estimates were very consistent.

Table 8.1

Mean heading estimates, mean bias, and standard deviations for head straight and head angled viewing conditions, N=150

Condition	Heading	Mean	Mean Bias	Std. Dev of Mean
Straight	-15	-7.42	-7.58	5.00
	-12	-6.94	-5.06	5.03
	-9	-5.46	-3.54	4.76
	-6	-3.57	-2.43	4.65
	-3	-1.33	-1.67	3.94
	0	0.37	-0.37	4.60
	3	2.17	-0.83	3.62
	6	3.53	-2.47	4.25
	9	5.11	-3.89	4.35
	12	5.84	-6.16	4.50
	15	6.50	-8.50	4.71
Angled	-15	-7.37	-7.63	4.89
	-12	-6.88	-5.12	4.72
	-9	-4.87	-4.13	4.62
	-6	-3.51	-2.49	4.38
	-3	-2.02	-0.98	4.38
	0	-0.43	-0.43	4.17
	3	2.30	-0.70	3.01
	6	4.36	-1.64	4.77
	9	5.27	-3.73	4.07
	12	6.04	-5.96	4.28
	15	6.13	-8.87	4.53

Regression analyses were then carried out on the actual heading estimates for each condition. Curve fitting showed that linear regression was appropriate for both conditions, ($p < .0001$). The results are shown below in Table 8.2, and a graph of the straight condition is shown in Figure 8.2. Only this condition is shown as there was no significant difference between the conditions as shown by the 95% confidence intervals in Table 8.2.

The p values for the slopes reach significance, showing them to be greater than zero. However, the 95% confidence intervals do not include 1.0, therefore a significant bias towards the centre of the screen occurred. The 95% confidence intervals also show that the two conditions were not significantly different from one another.

Table 8.2.

Linear regression statistics for estimated headings for head turned and head straight test conditions.

Condition	Slope	95% C.I.	Intercept	95% C.I.	R^2	p
Turned	0.514	0.492 to 0.537	-0.087	-0.301 to 0.126	0.742	<.0001
Straight	0.516	0.492 to 0.539	0.111	-0.330 to 0.108	0.733	<.0001

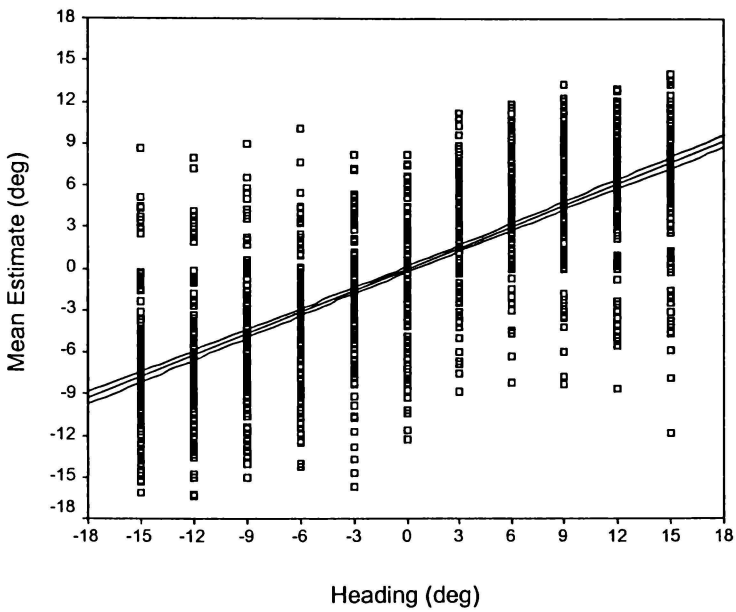

Figure 8.2. Scatterplot and regression line (± 95% C.I.) for heading estimates for the head turned condition.

In order to test which of the experimental factors significantly affected estimates of heading, two two-way within-subjects analysis of variance were conducted to evaluate the effect of head direction upon estimates of heading. The dependent variable was the mean heading estimate. The within subjects factors were head direction with two levels (turned and not), and heading with eleven headings (-15, -12, -9, -6, -3, 0, 3, 6, 9, 12, 15° of visual angle). Any violations of sphericity were corrected using Mauchly's Test of Sphericity.

There was a significant main effect for heading [$F(10, 140) = 33.367$, $p < .0001$, $\eta^2 = .704$]. There was no effect for head direction [$F(1,14) = .015$, $p = .904$, $\eta^2 = .001$], and no significant interaction effect for head direction x heading [$F(10, 140) = 1.460$, $p = .203$, $\eta^2 = .094$].

Discussion

The hypothesis that the orientation of the head would affect the accuracy of estimates of heading was not supported by the results of this experiment. For both conditions there was a considerable bias towards the centre of the screen.

The heading bias found in the experiments completed so far in this thesis has been directed towards the centre of the screen, rather than towards fixation, or the centre of a head- or body-based coordinate system. This finding has interesting implications for heading research in that it suggests that such bias is a direct consequence of the visual scene itself. An examination of the contribution of various scene parameters to heading estimates is therefore required.

CHAPTER 9

Experiment Eight – Number of Dots

Experiments 5, 6 and 7 examined the possibility of bias being caused by an error in perceived space, by having dots remain on-screen, by varying fixation direction and by the manipulating the angle between the observer's head and the screen. None of these factors was found to have a significant impact, and consequently it seems increasingly likely that it is some factor or factors relating to the flow field that are responsible.

One such factor is the possible influence of the number of dots present in the field of view. In the previous experiments reported in this thesis, the number of dots used in the simulated observer motion stimuli has been close to the average used in typical heading experiments. However it is possible that because of the particular display parameters being used, this number of dots may not be sufficient for good heading performance and the bias may be arising from this source.

The question of whether the number of dots affects estimates of heading has been reasonably well researched in the general field of heading estimation, and it is generally agreed that increasing dot number leads to improved estimates of heading, although heading can be estimated with reasonable accuracy even with low densities.

W.H. Warren, Morris, and Kalish (1988) used forward translation with a ground plane display and found heading estimation thresholds of around 1.2°, and with high dot numbers and speed they obtained thresholds to within 0.66°. They found that performance remained high with displays of 10 -63 dots, but dropped significantly when only 2 dots were present in the display. As the number of dots increased from 2 to 63, performance improved linearly, thresholds being above 3° with only 2 dots, better than 2° with 3 dots

and appearing to asymptote at around 0.5° with 30 dots. According to the authors, the visual field exhibits a redundancy gain with the addition of more dots to the display. Two non-collinear motion vectors are theoretically sufficient to determine translational heading, for the lines they define in the projection plane intersect at the FOE. There is therefore a great deal of redundancy in the visual field in theory, because each pair of vectors provides an independent estimate of the location of the focus of expansion, and constrains the solution more.

W.H. Warren, Mestre, Blackwell, and Morris (1991) examined heading on a curved path, and found thresholds better than 1.5° with ground, wall, and cloud displays, down to 2 dots. As the number of dots increased, performance improved linearly with square root of N dots (r =.97). This finding was supported by Andersen and Saidpour (2002), who also found that for movement through a 3-D cloud of objects, performance improved when the number of objects was increased.

The influence of the number of dots will be tested in the present work by using a range of dot numbers in a standard heading experiment. Because W.H. Warren, Morris, and Kalish (1988) found that the speed of observer translation was an important factor for reducing heading thresholds, and it because is possible that observer translation speed interacts with the number of dots, two observer speeds will also be used in this experiment.

Method

Participants

Ten students from the University of Waikato, 6 female and 4 male, aged between 18 and 25 years, participated in this experiment. All were first year psychology students who received partial course credit for taking part. All participants had visual acuity of 20:25 or better. None had previously participated in a heading experiment.

Apparatus

The apparatus for this experiment was the same as that for Experiment 1.

Procedure

The procedure was the same as that for Experiment 1, with the following changes. Four experimental conditions were run, crossing two simulated observer speeds (2 $m.s^{-1}$ and 4 $m.s^{-1}$) with four dot numbers (50, 100, 200 and 500 dots). These dot numbers gave a density of 0.42, 0.84, 1.68, 4.2 $dots/deg^2$respectively. Each heading was presented five times during an experimental condition, giving a total of 55 trials per condition. Each condition took about 5 min to run, for a total session time of approximately 50 min.

Results

The results of the experiment are shown below in Figures 9.1 and 9.2, with the mean estimated heading plotted against the actual direction of heading for both 2 $m.s^{-1}$ and 4 $m.s^{-1}$ translation speeds. Descriptive statistics for the data are shown in Tables 9.1 and 9.2.

The data summarised in Figures 9.1 and 9.2 shows that for both speeds and all dot numbers, there was still bias to the centre. The faster speed of translation led to more accurate estimates overall.

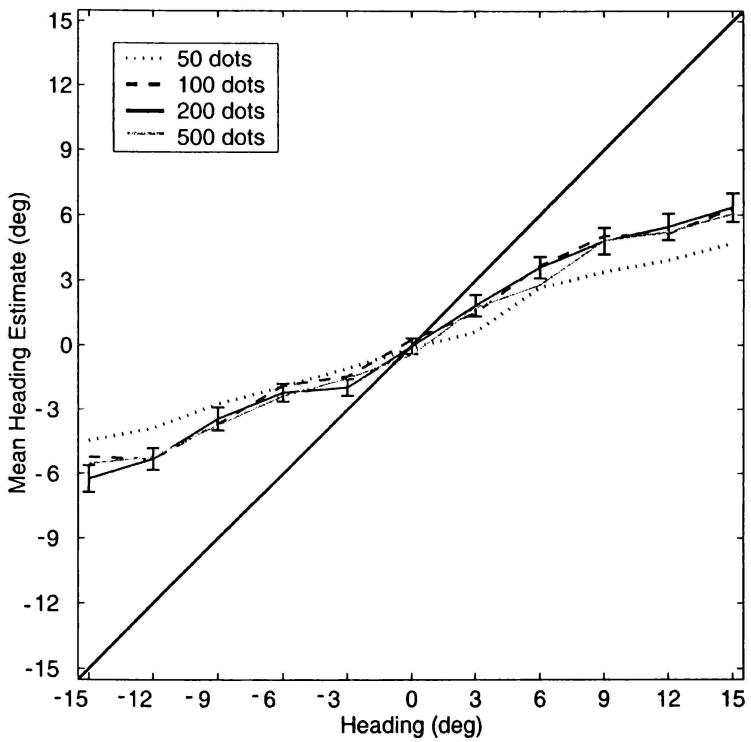

Figure 9.1. Mean heading estimates as a function of heading direction for different dot numbers with a translation speed of 2 $m.s^{-1}$, ±2 SE for 200 dot condition. Veridical performance is shown by the 45° line.

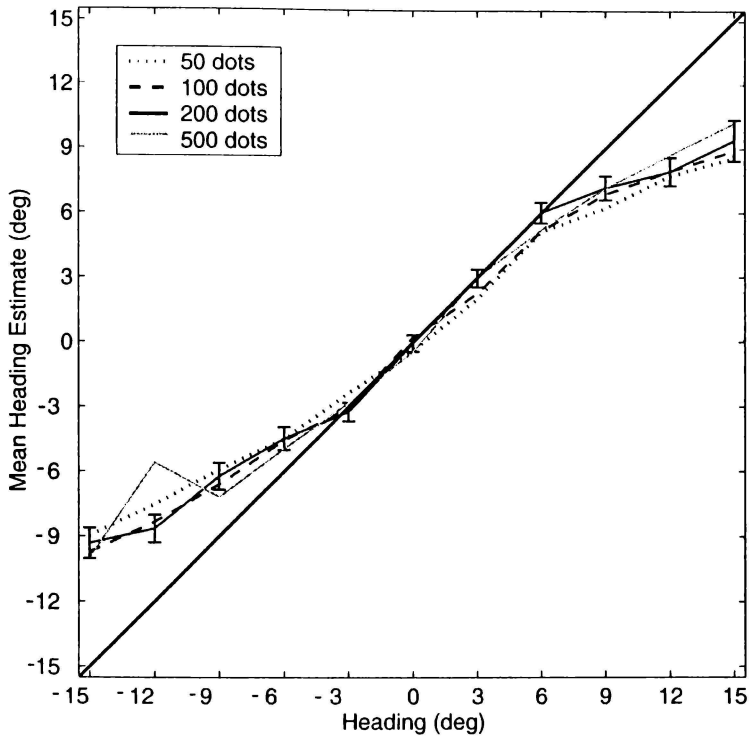

Figure 9.2. Mean heading estimates as a function of heading direction for different dot numbers with a translation speed of 4 $m.s^{-1}$, ±2 SE for 200 dot condition. Veridical performance is shown by the 45° line.

Table 9.1.

Mean heading estimates, mean bias, and standard deviations for dot number at 2 $m.s^{-1}$, N=50

Condition	Heading	Mean	Mean Bias	Std. Dev. of Mean
50 dots	-15	-4.46	-10.54	4.00
	-12	-3.87	-8.13	4.48
	-9	-2.74	-6.23	3.63
	-6	-1.92	-4.08	3.30
	-3	-1.08	-1.92	3.12
	0	-0.14	-0.14	3.14
	3	0.62	-2.38	3.10
	6	2.66	-3.34	3.81
	9	3.39	-5.51	4.22
	12	3.92	-8.08	4.13
	15	4.71	-10.29	4.66
100 dots	-15	-5.22	-9.78	4.76
	-12	-5.31	-6.69	4.37
	-9	-3.69	-5.31	4.35
	-6	-1.87	-4.13	3.70
	-3	-1.45	-1.55	3.43
	0	0.27	-0.27	3.00
	3	1.50	-1.50	3.73
	6	3.68	-2.32	3.52
	9	5.04	-3.96	4.57
	12	5.15	-6.85	4.76
	15	6.30	-8.70	5.17
200 dots	-15	-6.24	-8.76	4.42
	-12	-5.32	-6.48	3.59
	-9	-3.44	-5.56	3.78
	-6	-2.21	-3.79	2.96
	-3	-1.97	-1.03	2.71
	0	-0.04	-0.04	2.61
	3	1.84	-1.16	2.49
	6	3.59	-2.41	3.47
	9	4.81	-4.19	4.32
	12	5.46	-6.54	4.30
	15	6.35	-8.65	4.64
500 dots	-15	-5.53	-9.47	4.42
	-12	-5.23	-6.77	4.43
	-9	-3.74	-5.26	4.20
	-6	-2.37	-3.63	3.65
	-3	-1.54	-1.46	3.27
	0	-0.44	-0.44	2.54
	3	1.74	-1.26	3.41
	6	2.79	-3.21	3.75
	9	4.83	-5.17	4.39
	12	5.22	-6.78	4.57
	15	6.05	-8.95	4.84

Table 9.2.

Mean heading estimates, mean bias, and standard deviations for dot number at 4 m.s^{-1}, N=50

Condition	Heading	Mean	Mean Bias	Std. Dev. of Mean
50 dots	-15	-8.96	-6.04	4.73
	-12	-7.52	-4.48	4.42
	-9	-5.91	-3.09	3.96
	-6	-4.50	-1.50	3.53
	-3	-2.37	-0.63	3.24
	0	-0.39	-0.39	3.06
	3	2.02	-0.98	3.71
	6	5.13	-0.87	3.57
	9	6.24	-2.76	4.44
	12	7.74	-4.26	4.54
	15	8.58	-6.42	5.05
100 dots	-15	-9.73	-5.27	4.92
	-12	-8.34	-3.66	4.72
	-9	-6.60	-2.40	4.05
	-6	-4.57	-1.43	3.05
	-3	-3.07	0.07	3.39
	0	0.23	0.23	2.63
	3	2.27	-0.73	7.95
	6	5.16	-0.84	4.01
	9	6.88	-2.12	4.10
	12	7.96	-4.04	4.31
	15	8.92	-6.08	4.96
200 dots	-15	-9.32	-5.68	4.99
	-12	-8.65	-3.35	4.52
	-9	-6.23	-2.77	4.39
	-6	-4.48	-1.52	3.75
	-3	-3.24	0.23	3.03
	0	-0.05	-0.05	2.74
	3	2.98	-0.02	2.92
	6	6.03	0.03	3.43
	9	7.18	-1.82	3.96
	12	7.94	-4.06	4.63
	15	9.40	-5.60	6.73
500 dots	-15	-10.00	-5.00	5.32
	-12	-5.59	-6.41	5.04
	-9	-7.19	-1.81	4.35
	-6	-4.96	-1.04	3.86
	-3	-2.83	-0.17	3.61
	0	-0.44	-0.44	3.19
	3	3.02	0.02	3.21
	6	5.23	-0.77	4.01
	9	7.16	-1.84	4.56
	12	8.71	-3.29	4.83
	15	10.21	-4.79	6.53

In order to characterise the trends in the data across the different conditions, regression analyses were carried out on the actual heading estimates. Prior to carrying out the regression, curve fitting was done to ensure that linear regression was appropriate. A linear fit was found to be significant for all outcomes ($p < .0001$).

The full details of the regression equations for 2 $m.s^{-1}$ and 4 $m.s^{-1}$ conditions respectively are shown below in Table 9.3 and 9.4, while the scatter-plots for the 2 $m.s^{-1}$, 50 and 100 dot conditions are shown in Figures 9.3 and 9.4. These graphs have been selected because the 50-dot condition is different from all others at 2 $m.s^{-1}$, as well as being different from the 500-dot condition at 4 $m.s^{-1}$.

Table 9.3

Linear regression statistics for estimated headings for different dot numbers with a translation speed of 2 $m.s^{-1}$

Condition	Slope	95% C.I.	Intercept	95% C.I.	R	p
50 dots	0.322	0.298 to 0.346	0.100	-0.125 to 0.326	0.625	<.0001
100 dots	0.423	0.397 to 0.449	0.399	0.151 to 0.647	0.692	<.0001
200 dots	0.426	0.396 to 0.455	0.119	-0.129 to 0.368	0.652	<.0001
500 dots	0.384	0.354 to 0.415	0.194	-0.064 to 0.451	0.600	<.0001

Table 9.4

Linear regression statistics for estimated headings for different dot numbers with a translation speed of 4 $m.s^{-1}$

Condition	Slope	95% C.I.	Intercept	95% C.I.	R	p
50 dots	0.633	0.607 to 0.658	0.004	-0.239 to 0.247	0.826	<.0001
100 dots	0.678	0.649 to 0.706	-0.07	-0.344 to 0.201	0.814	<.0001
200 dots	0.683	0.657 to 0.709	0.104	-0.142 to 0.350	0.842	<.0001
500 dots	0.732	0.704 to 0.759	-0.09	-0.358 to 0.162	0.845	<.0001

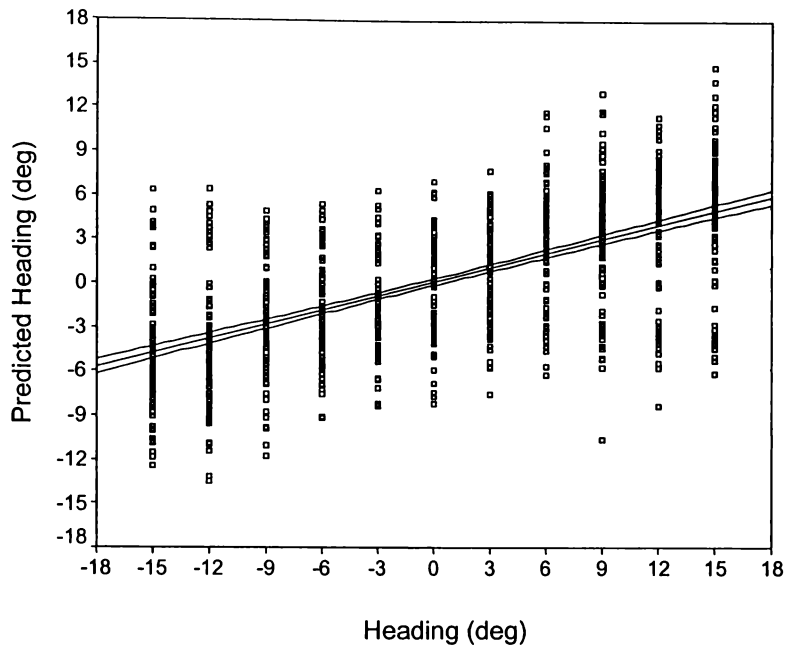

Figure 9.3. Scatterplot and regression line (± 95% C.I.) for heading estimates for the 200 dots - 2 $m.s^{-1}$ condition.

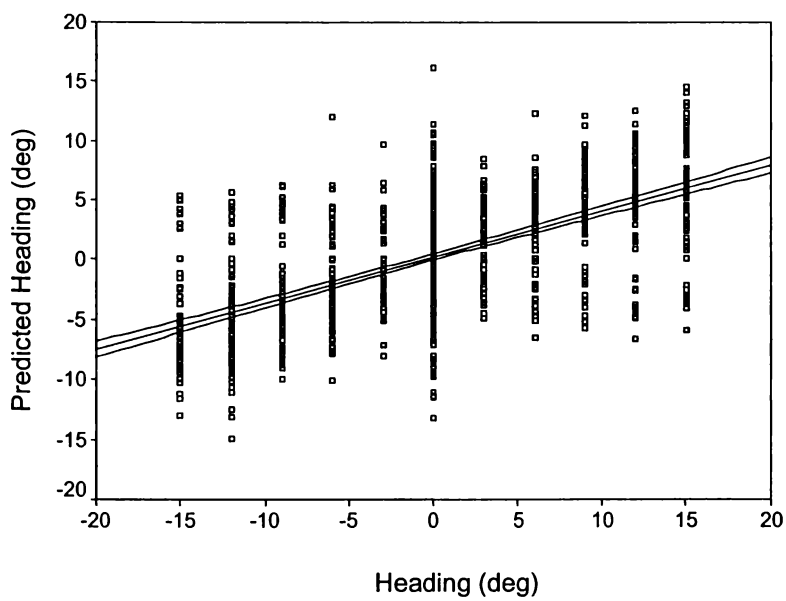

Figure 9.4. Scatterplot and regression line (± 95% C.I.) for heading estimates for the 500 dots - 2 $m.s^{-1}$ condition

Heading estimates made for the 50-dot condition are significantly different to the other conditions, and the 100 and 200 dot conditions were different to the 500 dot condition at 2 $m.s^{-1}$. At the higher speed of 4 $m.s^{-1}$ only heading estimates for the 50-dot condition differed significantly from the other dot conditions. The heading estimates made in the lower speed conditions are all significantly different from those made in the higher speed conditions.

A three-way within-subjects analysis of variance was conducted to evaluate the effect of depth, dot number, and heading upon estimates of heading. The dependent variable was the mean heading estimate. The within subjects factors were speed with 2 levels (2 $m.s^{-1}$ and 4 $m.s^{-1}$), dot number with 4 levels (50, 100, 200 and 500) and heading with 11 levels (-15, -12, -9, -6, -3, 0, 3, 6, 9, 12, 15° of visual angle). Any violations of sphericity were corrected using Mauchly's Test of Sphericity.

There was a significant main effect for speed [$F(1, 9) = 7.945$. $p = .02$, partial $\eta^2 = .771$] and heading [$F(1.065, 9.589) = 18.338$ $p = .002$, partial $\eta^2 = .671$]. Significant interaction effects were found for speed x heading [$F(2.090, 9)) = 24.484$. $p = .0001$, partial $\eta^2 = .731$] and also for dot number x heading [$F(9.141, 9) = 3.564$. $p = .001$, partial $\eta^2 = .284$].

However there was no significant main effect for dot number [$F(1.474,13.263) = 0.347$. $p = .649$ partial $\eta^2 = .037$], and no significant interactions were found for speed x dot number [$F(5.527, 49.739) = .792$. $p = .506$, partial $\eta^2 = .081$] or for the three way interaction between speed, heading and dot number [$F(1.492, 49.859) = 1.408$. $p = .234$, partial $\eta^2 = .135$].

Discussion

The results of this experiment support the initial hypothesis that the number of dots can have an effect upon estimates of heading, with 50 dots leading to a significant increase in heading bias for both speeds. Dot number was found to have a significant interaction effect with heading, and an examination of Figures 9.1 and 9.2 show that as eccentricity increases the benefit of having an increased numbers of dots also increases to a certain extent.

Translation speed was also found to have a significant main effect upon heading estimates, with the lower speed leading to worse estimates than did the higher one across all densities. This was not entirely unexpected, but the extent of the improvement suggests a dominant role for speed in the accurate estimation of heading. Therefore a further examination of this factor is also required (see Chapter 11).

CHAPTER 10

Experiment Nine – Depth

Experiment 8 demonstrated that an increased number of dots could improve heading performance slightly, but a substantial amount of heading bias still occurred even for the 'optimal' condition of 500 dots and a observer translation speed of 4 m.s-1 ($\beta = 0.7$, where β is equal to the slope of the regression line).

Some other factor is obviously at work, and I therefore in this chapter I intend to examine the effect of scene depth on heading performance. Few experiments overtly examining the role of scene depth in heading estimation have been conducted, and these have led to somewhat equivocal results. For example, van den Berg and Brenner (1994) used a 2-AFC task with a ground plane with a depth of 12 m or 40 m, with simulated pursuit eye motion, and found an increase in heading bias as depth was reduced. In another experiment Beintema and van den Berg (2000) also found that a lack of depth, combined with eye movements, led to an increase in heading estimation bias.

Further, differential motion models of self-motion estimation rely on large depth differences in order to work. They predict that heading estimation should be impossible (or very poor) at very low depths (e.g. a single fronto-parallel plane of dots) and this has been confirmed experimentally for the case of combined translation and rotation (Rieger & Toet, 1985; W.H. Warren & Hannon, 1988, 1990). Therefore the practitioners of one main class of heading model would argue that large depth differences are required for good heading estimation performance.

By contrast, Frey and Owen (1999) used an active heading task and found an improved performance in heading estimation with smaller depths. Improvement in heading estimation with decreased depth was also found by Crowell and Banks (1996).

The experimental paradigms of these studies are not identical to that of the current work, however they do suggest that scene depth may have an impact upon heading performance. However, because of the lack of consistency between the theoretical predictions and experimental results, a detailed examination of the role of depth in heading estimation bias is warranted. This will be achieved by a series of heading experiments using a variety of scene depths.

Because the amount of image motion generated during forward translation depends both on the depth of objects in the world and the speed of forward motion (see Equations 5 & 6, Chapter 1) it was decided to also include two levels of observer speed in the experiment. It may be that slow observer speeds do not generate sufficient image motion in the case of high depth scenes and this may affect the heading estimation process.

Method

Participants

Ten students from the University of Waikato, 6 female and 4 male, aged between 18 and 28 years, participated in this experiment. All were first year psychology students who received partial course credit for taking part. All participants had visual acuity of 20:25 or better. None had previously taken part in a heading experiment.

Apparatus

The apparatus used in this experiment was the same as that used in Experiment 1.

Procedure

The procedure is as for Experiment 1, with the following changes. For this experiment, seven azimuthal headings (-15, -10, -5, 0, 5, 10, 15° of visual angle) were used. Ten experimental conditions were run, crossing two speeds (1 $m.s^{-1}$and 2 $m.s^{-1}$) with depth, using five depths (12.5 m, 25 m, 50 m, 75 m, and 100 m). Each heading was presented 10 times during an experimental condition, giving a total of 70 trials per condition. Each condition took about 5 min to run, for a total session time of approximately 60 min.

Results

The results of the experiment are shown below in Figures 10.1 and 10.2, with the mean estimated heading plotted against the actual direction of heading for both the 1 $m.s^{-1}$ and 2 $m.s^{-1}$ translations speeds. Descriptive statistics for these data are shown in Tables 10.1 and 10.2.

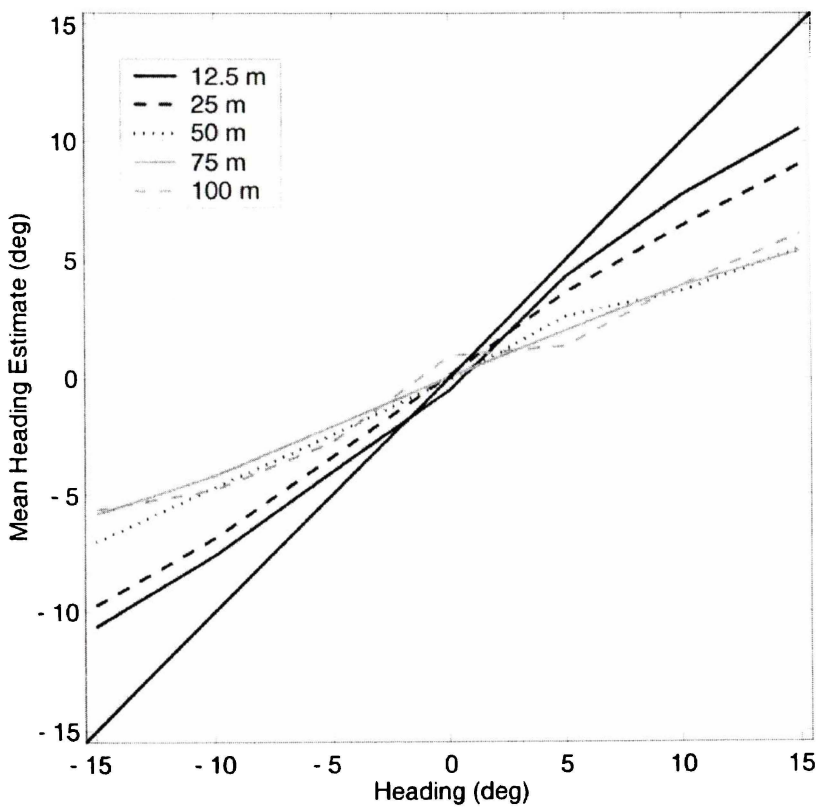

Figure 10.1. Mean heading estimates as a function of heading direction for different depths with a translation speed of 1 $m.s^{-1}$, ±2 SE for 100 m depth. Veridical performance is shown by the 45° line.

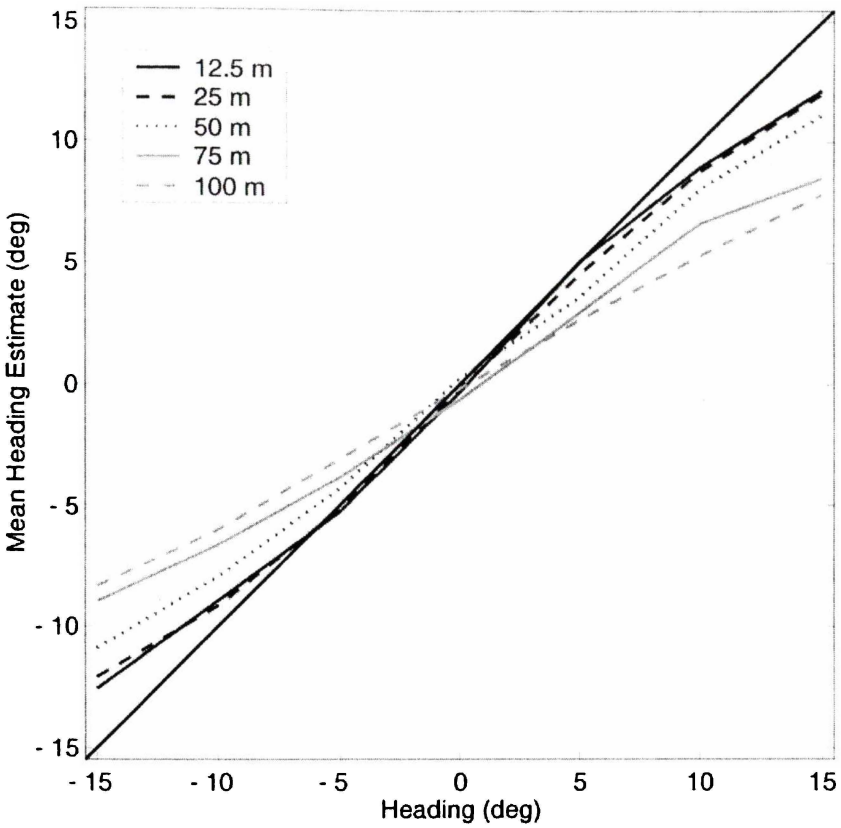

Figure 10.2. Mean heading estimates (±2 SE) as a function of heading direction for different depths with a translation speed of 2 $m.s^{-1}$, ±2 SE for 100 m depth. Veridical performance is shown by the 45° line.

Table 10.1

Mean heading estimates, mean bias, and standard deviations for depth at 1 m.s^{-1}, N=100

Condition	Heading	Mean	Mean Bias	Std. Dev of Bias
12.5 m	-15	-10.63	-4.37	4.05
	-10	-7.60	-2.40	3.68
	-5	-4.02	-0.98	2.78
	0	-0.52	-0.52	2.36
	5	4.29	-0.71	3.51
	10	7.75	-2.29	3.32
	15	10.56	-4.44	3.87
25 m	-15	-9.73	-5.27	3.74
	-10	-6.86	-3.14	3.85
	-5	-3.38	-1.62	3.32
	0	0.12	-0.12	3.25
	5	3.62	-1.28	3.69
	10	6.45	-3.55	3.51
	15	9.06	-5.94	4.37
50 m	-15	-7.03	-7.97	3.51
	-10	-4.68	-10.32	4.14
	-5	-2.44	-2.56	3.65
	0	-0.09	-0.09	3.52
	5	2.60	-2.40	3.30
	10	3.68	-6.32	4.16
	15	5.50	-9.50	3.89
75 m	-15	-5.84	-9.16	4.86
	-10	-4.18	-5.82	4.22
	-5	-2.08	-2.92	3.41
	0	0.04	-0.04	3.26
	5	2.01	-2.99	3.97
	10	3.92	-6.08	3.81
	15	5.40	-9.60	4.14
100 m	-15	-5.65	-9.35	4.37
	-10	-4.79	-5.21	4.02
	-5	-2.75	-2.25	4.52
	0	0.93	-0.93	4.21
	5	1.34	-3.56	4.36
	10	3.96	-6.04	3.71
	15	6.13	-8.87	3.95

Table 10.2

Mean heading estimates, mean bias, and standard deviations for depth at 2 $m.s^{-1}$, N=100

Condition	Heading	Mean	Mean Bias	Std. Dev of Bias
12.5 m	-15	-12.56	-2.44	2.86
	-10	-8.95	-1.05	2.62
	-5	-5.27	0.27	2.01
	0	-0.31	-0.31	1.90
	5	5.02	0.02	1.80
	10	8.92	-1.08	2.40
	15	12.12	-2.88	2.50
25 m	-15	-12.08	-2.92	3.65
	-10	-9.16	-0.84	2.94
	-5	-5.16	0.16	2.29
	0	-0.18	-0.18	3.03
	5	4.52	-0.48	2.38
	10	8.75	-1.25	2.70
	15	11.99	-3.01	3.54
50 m	-15	-10.89	-4.11	4.62
	-10	-7.95	-2.05	3.82
	-5	-4.30	-0.70	3.34
	0	0.25	0.25	2.33
	5	3.58	-1.42	2.99
	10	8.02	-1.98	3.61
	15	11.12	-3.88	4.02
75 m	-15	-8.97	-6.03	4.16
	-10	-6.63	-3.37	3.58
	-5	-3.84	-1.16	2.88
	0	-0.62	-0.62	2.42
	5	2.93	-2.07	3.44
	10	6.62	-3.38	3.22
	15	8.50	-6.50	4.31
100 m	-15	-8.33	-6.67	4.50
	-10	-6.01	-3.99	3.76
	-5	-3.08	-1.92	3.84
	0	-0.18	-0.18	3.36
	5	2.64	-1.36	3.78
	10	5.27	-4.37	3.91
	15	7.83	-7.17	4.44

In order to characterise the trends in the data across the different conditions, regression analyses were carried out on the actual heading estimates. Prior to carrying out the regression, curve fitting was done to ensure that linear regression was appropriate. A linear fit was found to be significant for all outcomes ($p < .0001$), and therefore linear regression was used for all conditions.

The full details of the regression equations for the 1 $m.s^{-1}$ and 2 $m.s^{-1}$conditions are given in Tables 10.3 and 10.4, while the scatter-plots for the 1 $m.s^{-1}$-12.5 m and -100 m conditions and the, 2 $m.s^{-1}$-12.5 m and -100 m depth conditions are shown in Figures 10.3 to 10.6. These have been chosen as representing the shortest and longest depths in the experiment.

Table 10.3.

Linear regression statistics for estimated headings for different scene depths with a translation speed of 1 $m.s^{-1}$

Condition	Slope	95% C.I.	Intercept	95% C.I.	R	p
12.5 m	0.733	0.707 to 0.758	-0.023	-0.278 to 0.231	0.906	<.0001
25 m	0.643	0.615 to 0.670	-0.104	-0.378 to 0.170	0.869	<.0001
50 m	0.424	0.396 to 0.452	-0.352	-0.631 to -0.073	0.749	<.0001
75 m	0.386	0.356 to 0.415	-0.104	-0.399 to -0.191	0.697	<.0001
100 m	0.341	0.375 to 0.438	-0.121	-0.432 to 0.191	0.696	<.0001

Table 10.4.

Linear regression statistics for estimated headings for different scene depths with a translation speed of 2 $m.s^{-1}$

Condition	Slope	95% C.I.	Intercept	95% C.I.	R	p
12.5 m	0.841	0.841 to 0.877	-0.144	-0.239 to 0.247	0.963	<.0001
25 m	0.819	0.819 to 0.864	-0.184	-0.344 to 0.201	0.941	<.0001
50 m	0.756	0.729 to 0.783	-0.002	-0.142 to 0.350	0.902	<.0001
75 m	0.548	0.519 to 0.578	-0.262	-0.358 to 0.162	0.810	<.0001
100 m	0.612	0.585 to 0.638	-0.287	-0.358 to 0.162	0.869	<.0001

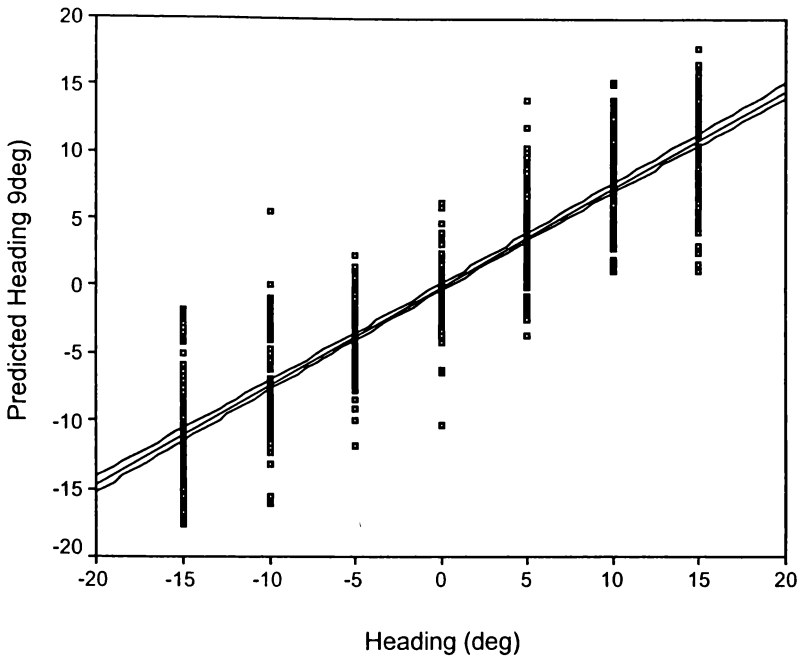

Figure 10.3. Scatterplot and regression line (± 95% C.I.) for heading estimates for the 12.5 m – 1 $m.s^{-1}$ condition

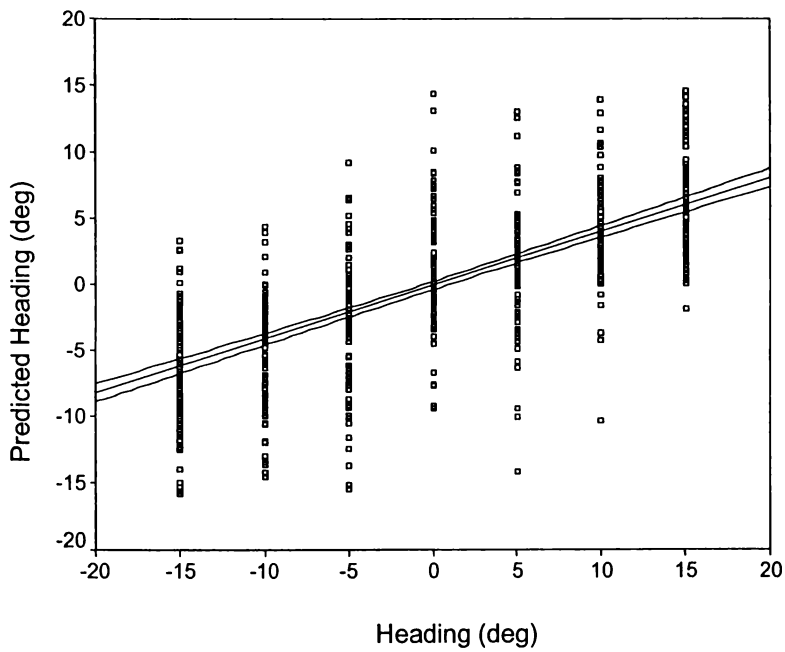

Figure 10.4. Scatterplot and regression line (± 95% C.I.) for heading estimates for the 100 m - 1 $m.s^{-1}$ condition

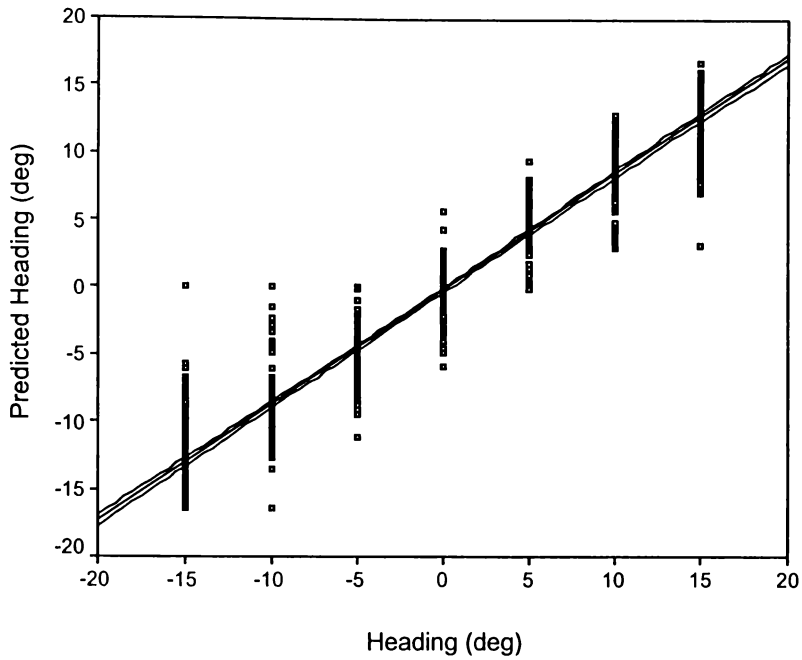

Figure 10.5. Scatterplot and regression line (± 95% C.I.) for heading estimates for the 12.5 m - 2 $m.s^{-1}$ condition

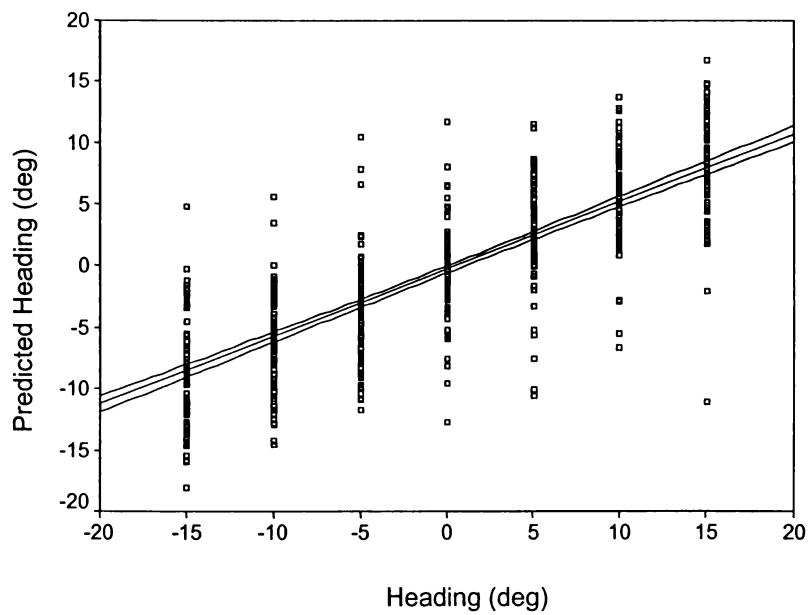

Figure 10.6. Scatterplot and regression line (± 95% C.I.) for heading estimates for the 100 m - 2 $m.s^{-1}$ condition

The 95% confidence interval for the slope does not include 1.0, meaning that a significant bias to the screen centre occurred in all conditions.

Overall, bias was greatest with the slower translation speed. At 1 $m.s^{-1}$ results for the 12.5 m and25 m distances are different to each other and those for all other depths, while results the three furthest depths are not significantly different from one another. For the 2 $m.s^{-1}$ speed, results for the 12.5 m and 25m depths are not significantly different from one another, but results for all other distances are significantly different to one another. Results for 12.5m at the slower speed are comparable to 50 m at the faster speed. Note that for both speeds, accuracy decreases as depth increases.

In order to test which of the experimental factors significantly affected estimates of heading, a three-way within subjects analysis of variance and two two-way within-subjects analyses of variance, one for each speed, were conducted to evaluate the effect of speed, depth and heading upon estimates of heading. The dependent variable was the Mean heading estimate. Within subjects factors were speed, with two levels (1 $m.s^{-1}$ and 2 $m.s^{-1}$), depth with five levels (12.5 m, 25 m, 50 m, 75 m, and 100 m) and heading with seven levels (-15, -10, -5, 0, 5, 10, 15° of visual angle). Any violations of sphericity were corrected using Mauchly's Test of Sphericity.

For the three-way analysis there was a significant main effect for heading [$F(6, 54) = 29.689$, $p < .0001$, $\eta^2 = .767$] and significant interaction effect for speed x depth [$F(3.221, 28.992) = 3.097$, $p = .039$, $\eta^2 = .256$] for speed x heading [$F(6, 54) = 13.819$, $p < .0001$, $\eta^2 = .606$] for depth x heading [$F(5.188, 46.690) = 22.313$, $p < .0001$, $\eta^2 = .713$] and for speed x depth x heading [$F(6.049, 54.445) = 5.097$, $p < .0001$, $\eta^2 = .362$]. There was no significant main effect for speed [$F(1, 9) = .457$, $p = .516$, $\eta^2 = .048$] , or depth [$F(3.912, 35.209) = 2.029$, $p = .113$, $\eta^2 = .184$].

For 1 $m.s^{-1}$there was a significant main effect for depth [$F(3.374, 30.369) = .5.245$, $p = .004$, $\eta^2 = .368$] and heading [$F(6, 54) = 58.563$, $p = .000$, $\eta^2 = .867$] and a significant interaction effect for depth x heading [$F(6.448, 58.031) = 21.558$, $p < .0001$, $\eta^2 = .705$].

For 2 $m.s^{-1}$ there was a significant main effect for heading [$F(6, 54) = 18.682$, $p < .0001$, $\eta^2 = .675$] , and a significant interaction effect for depth x heading [$F(6.593, 59.335) = 12.334$, $p < .0001$, $\eta^2 = .578$]. There was no significant main effect for depth [$F(2.423, 21.806) = .811$, $p = .479$, $\eta^2 = .083$].

Discussion

The data summarised in Figures 10.1 and 10.2 shows that for both speeds and all depths, there was still bias to the centre. However for this experiment, the different conditions appear to have had a definite influence on the amount of bias that occurred.

In this experiment, there was a clear trend showing that the smaller the depth in the scene, the smaller the amount of heading bias (i.e. the regression line slope increased with decreasing scene depth). Therefore the results of this experiment offer support to the results of Frey and Owen (1999), and Crowell and Banks (1996). However they are counter to the predictions of vector decomposition heading models (e.g. Hildreth, 1992; Rieger & Toet, 1985) because these models rely on large depth differences for their vector subtraction process to work properly. One would expect greater depth differences to lead to larger difference vectors and hence improved heading performance. However the results of Experiment 9 show that better heading performance was obtained with a scene depth of 12.5 m (β = .73, .84 for 1 $m.s^{-1}$ and 2 $m.s^{-1}$ respectively) compared to the larger 100 m depth (β = .34, .55).

A significant interaction effect between depth and heading eccentricity was found, which suggests that when heading direction lies in the peripheral region of vision it becomes more difficult to correctly estimate the direction of heading.

In this experiment a faster simulated observer speed was found to have a significant effect upon the accuracy of estimates (e.g., for 100 m depth, β = .34, .55 for 1 $m.s^{-1}$ and 2 $m.s^{-1}$ respectively). An examination of the effect of speed upon heading estimation performance was therefore undertaken. This is detailed in Chapter 11.

CHAPTER 11

Experiment Ten – Speed

Scene depth was found to improve heading performance quite effectively, but some heading bias occurred even with the best condition of 12.5 m scene depth and 2 $m.s^{-1}$ observer translation speed (slope = .84).

Next it was desirable to examine more closely the effect of observer translation speed on heading estimation. In a study looking at the ability of observers to estimate their direction of heading through a naturalistic environment, Vishton and Cutting (1995) found that a faster observer translation speed leads to improved navigation performance. This finding is supported by the work of W.H. Warren and colleagues (W.H. Warren, Morris, & Kalish, 1988; W.H. Warren, Blackwell, Kurtz, Hatsopoulos, & Kalish, 1991), who found thresholds of 1.5° at a simulated slow walk (1 $m.s^{-1}$), improving to 0.7° at a run (3.8 ms^{-1}).

It has been suggested that the improvement due to speed may be attributable to improved signal-to-noise ratio (SNR) in local motion extraction (W.H. Warren, 1995). van den Berg and Brenner (1994) also looked at signal to noise ratios, and found that as more noise was introduced (lower SNR) the bias towards fixation became more pronounced. Turano and Wang (1994) varied forward observer speed in a combined translation and rotation task, and asked observers to differentiate between straight and curved paths with a scene depth of 100 m and a variety of locomotion speeds. The results showed that their observers could discriminate between the straight and curved paths at fast but not slow speeds. These authors also suggested that problems with low speed displays are probably noise related. Although the experimental paradigms of this research differ substantially from that of the present work, it seems likely that that increased speed will lead to improved performance in heading.

Even without the above research indicating an improvement in heading estimation with faster observer speeds, there are theoretical grounds for suspecting this relationship. In computer generated displays such as the ones used in this thesis and in many cases of heading research, an increase in simulated observer speed produces an increase in the rate and amount of image motion on the screen. During observer translation, points in the distance have very low or zero image motion (see Figure 1.2, Chapter 1.). Points that lie close to the heading direction also have a very low image speed because of their proximity to the FOE. An increase in observer speed leads to an increase in the speed of the image motion close to the FOE. Image motion close to the FOE constrains its possible location because (by definition) the FOE is the point in the image from which the image motion radiates outwards. Therefore if image motion is being used by the observer to locate or constrain the position of the FOE, a greater observer speed should lead to improved heading estimation performance. Changes to the depth of the scene should also influence the heading estimates, because the amount of image motion around the FOE is also determined by the depth of the points in the scene (equations 7 and 8, on page 7).

These ideas are tested in this work by using a variety of translation speeds in a standard heading experiment. The effect of depth is also examined because of the possibility (discussed above) of this having an effect.

Method

Participants

Ten students from the University of Waikato, 7 female and 3 male, aged between 18 and 37 years, participated in this experiment. All were first year psychology students who received partial course credit for taking part. All participants had visual acuity of 20:25 or better.

Apparatus

The apparatus was as for Experiment 1.

Procedure

The procedure was as for Experiment 1, with the following changes. For this experiment, seven headings (-15, -10, -5, 0, 5, 10, 15° of visual angle) were used. Nine experimental conditions were run, crossing two depths (25 m and 100 m) with five speeds (1 $m.s^{-1}$, 2 ms^{-1}, 3$m.s^{-1}$, 4 $m.s^{-1}$, and 5$m.s^{-1}$). The smaller depth was tested with the first four speeds only (in order to prevent excessively high image speeds which the computer display would not have been able to present adequately), while the greater depth was used with all five speeds. Each heading was presented 10 times during an experimental condition, giving a total of 70 trials per condition. Each condition took about 5 min to run, for a total session time of approximately 60 min.

Results

The results of the experiment are shown in Figures 11.1 and 11.2, with the mean estimated heading plotted against the actual direction of heading for 25 m and 100 m scene depths. Descriptive statistics for this data are shown in Tables 11.1 and 11.2.

The data summarised in Figures 11.1 and 11.2 shows that for both depths and all speeds, there was still bias to the centre.

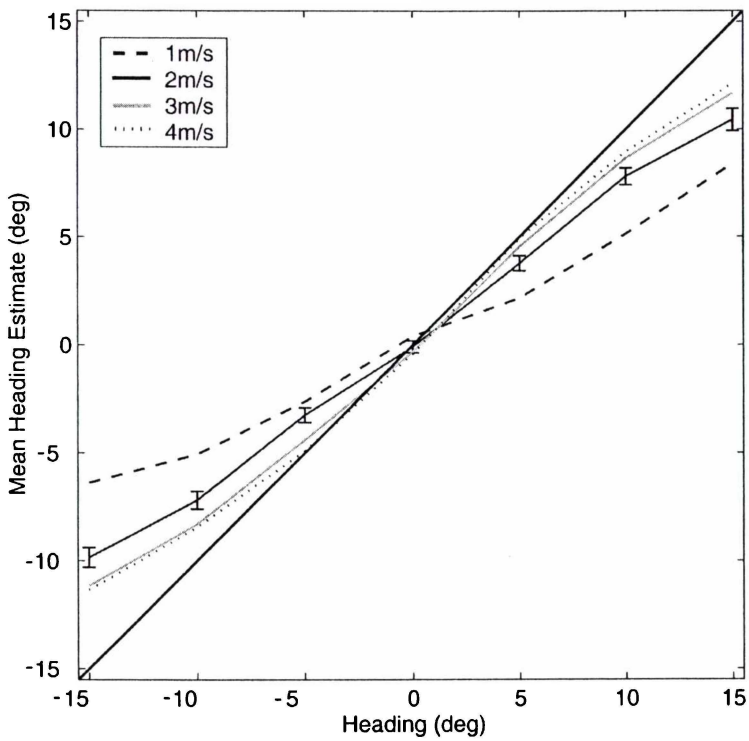

Figure 11.1. Mean heading estimates as a function of heading direction for different translation speeds with a scene depth of 25 m, ±2 SE for 2 $m.s^{-1}$ speed. Veridical performance is shown by the 45° line.

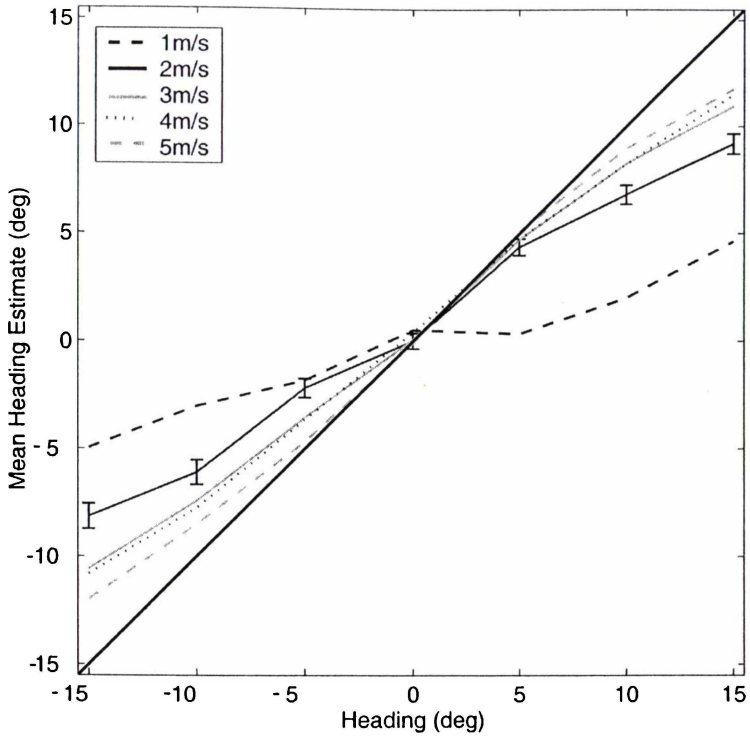

Figure 11.2. Mean heading estimates as a function of heading direction for different translation speeds with a scene depth of 100 m, ±2 SE for 2 $m.s^{-1}$ speed. Veridical performance is shown by the 45° line.

Table 11.1

Mean heading estimates, mean bias, and standard deviations for speed at 25 m, N=100

Condition	Heading	Mean	Mean Bias	Std. Dev. of Mean
1 $m.s^{-1}$	-15	-6.39	-8.61	5.57
	-10	-5.06	-4.94	3.82
	-5	-2.62	-2.38	3.64
	0	0.40	-0.4	2.87
	5	2.16	2.84	4.00
	10	5.13	4.87	4.28
	15	8.39	6.61	5.70
2 $m.s^{-1}$	-15	-9.85	-5.15	4.58
	-10	-7.19	-2.81	4.05
	-5	-3.24	-1.76	3.38
	0	-0.09	0.09	2.79
	5	3.77	1.23	3.47
	10	7.80	2.2	3.95
	15	10.44	4.56	5.15
3$m.s^{-1}$	-15	-11.16	-3.84	4.75
	-10	-8.30	-1.7	3.35
	-5	-4.39	-0.61	2.63
	0	-0.33	0.33	1.95
	5	4.55	0.45	2.37
	10	8.65	1.35	3.56
	15	11.68	3.32	4.62
4 $m.s^{-1}$	-15	-11.36	-3.64	4.55
	-10	-8.45	-1.55	3.21
	-5	-4.90	-0.1	2.31
	0	-0.42	0.42	1.84
	5	4.94	0.06	2.28
	10	8.95	1.05	3.36
	15	12.14	2.86	4.79

Table 11.2

Mean heading estimates, mean bias, and standard deviations for speed at 100 m, N=100

Condition	Heading	Mean	Mean Bias	Std. Dev. of Mean
1 $m.s^{-1}$	-15	-4.96	-10.04	6.35
	-10	-3.02	-6.98	5.67
	-5	-1.82	-3.18	5.22
	0	0.52	-0.52	4.43
	5	0.36	-4.64	4.25
	10	2.01	-7.99	4.93
	15	4.63	-10.37	6.03
2 $m.s^{-1}$	-15	-8.15	-6.85	5.82
	-10	-6.10	-3.90	5.67
	-5	-2.18	-2.82	4.45
	0	0.02	-0.02	3.55
	5	4.38	-0.62	3.88
	10	6.82	-3.18	4.43
	15	9.19	-5.81	4.69
3$m.s^{-1}$	-15	-10.58	-5.42	4.74
	-10	-7.43	-2.57	4.16
	-5	-3.55	-1.45	3.46
	0	0.07	-0.07	3.45
	5	4.72	-0.28	3.41
	10	8.26	-1.74	3.59
	15	10.94	-4.06	4.79
4 $m.s^{-1}$	-15	-10.82	-4.18	5.41
	-10	-7.75	-2.25	4.19
	-5	-3.65	-1.35	3.25
	0	0.40	-0.40	2.29
	5	4.75	-0.25	3.30
	10	8.25	-1.75	4.17
	15	11.48	-3.52	5.00
5$m.s^{-1}$	-15	-11.99	-3.01	4.66
	-10	-8.51	-1.49	3.64
	-5	-4.67	-0.33	2.52
	0	-0.10	-0.10	2.13
	5	5.10	-0.10	3.21
	10	8.97	-1.03	3.48
	15	11.74	-3.26	4.91

Regression analyses were then carried out on the actual heading estimates. Curve fitting indicated that linear regression was significant for all outcomes ($p < .0001$), and therefore linear regression was used for all conditions.

The full details of the regression equations are shown below in Tables 11.1 and 11.2, with scatter-plots for the 100 m - 2 $m.s^{-1}$ and - 4 $m.s^{-1}$ conditions in Figures 11.3 and 11.4. These speeds were chosen because they are significantly different to one another for both depths.

Table 11.3

Linear regression statistics for estimated headings for different translation speeds with a scene depth of 25 m.

Condition	Slope	95% C.I.	Intercept	95% C.I.	R	p
1 $m.s^{-1}$	0.496	0.464 to 0.529	0.286	-0.040 to 0.611	0.750	<.0001
2 $m.s^{-1}$	0.699	0.669 to 0.729	0.234	-0.061 to 0.530	0.869	<.0001
3 $m.s^{-1}$	0.796	0.770 to 0.821	0.101	-0.158 to -0.360	0.916	<.0001
4 $m.s^{-1}$	0.822	0.797 to 0.848	0.129	-0.124 to 0.382	0.924	<.0001

Table 11.4

Linear regression statistics for estimated headings for different translation speeds with a scene depth of 100 m.

Condition	Slope	95% C.I.	Intercept	95% C.I.	R	p
1 $m.s^{-1}$	0.293	0.253 to 0.333	-0.326	-0722 to 0.069	0.483	<.0001
2 $m.s^{-1}$	0.603	0.568 to 0.683	0.569	0.219 to 0.919	0.788	<.0001
3 $m.s^{-1}$	0.744	0.715 to 0.774	0.349	0.053 to 0.646	0.882	<.0001
4 $m.s^{-1}$	0.766	0.736 to 0.797	0.380	0.078 to 0.682	0.884	<.0001
5 $m.s^{-1}$	0.828	0.801 to 0.855	0.007	-0.196 to 0.349	0.915	<.0001

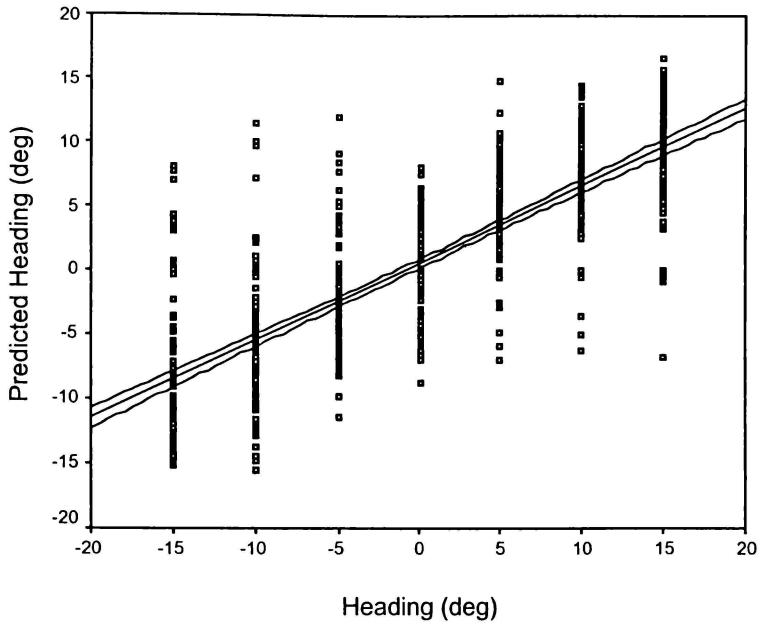

Figure 11.3. Scatterplot and regression line (± 95% C.I.) for heading estimates for the 100 m - 2 $m.s^{-1}$ condition.

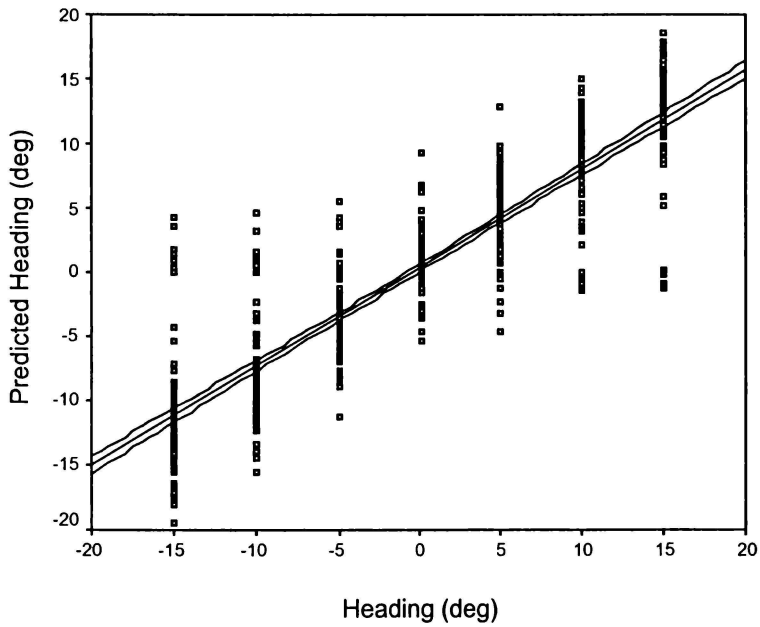

Figure 11.4. Scatterplot and regression line (± 95% C.I.) for heading estimates for the 100 m – 4 $m.s^{-1}$ condition.

The slopes for the regressions are significantly greater than zero in all cases, however they are also less than one, as shown by the 95% C.I.s indicating that a significant bias occurred.

At 25 m, the results for all speeds are significantly different from one another.

At the 100 m scene depth, results for the 1 $m.s^{-1}$, 2 $m.s^{-1}$, and 5 $m.s^{-1}$ condition were significantly different to those for other speeds. Comparing speeds, only the 1 $m.s^{-1}$ speed differed by depth, and all other speeds showed no significant difference by depth, indicating that observer speed is an important factor in heading estimation.

A three-way within subjects analysis of variance and two two-way within-subjects analyses of variance, one for each depth, were conducted to evaluate the effect of depth, speed and heading upon estimates of heading. The dependent variable was the mean heading estimate. The within subjects factors were depth with two levels (25 m and 100 m), speed with four levels (1 $m.s^{-1}$, 2 ms^{-1}, 3$m.s^{-1}$, and 4 $m.s^{-1}$) and heading with seven levels (-15, -10, -5, 0, 5, 10, 15° of visual angle). Any violations of sphericity were corrected using Mauchly's Test of Sphericity.

For the three-way analysis there was a significant main effect for heading [$F(1.071, 9.637) = 16.554$, $p = .002$, $\eta^2 = .648$] and a significant interaction effect for depth x speed [$F(2.418, 21.765) = 4.399$, $p = .020$, $\eta^2 = .328$] for speed x heading [$F(3.826, 34.435) = 13.293$, $p < .0001$, $\eta^2 = .596$] for speed x depth x heading [$F(3.100, 27.896) = 3.467$, $p = .028$, $\eta^2 = .278$]. There was no significant main effect for speed [$F(2.526, 22.737) = .391$, $p = .728$, $\eta^2 = .042$].

There were no significant main effect for speed [$F(1.861, 16.750) = 1.054$, $p = .366$, $\eta^2 = .105$] or for depth [$F(1, 9) = .121$, $p = .736$, $\eta^2 = .013$], and no significant interaction effect for depth x heading [$F(1.124, 10.113) = .724$, $p = .431$, $\eta^2 = .074$].

For 25 m there was a significant main effect for heading [$F(1.064, 9.580) = 12.325$, $p = .006$, $\eta^2 = .578$] and a significant interaction effect for speed x heading [$F(3.425, 30.827) = 4.887$, $p = .005$, $\eta^2 = .352$]. There was no significant main effect for speed [$F(2.526, 22.737) = .391$, $p = .728$, $\eta^2 = .042$].

For 100 m there was a significant main effect for heading [$F(1.095, 9.852) = 13.408$, $p = .004$, $\eta^2 = .598$] and a significant interaction effect for speed x heading [$F(5.478, 49.303) = 12.573$, $p = .0001$, $\eta^2 = .583$]. There was no significant main effect for speed [$F(2.325, 20.927) = 2.376$, $p = .111$, $\eta^2 = .207$].

Discussion

The results of this experiment show that increasing observer forward translation speed and/or reducing the overall amount of depth in a scene, has a significant positive effect upon estimates of heading. For both depths, the two slowest speeds of 1 $m.s^{-1}$ and 2 $m.s^{-1}$ were found to lead to significantly worse performance (slope = 0.5, 0.7 and 0.29, .60) than did the higher speeds (slope = 0.80, 0 .82 and .77, .83), while at 100 m, the fastest speed was found to lead to significantly better performance (slope = 0.83). However note that even in the near depth condition (25 m) and at the fastest speed (5 $m.s^{-1}$) the slope of the regression line (slope = .83) is still significantly less than 1.0 and so heading bias is still present. The image motion generated in this condition is very high, and there is no added noise (as in van den Berg & Brenner, 1994) yet the participants were still not able to determine their heading correctly and tended to perceive heading to be closer to the straight ahead direction than it actually was.

The regression analysis revealed no significant differences in performance between the two depths except at the very lowest simulated observer speed of 1 $m.s^{-1}$. This is a very revealing finding, because it suggests that observer speed exerts a stronger influence over heading estimation than does depth. This small effect for depth can be seen in Figures 11.1 and 11.2. When combined with the results of Experiment 9, which examined the impact of changing depth at the observer speeds of 1 $m.s^{-1}$ and 2 $m.s^{-1}$, it appears that observer speed plays the primary role in controlling bias in heading, with depth being of secondary importance.

At each depth there was also a significant interaction effect between speed and heading, with a higher speed and a more central heading direction leading to less bias.

CHAPTER 12

Experiment Eleven – Viewing Time

Experiments 8, 9 and 10 have demonstrated the importance of the number of dots, depth, and translation speed upon heading performance, with the optimal conditions of each leading to regression slopes of 0.70, 0.84, and 0.82 respectively. Some bias still occurred however, even under these conditions. It was therefore desirable to examine the effect of viewing time on heading performance.

The question of how much viewing time is required in order to achieve a satisfactory level of accuracy in heading estimation has been examined before. For simple translation, the consensus appears to be that people can recover heading accurately from only 2 or 3 frames (W.H. Warren et al., 1991a) but improve up to approximately 300 ms of viewing time (Crowell et al., 1990).

However at pedestrian speeds, people have been found to require quite long stimulus durations to reach 95% accuracy (Vishton & Cutting, 1995). These authors propose that viewing times of 3 - 4 s will be needed to achieve this level of performance during normal gait. Gaze durations 1/8 as long allowed 75 % accuracy, but these are believed to be insufficient for real-life navigation in view of the danger of accidents.

In computer-generated displays such as the ones used in this thesis, and in many cases of heading research, an increase in simulated observer speed produces an increase in the rate of image motion on the screen. Viewing time creates changes in the amount of image motion alone. Consequently a variety of viewing times will be combined with two observer speeds to test for a possible interaction between viewing time and speed.

Method

Participants

Ten students from the University of Waikato, 5 female and 5 male, aged between 17 and 26 years, participated in this experiment. All were first year psychology students who received partial course credit for taking part. All participants had visual acuity of 20:25 or better.

Apparatus

The apparatus for this experiment is as for Experiment 1.

Procedure

The procedure was as for Experiment 1, with the following changes. For this experiment, the response screen was black for all trials and heading was only in the azimuth plane, and seven headings (-15, -10, -5, 0, 5, 10, 15° of visual angle) were used. Ten experimental conditions were run, crossing 2 speeds (2 $m.s^{-1}$ and 4 $m.s^{-1}$) with 5 presentation times (200, 400, 600, 800 and 1000 ms) and a scene depth of 100 m. Each heading was presented 10 times during an experimental condition, giving a total of 70 trials per condition. Each condition took about 5 min to run, for a total session time of approximately 55 min.

Results

The results of the experiment are shown below in Figures 12.1 and 12.2, with the mean estimated heading plotted against the actual direction of heading for both 2 $m.s^{-1}$ and 4 $m.s^{-1}$ speeds. Descriptive statistics are provided in Tables 12.1 and 12.2.

The data summarised in Figures 12.1 and 12.2 shows that for both speeds and all times, there was still bias to the centre.

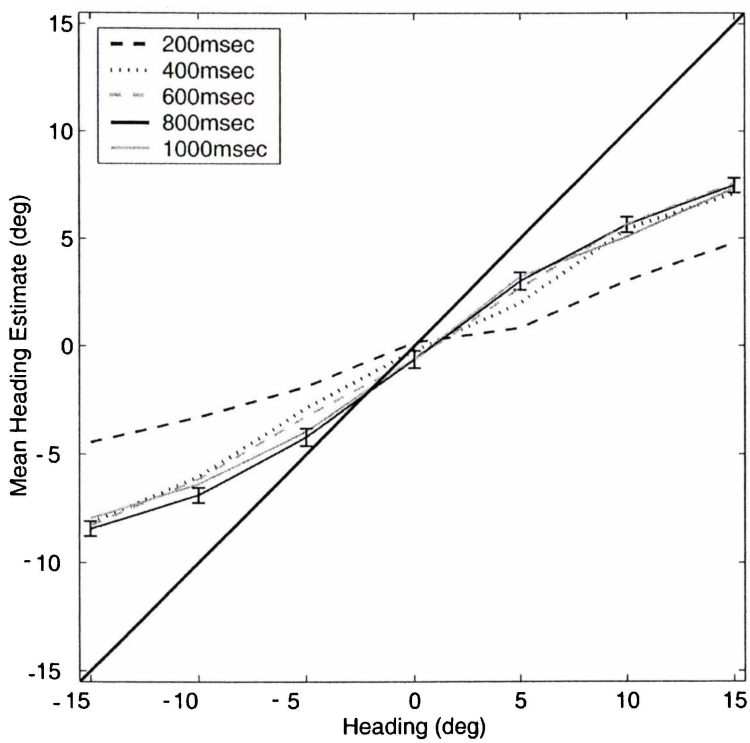

Figure 12.1. Mean heading estimates as a function of heading direction for different viewing times with a translation speed of 2 $m.s^{-1}$, ±2 SE for 800 ms condition. Veridical performance is shown by the 45° line.

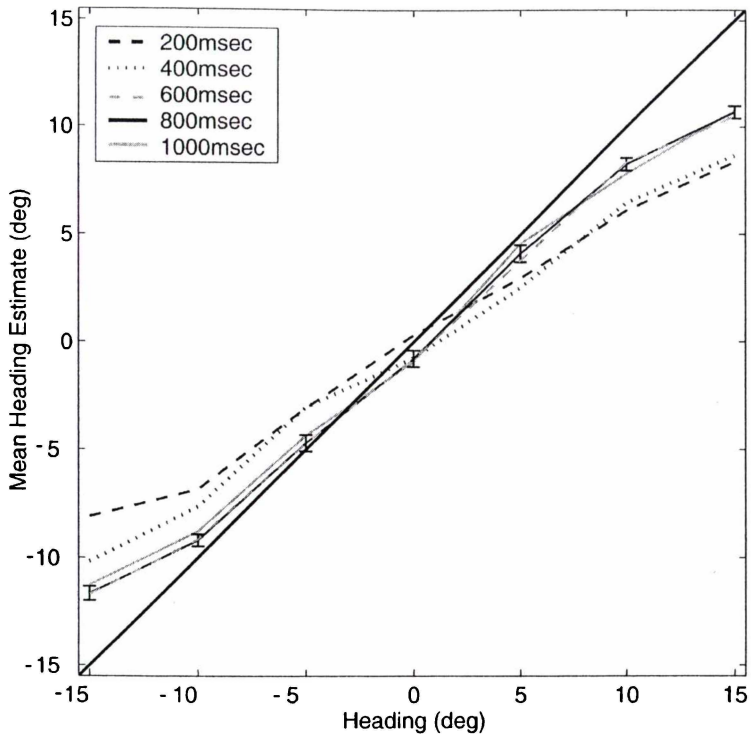

Figure 12.2. Mean heading estimates as a function of heading direction for different viewing times with a translation speed of 4 $m.s^{-1}$, ±2 SE for 800 ms condition. Veridical performance is shown by the 45° line.

Table 12.1

Mean heading estimates, mean bias, and standard deviations for viewing time at 2 $m.s^{-1}$. N=100

Condition	Heading	Mean	Mean Bias	Std. Dev. of Mean
200 ms	-15	-4.45	-10.55	5.77
	-10	-3.29	-6.71	5.48
	-5	-1.88	-3.12	5.34
	0	0.16	-0.16	5.26
	5	0.83	-4.17	5.12
	10	3.03	-6.97	4.83
	15	4.78	-10.12	4.49
400 ms	-15	-8.18	-6.82	3.32
	-10	-6.03	-3.97	3.81
	-5	-2.87	-2.13	4.20
	0	-0.22	-0.22	4.16
	5	1.99	-3.01	4.82
	10	5.44	-9.56	3.46
	15	7.10	-7.90	3.10
600 ms	-15	-7.95	-7.05	3.48
	-10	-6.37	-3.63	3.46
	-5	-3.95	-1.05	3.96
	0	-0.58	-0.58	4.04
	5	3.21	-1.79	3.92
	10	5.07	-9.93	4.01
	15	7.33	-7.67	3.63
800 ms	-15	-8.44	-6.56	3.45
	-10	-6.89	-3.11	3.49
	-5	-4.21	-0.79	4.04
	0	-0.62	-0.62	4.01
	5	3.01	-1.99	4.04
	10	5.64	-4.36	3.66
	15	7.47	-7.53	3.38
1000 ms	-15	-8.28	-6.72	4.50
	-10	-6.14	-3.86	4.04
	-5	-3.25	-1.75	4.20
	0	-0.63	-0.63	3.59
	5	2.69	-2.31	4.39
	10	5.67	-4.33	3.78
	15	7.57	-7.43	3.95

Table 12.2

Mean heading estimates, mean bias, and standard deviations for viewing time at 4 m.s^{-1}, N=100

Condition	Heading	Mean	Mean Bias	Std. Dev. of Mean
200 ms	-15	-8.10	-6.90	4.52
	-10	-6.84	-3.16	4.44
	-5	-3.07	-1.97	4.41
	0	0.32	-0.32	3.98
	5	2.97	-2.03	4.23
	10	6.11	-3.89	3.46
	15	8.36	-6.64	3.08
400 ms	-15	-10.17	-4.83	3.77
	-10	-7.64	-2.36	3.64
	-5	-3.03	-1.97	3.99
	0	-0.73	-0.73	3.58
	5	2.53	-2.47	3.78
	10	6.47	-3.53	3.75
	15	8.67	-1.33	3.07
600 ms	-15	-11.26	-3.74	3.34
	-10	-8.78	-1.22	3.49
	-5	-4.35	-0.65	4.07
	0	-0.92	-0.08	4.72
	5	4.59	-0.41	4.39
	10	7.81	-2.19	3.03
	15	10.76	-4.24	2.76
800 ms	-15	-11.66	-3.34	3.27
	-10	-9.20	-0.80	2.75
	-5	-4.70	-0.30	3.79
	0	-0.77	-0.77	3.78
	5	4.12	-0.88	3.97
	10	8.26	-1.74	2.98
	15	10.69	-4.31	2.87
1000 ms	-15	-11.70	-2.20	3.92
	-10	-9.16	-0.84	2.60
	-5	-4.70	-0.30	3.53
	0	-0.78	-0.78	3.83
	5	3.79	-1.21	3.72
	10	8.34	-1.66	2.69
	15	10.48	-4.52	3.12

In order to characterise the trends in the data across the different conditions, regression analyses were carried out on the actual heading estimates. Although the mean estimate lines appear somewhat curved, a linear fit was found to be significant for all conditions ($p < .0001$), and therefore linear regression was used for all conditions. The full details of the regression equations are shown in Tables 12.1 and 12.2, while the scatter-plots for the 2 $m.s^{-1}$ and 4 $m.s^{-1}$ 200 and 600 ms conditions are shown in Figures 12.3 to 12.6. These speeds were chosen because the heading estimates recorded at these speeds are significantly different from one another for both depths.

The p values for the slopes reach significance, however, the 95% confidence interval for the slope does not include 1.0, therefore a significant bias to the screen centre occurred. For both speeds, the slopes appear to reach an upper limit in accuracy.

Table 12.3

Linear regression statistics for estimated headings for different viewing times with a translation speed of 2 $m.s^{-1}$.

Condition	Slope	95% C.I.	Intercept	95% C.I.	R	p
200 ms	0.307	0.274 to 0.341	-0.117	-0.455 to 0.220	0.510	<.0001
400 ms	0.526	0.501 to 0.551	-0.395	-0.648 to -0.143	0.805	<.0001
600 ms	0.543	0.517 to 0.567	-0.642	-0.711 to -0.213	0.817	<.0001
800 ms	0.571	0.547 to 0.596	-0.580	-0.825 to -0.334	0.835	<.0001
1000 ms	0.551	0.524 to 0.577	-0.339	-0.605 to -0.074	0.804	<.0001

Table 12.4

Linear regression statistics for estimated headings for different viewing times with a translation speed of 4 $m.s^{-1}$.

Condition	Slope	95% C.I.	Intercept	95% C.I.	R	p
200 ms	0.594	0.567 to 0.620	-0.122	-0.386 to -0.142	0.826	<.0001
400 ms	0.645	0.621 to 0.669	-0.556	-0.796 to -0.317	0.869	<.0001
600 ms	0.773	0.748 to 0.797	-0.304	-0.551 to -0.058	0.898	<.0001
800 ms	0.791	0.769 to 0.814	-0.466	-0.689 to -0.243	0.918	<.0001
1000 ms	0.786	0.763 to 0.808	-0.535	-0.758 to -0.311	0.916	<.0001

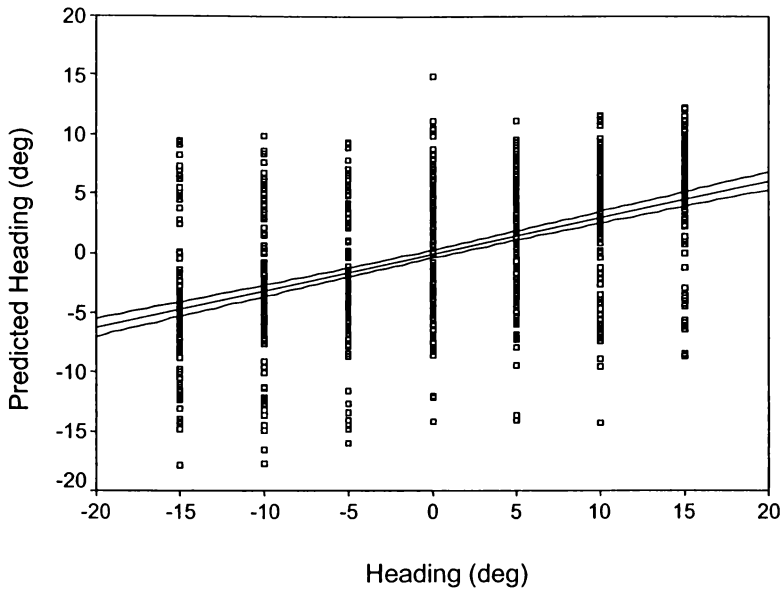

Figure 12.3. Scatterplot and regression line (± 95% C.I.) for heading estimates for the 200 ms – 2 $m.s^{-1}$ condition

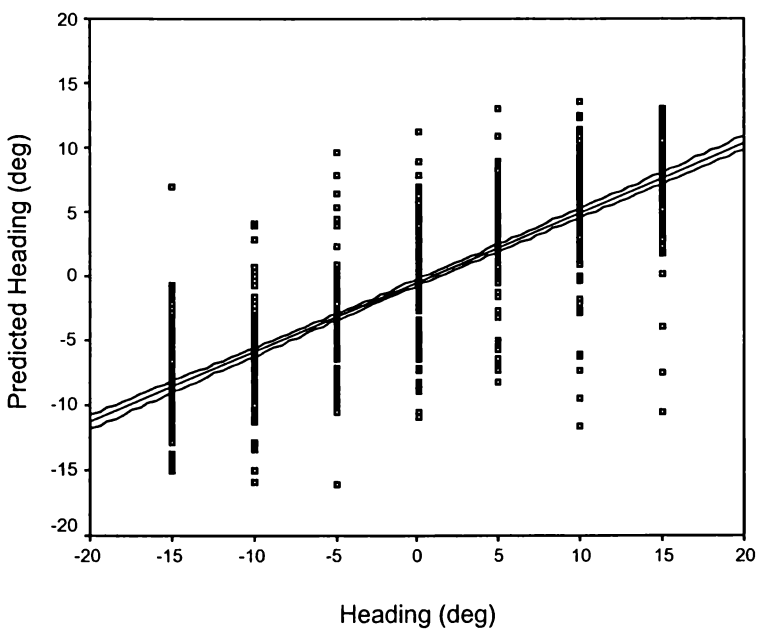

Figure 12.4. Scatterplot and regression line (± 95% C.I.) for heading estimates for the 600 ms – 2 $m.s^{-1}$ condition

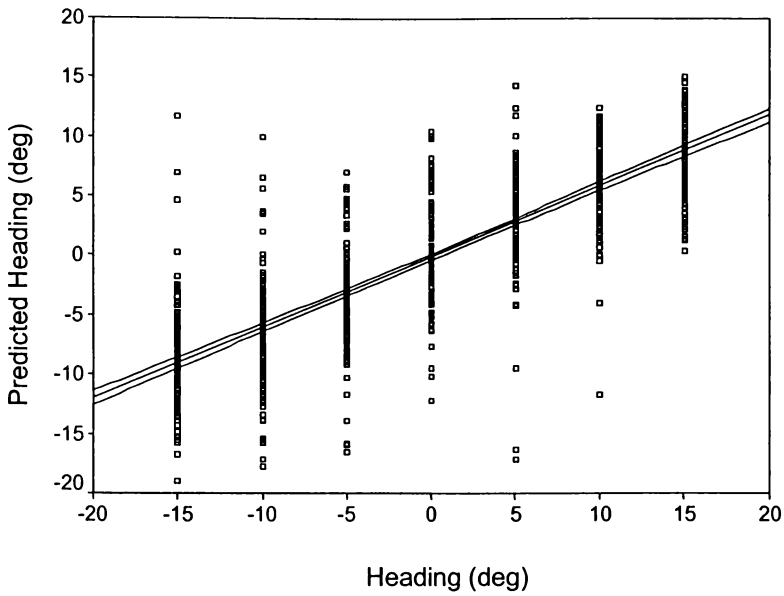

Figure 12.5. Scatterplot and regression line (± 95% C.I.) for heading estimates for the 200 ms – 4 $m.s^{-1}$ condition

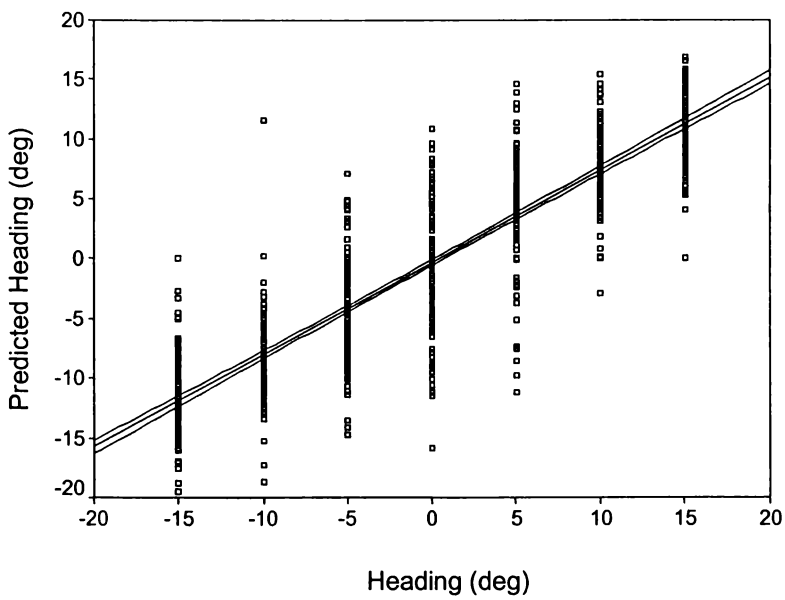

Figure 12.6. Scatterplot and regression line (± 95% C.I.) for heading estimates for the 600 ms – 4 $m.s^{-1}$ condition

The results for the two depths are different. At 2 $m.s^{-1}$ the results from the 200 ms condition differ significantly from the results from all other conditions. Results for the 400 ms condition are different from 800 and 1000 ms conditions, and results from the 600 ms condition are different from 800. There was no significant difference between results for the 800 and 1000 ms conditions.

At 4 $m.s^{-1}$, the 200 ms and 400 ms conditions differ from all of the others and from each other. Results for the other viewing conditions are not significantly different from one another.

Results from the 2 $m.s^{-1}$ condition are significantly less accurate than those from the 4 $m.s^{-1}$ condition, across all viewing conditions.

In order to test which of the experimental factors significantly affected estimates of heading, a three-way within subjects analysis of variance and two two-way within-subjects analyses of variance, one for each depth, were conducted to evaluate the effect of time, speed and heading upon estimates of heading. The dependent variable was the mean heading estimate. The within subjects factors were speed with 2 levels (2 $m.s^{-1}$ and 4 $m.s^{-1}$), time with 5 levels (200, 400, 600, 800, 1000 ms) and heading with 7 levels (-15, -10, -5, 0, 5, 10, 15° of visual angle). Any violations of sphericity were corrected using Mauchly's Test of Sphericity.

For the three-way analysis there was a significant main effect for heading [$F(6, 72) = 129.974$, $p < .0001$, $\eta^2 = .915$] and significant interaction effects for speed x heading [$F(6, 72) = 29.919$, $p < .0001$, $\eta^2 = .714$] and time x heading [$F(7.363, 88.361) = 8.486$, $p < .0001$, $\eta^2 = .414$].

There was no significant main effect for speed [$F(1, 12) = .022$, $p = .885$, $\eta^2 = .002$] and time [$F(4, 48) = 1.248$, $p = .303$, $\eta^2 = .099$] and no significant interaction effects for

speed x time [$F(5.049, 160.916) = 3.352$, p =.824, $\eta^2 = .030$] or for speed x time x heading [$F(9.342, 112.098) = 1.138$, p =.342, $\eta^2 = .087$].

For 2 $m.s^{-1}$ there was a significant main effect for heading [$F(6, 72) = 181.99$, p <.0001, $\eta^2 = .938$] and a significant interaction effect for time x heading [$F(7.101, 85.215) = 3.804$, p =.001, $\eta^2 = .241$]. There was no significant main effect for time [$F(3.874, 46.484) = .109$, p =.977, $\eta^2 = .009$].

For 4 $m.s^{-1}$ there was a significant main effect for heading [$F(6, 72) = 41.734$, p <.0001, $\eta^2 = .777$] and a significant interaction effect for time x heading [$F(15.790, 189.476) = 7.668$, p <.0001, $\eta^2 = .390$]. There was no significant main effect for time [$F(4, 48) = 1.92$, p =.122, $\eta^2 = .138$].

Discussion

The results of this experiment confirm our hypothesis that viewing time can have an effect upon estimates of heading. For both translation speeds the smallest viewing time of 200 ms led to the worst estimation overall, and for the slower speed, 400 ms also led to significantly more bias than did the longer viewing times. This suggests that for a slower translation speed somewhat more viewing time will be required, and that viewing time will mainly be of importance when it is too short for adequate processing of heading. This effect could reflect the fact that longer viewing times lead to more image motion for points near the FOE.

These results lend somewhat conditional support to the previous finding that estimates of heading improve up to approximately 300 ms of viewing time (Crowell, et a., 1990), in that this amount of time appears to be adequate only when observer speed is high. However, when speed is lower, more processing time will be required. A viewing time of 600-800 ms should be sufficient for the range of translation speeds used in this thesis. Previous experiments have used a viewing time of 800 ms with an observer translation speed of $2m.s^{-1}$, and therefore the bias cannot be blamed upon viewing time.

A significant interaction between viewing time and heading was found for both speeds. Figures 12.1 and 12.2 showing that, as for depth and speed, viewing time has an increasing effect with eccentricity. Again this suggests the need for increased amounts of stimulation with extreme heading angles.

CHAPTER 13

Summary and Discussion

Summary

The first part of this thesis was designed as an investigation into the nature and cause of bias in heading judgments in computer-based tasks. The experiments detailed in this section have revealed some interesting insights into the nature of this bias. Although the general consensus among researchers has been that heading estimation can be estimated with reasonable efficiency, the current work has discovered that, under a range of conditions, bias was a significant problem, and would cause severe difficulty if encountered during real-world navigation.

The experiments themselves fell into four broad categories: methods of heading estimation, perspective cues, proprioceptive information, and factors affecting vector magnitude, each of which will be considered in turn.

The first aspect of interest in this research was the question of how well heading estimation could be carried out using naturalistic scene depths and observer translation speeds. A significant central bias was found. The next question concerned whether heading estimation is performed as a simple static task or a motion-based one. The static task gives line traces that are the resulting pattern of radial lines traced by the moving dots across the screen surface, and these could be used as a single 'snapshot' of the pattern of flow. One possible source of line traces in heading displays is provided by the phosphor trails, which remain on the screen after each trial. Two experimental factors were used to assist in determining whether static or motion techniques are used. The first involved using two response screens: black and grey. The second involved using two types of dot display:

static and motion. No significant difference in performance was found between the black and grey response screens, which lead me to conclude that phosphor trails are not used to facilitate estimation despite their salience in such displays. Further support for this finding was provided by comparing results using the two different types of display static and motion. Results showed that heading was more accurately estimated with a static display than with a motion one. With a motion display bias was found to increase with heading eccentricity. The extent of the difference in bias between the line-traces and motion displays also suggests that static-based estimation is not used for heading in depth. Taken together, there is reason to believe that heading estimation in computer-based experiments is not carried out using phosphor traces.

Experiment 3 aimed to investigate whether the bias found in Experiment 2 was due to errors in memory, response or calculation errors. The bias was found to disappear when observers were simply required to locate a dot positioned at the focus of expansion. Therefore bias was presumed not to be due to response errors of memory or pointing, but instead to have arisen during the computational phase of heading extraction.

The second series of experiments examined the role of various perspective cues upon bias. Experiment 4 used a series of objects: non-growing dots, growing dots and growing cubes, to test the importance of size and shape perspective upon heading. It was proposed that the extra perspective these cues would provide could be enough to counter the central bias found in the previous experiment. However, neither size nor shape was found to have a significant effect upon the size of the bias found in the current experimental design.

Experiment 5 looked at the possible role of the disappearance of the dots during the response phase. It was proposed that this could lead to shrinkage of perceived space, in which case, having the dots remain during the response phase should go some way towards

solving the bias problem. However it was found that this had no significant effect upon heading accuracy.

The third series of experiments examined the role of proprioceptive cues. Experiment 6 involved changing eye fixation between five different directions: central and 9° eccentricity in elevational and azimuthal directions. This was found to have some effect upon heading estimation, with accuracy being the greatest near to fixation. However, this effect was not great enough to overcome the overall bias to centre found in the previous experiments, and when heading directions lay outside of the fixation point, a bias towards the centre of the screen was still observed. Thus it appears that bias is towards the screen centre.

Experiment 7 examined a different proprioceptive cue, those from neck muscle signals. This involved participants having their head locked in an angled position in relation to the body while gaze was fixed as in earlier experiments. Heading estimates were found to contain the same bias to centre as before. Therefore on the basis of the results of these two experiments, proprioceptive cues were concluded not to be of great importance in causing heading bias.

The fourth group of experiments involved the manipulation of the properties of the vector flow field in order to investigate the role of various factors upon heading accuracy. Experiment 8 used different quantities of dots to examine the role of the number of dots in heading bias. It was found that this had a minor role to play, with optimal heading estimation being made with more than 50 dots and fewer than 500. This finding has two implications for heading estimation. Firstly, the dot number is not likely to be a major factor in causing heading bias provided their are sufficient. Secondly, that the quantity of 200 dots used in the current experiments should be more than sufficient for the task.

Experiment 9 looked at the effect of scene depth, which was found to have a significant effect upon heading bias, with a decrease in depth leading to an improvement in estimation. Two translation speeds were used, and speed was also found to be a significant factor in estimation accuracy, with the faster speed leading to less bias.

Experiment 10 therefore examined the influence of translational speed on bias, and it was found to have a significant effect, and the faster the forward speed of travel, the greater the accuracy of estimation, although performance began to reach an asymptote at higher speeds. Perfect average accuracy was never obtained with the range of speeds considered in this experiment.

Experiment 11 looked at the role of viewing time in heading estimation. Time was found to have a significant interaction effect with heading, with greater viewing time being more influential at greater eccentricities. For a slower approach speed (2 $m.s^{-1}$) a viewing time of greater than 400 ms led to significantly more accurate estimation, but under more optimal conditions observers could make reasonably accurate estimates down to a viewing time of 200 ms. Thus it appears as though viewing time is not a major cause of bias in the present work, and that the use of 800 ms of viewing time is sufficient for optimum performance without the problems associated with prolonged viewing.

Two other factors of interest arose as a result of these experiments. The first involves the small proportion of individuals who were found to invert their estimation of heading such that, if the actual direction lay 15° to the left, they would indicate perceived heading lay far to the right, and vice versa. This did not happen in all the experiments, but there was a large enough group of them across the entire series for them to be considered as a separate group in their own right. These people were not simply responding randomly as the error bars for their data are generally quite small. They simply perceived heading as being inverted relative to its true direction, and these errors were consistent across the range

of conditions used in each experiment. It is not known what leads to these specific errors of estimation, but the fact that there is a small but consistent proportion of the study population in this category leads to the question of whether this form of error could be related to the more general issue of bias in some way.

The second factor involves the finding of a difference in bias between observers who had spent considerable time playing 3-D computer games (self-reported) as opposed to those who had not. Those who had spent more time on games showed much less bias under all conditions. In previous research, a trend towards males having less heading bias had been noted. However, early on in this series of experiments a female participant was found to have estimates that more accurate than most, and she was found to have considerable experience with computers. Consequently, I carried out an informal survey of students as to the time they spent playing 3-D computer games. No statistical analysis of results was carried out, but overall results strongly suggest that hours spent playing with computer games has a more positive association with accuracy than gender. This finding puts a caution not only upon dividing observers simply on the basis of gender, but also upon the use of highly experienced computer users as participants in heading experiments, particularly when the overall number of participants is low. The potential for getting an overly optimistic view of performer abilities in such cases is high. This finding is lent support by Bavelier and Green (2003), who discovered that computer gamers scored off the charts in several standard vision tests, and that the visual skills of non-gamers improved dramatically after only 10 hours of playing action computer games.

Discussion

The results of the experiments summarised above show heading bias to be extremely robust to changes in a variety of experimental factors. Bias in Motion conditions was consistently larger than that found for Line conditions, however even for Line conditions some central bias occurred, and this indicates some amount of constant error that occurs in all heading estimates.

For Motion conditions, the consistent increase in bias with eccentricity of heading shows that whatever factor is leading to the bias increases with distance from the fovea. Because this bias was so robust to changes in object perspective and proprioceptive information, it must have derived from the motion of the flow field itself rather than from some other factor. Indeed, those experiments investigating various properties of the vector flow field demonstrated that scene depth and translation speed exert the major influence upon the bias. Speed appears to be the most important factor, with faster speed leading to more accurate estimates, although performance reached an asymptote at around $5m.s^{-1}$. Depth plays a secondary role in heading, and becomes important mainly when the translation speed is low, presumably because it increases dot speed. Overall screen motion is a function of the dot layout and heading direction, global image speed therefore needs to be calculated for each display. However, for any one point in the field, image speed is related to distance by a function such as: $\omega' = (v \sin w)/D$ (for the horizontal dimension)

v = speed
D = radial distance to a point
W = angle from heading vector to a point

As distance doubles, speed falls off at 1/D. i.e. it is a linear change, such that when distance increases from 12.5m to 100m (increasing 8x), the average speed decreases by eight times.

SECTION B

AN EXAMINATION OF THE ROLE OF ROTATION IN HEADING BIAS

Chapter 14

Rotation

The first section of this thesis has demonstrated the existence of a strong heading bias error that occurs when observers are asked to judge their heading direction in virtual computer generated 3-D worlds depicting motion through a field of random dots. The obvious question remaining to be answered is, why does this bias occur? This section of the thesis attempts to answer that question.

The results of the experiments summarised at the end of Section A show the bias to be extremely robust to changes in a variety of experimental factors. The consistent increase in bias with eccentricity of heading suggests that whatever factor(s) is/are leading to the bias must also increase as the distance of the FOE from the fovea increases. Because the bias was so robust to changes in object /scene perspective features and proprioceptive information it is most likely derived from the motion of the flow field. Indeed, those experiments investigating various properties of the vector flow field demonstrated that scene depth and translation speed exert the major influence upon the bias. Observer speed appears to be the most important factor, with faster speed leading to more accurate estimates, although the capacity for improvement appears to level out at $5m.s^{-1}$. When there was zero observer speed and no image motion (as in the line experiments reported in Experiment 2), the bias was greatly reduced. Depth appears to play a secondary role in heading, and becomes important mainly when the observer translation speed is low, presumably because the flow vector magnitudes increase with decreasing depth.

A matter of concern when trying to extrapolate the findings of computer-based experiments to locomotion in the real world is that the visual schema portrayed in them is

extremely artificial. There are very few settings in real-life navigation where one would gaze in a forward direction, not tracking any objects, while simultaneously moving towards a point to one side or the other. The difference between the motion portrayed in these computer displays and that experienced with physical navigation puts a note of caution over assuming that the results of the one should apply to the other.

In fact, the very artificiality of the present design could in fact be a factor contributing to the bias found in these experiments. With simple translatory motion, when one faces towards the current direction of heading, a radial pattern of flow is then located in the central visual area. In typical heading experiments and in the experimental design used in the present work, the heading direction is moved further and further out into the periphery while the observer is forced to maintain fixation on the centre of the screen. In real life scenarios, if we move our gaze away from the direction of heading so that the FOE moves into our peripheral visual field, we tend to start following objects in the world with our eyes. We tend not to experience the type of visual flow that is presented in heading experiments with the FOE well out in the periphery.

By maintaining fixation on the centre of the screen, the observer in these heading experiments experiences optical flow across the central visual area that grows increasingly unidirectional (lamellar) as heading eccentricity increases. This lamellar flow equates strongly with that experienced with rotational flow (usually generated by rotation of the body or eyes), and could potentially generate a rotation signal in the brain where none should occur. This rotation signal could, in theory, erroneously lead to a perception of visual rotation, either by triggering a physical eye movement or by eliciting a visual signal. This eye movement or rotation signal could in turn lead to a perceived shift in heading.

Figure 14.1 (a) shows screen shots of vector flow fields depicting translation motion to a point 15° to the right, compared with pure yaw rotations. Notice how the optical flow

in the central and left regions of the eccentric heading translation cases mainly has unidirectional motion (to the left in this case). This is very similar to the lamellar flow experienced during rotation of the body or eyes (Figure 14.1 (b)). It is therefore reasonable to expect that any system in the visual system designed to detect and respond to full field rotation would also be stimulated by the pattern of motion seen in this type of translation displays.

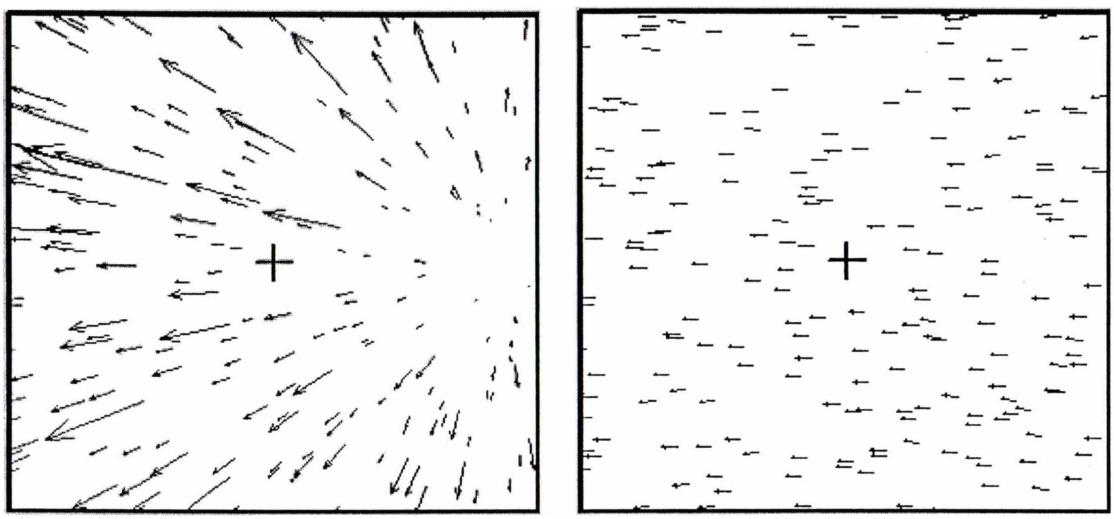

(a) (b)

Figure 14.1. Screen shots of vector flow field for: (a) translation through 25 m depth at 2 $m.s^{-1}$ with heading of +15°, and (b) yaw of $2°s^{-1}$

It is proposed here that the bias observed in the experiments reported in Section A of this work could be derived from the fact that lamellar components in the radial flow heading stimuli generate erroneous visual rotation signals in the visual system. In typical experiments on heading perception, the heading direction is moved further and further away from the direction of gaze and the observer is asked to judge their heading direction while maintaining fixation on the centre of the screen. The more eccentric the heading

direction becomes, the more unidirectional the image motion becomes (i.e. it becomes more lamellar). There are two possible ways in which this lamellar flow could affect a heading estimate: Either it could cause a retinal rotation signal, or it could drive a physical eye movement: either way, the pure translation stimulus specifying heading in a particular direction will be perturbed by the additional rotation signal and the apparent heading direction shifted.

Various models have been created that attempt to explain how rotational signals are dealt with retinally (e.g. Beintema & van den Berg, 2000; Perrone, 1992), but the exact physiological mechanisms by which such systems would operate are currently not clear. By contrast, there is a substantial body of work suggesting that a physical eye movement can be elicited by lamellar flow (see review following). It was therefore decided to proceed with the assumption that the flow drives a small eye movement, which in turn biases the perceived direction of heading.

The Effect of Lamellar Flow on Perceived Heading Direction

There is some evidence to suggest that perceived heading direction is biased by the superimposing of lamellar flow onto a radial flow field caused by forward translation. This support comes from research in two different areas. The first examines an illusory shift caused by combining radial and lamellar flow, and the second looks at the biasing effect of self-moving objects in the field. These will be considered in turn.

Illusory shift

Duffy and Wurtz (1993) described an illusory transformation of the flow field that provides further support for the idea of the biasing effect of lamellar flow. They presented

300 randomly distributed dots on a screen, of which half underwent radial motion centred on the centre of the screen, while the other half underwent unidirectional motion to the left or right. When human subjects were asked to find the FOE of the radial motion, they perceived it as being biased away from the centre of the display. The displacement was in the direction of the rotational motion, and opposite to the displacement predicted by the vector summation of the two types of motion. The explanation of this illusory shift offered by the authors was that the visual system interprets the rotational motion as a reafferent eye movement signal resulting from a horizontal eye rotation. This eye rotation is subtracted from the radial motion in order to compensate for the apparent eye rotation (Duffy & Wurtz, 1993, 1995a).

The mechanisms underlying this illusion were first investigated by Pack and Mingolla (1998). In a series of psychophysical experiments they added varying amounts of rotation to the expansion stimulus, and varied the speed and size of the planar motion field. Rotation was found to bias the perceived FOE in a direction perpendicular to the planar motion, and larger FOE shifts were found with greater speeds and sizes of planar motion fields, although the speed effect saturated at high speeds. They proposed that this points to the involvement of a global mechanism that subtracts coherent planar motion from the flow field, and may help to maintain visual stability during eye movements.

Grigo and Lappe (1998) examined the effect of stereoscopic vision upon the Duffy and Wurtz (1993) illusion and found that there was a significant decrease in error when stereoscopic cues were present. In a further experiment they varied monocular depth cues of dot size and dot number, and found that there was also a reduction in bias, but that this was not as large as for disparity. They concluded that the illusory optic flow transformation is modified by depth information, especially by binocular disparity.

Heading estimation in the presence of a moving object

While research into heading estimation has tended to concentrate upon motion generated by the movement of the observer, independent motion of objects in the visual field is also possible during self-motion (e.g. cars driving by or birds flying past). Although models of heading have not been designed to encompass such 'non-rigidity' of the environment, and the presence of moving objects would typically adversely affect their performance, people are able to move through a non-rigid environment with little difficulty. A range of experiments has been carried out to measure human heading ability in the presence of moving objects.

Both Royden and Hildreth (1994, 1995a, 1995b, 1996) and W.H. Warren and Saunders (1995a, 1995b) have reported that a moving object has no effect upon heading unless it crosses the observer's path. In the case when such a crossing did occur however, a biasing of the heading direction occurred. Unfortunately, the direction of the bias was different for each group. W.H. Warren and Saunders (1995 a, 1995 b) found biases in the direction opposite to the object's motion, while Royden and Hildreth (1996) obtained a small bias towards the object's direction of motion. It is not known why such a difference in the direction of bias should occur; however, in both cases the bias was only present when the FOE was obscured. Royden and Hildreth (1996) also found that no bias occurred when a static object obscured the FOE, which implies that motion of the object is necessary.

The nature of the occluding object may have other aspects of interest. W.H. Warren and Saunders (1995b) found that when the object outline contained no dots the bias disappeared, whereas Royden and Hildreth (1996), while still finding a bias, noted it was much reduced when no dots were present in the object. This suggests that, in addition to the presence or absence of the FOE, relative motion between texture elements in the scene

and within the object itself may enhance the bias.

Eye Movements Induced by Lamellar Flow

As mentioned above, heading experiments that use high eccentric heading angles (e.g., 10° or 15°) result in the observer being subjected to a fairly strong lamella type of flow (see Figure 14.1). It is important to note that this form of flow observed in these experiments is reasonably uncommon in real-life situations. In fact, the visual system appears to incorporate systems to avoid having such a pattern of rotational flow moving across the static eye. To do this, gaze stabilization mechanisms are used to keep the images of objects steady on the retina and it has been suggested that smooth pursuit developed especially for this purpose (Eckert & Buchsbaum, 1993; Miles, 1994). We know that deficits in gaze stabilization are associated with impaired vision during locomotion (Grossman & Leigh, 1990). As well as bringing the object onto the fovea and keeping the image as stable as possible in this region, smooth pursuit aids in the estimation of heading by reducing the dimensionality of the self-motion estimation problem (e.g. Longuet-Higgins & Prazdny, 1980, Perrone & Stone, 1994).

Visually driven reflexive movements produced in response to motion of the visual field have been observed. Such eye movements are involuntary, and are characterized by slow pursuit movements alternating with rapid saccadic return movements. The slow phase can be elicited by a movement of the visual surround and is produced by the ocular following reflex or optokinetic nystagmus (OKN). The ocular following reflex describes the initial (60 – 150 ms) ocular reaction to the onset of motion of a visible scene. Another reflexive movement is produced in response to the motion of the head, and is called the vestibulo-occular reflex (VOR). However as the observers used in the experiments

reported in this thesis had their heads held in a chin rest, this type of motion is not applicable to the current experimental design.

To record OKN, the observer is usually placed at the centre of a revolving cylinder, the inside of which is covered with vertical black and white stripes which fill the visual field completely, or contains no inhomogeneities upon which the person can anchor their gaze. As long as the drum is not moving too fast, the observer's eyes tend to follow the drum as it moves. Eventually the eyes are carried too far from the primary position and a fast saccade is made back to bring the gaze back to fixation. The velocity of the slow-phase of OKN is close to the speed of the stimulus up to a speed of $30°s^{-1}$, when it also has a mean duration of around 0.3 s and a deviation of some 2°. At faster speeds the eyes lag more and more behind the stimulus, until at about $100°s^{-1}$, the regular pattern of the OKN breaks down completely (Honrubia, Downey, Mitchell, & Ward, 1968). The velocity of the fast-phase of OKN is almost identical to that of normal saccades.

For accurate pursuit it is important for optokinetic nystagmus (OKN) to be suppressed during pursuit because OKN causes the eye to move in the same direction as the large stimulus, so an OKN triggered to track retinal motion of a background during pursuit would cause an eye movement in the opposite direction to the ongoing pursuit movement. However, background movement could also play an important role in estimating the velocity of pursuit eye movements, so the visual motion of the background has contradictory effects on the pursuit system.

The OKN and ocular following reflexes appear to be mediated primarily by the central visual field (Dubois & Colleqijn, 1979), whereby a lamellar flow pattern induces a tracking eye motion. The retinal image is used directly, as the eye movement follows the motion in order to minimize retinal image slip and generate a stable image. For rotations of the head or body, OKN will attempt to null retinal image motion by adjusting eye speed to

the speed of the visual motion, and this works best for low visual speeds. In the case of translation however, accurate image stabilization needs to take into account the geometry of the visual scene. If the object is close to the eye, the induced visual speed is much greater than if it is further away. A scaling of eye speed with viewing distance has been confirmed for humans (Busettini, Miles, Schwarz, & Carl, 1994).

Studies confirm that OKN is elicited by displays of optical flow simulating self-motion. Lappe and colleagues (Lappe, Pekel, & Hoffmann, 1998, 1999; Niemann, Lappe, Büscher, & Hoffmann, 1999) recorded spontaneous OKN – type eye movements for humans and macaque monkeys watching large-field radial optic flow simulating motion over a ground plane with heading directions of 0, 10 or 20° to the left or right. When observers were asked to attend to motion across the entire field, a typical oculomotor response consisting of alternating slow tracking phases and saccades at a frequency of approximately 2 Hz was found. There was a close correspondence between the eye movement direction of the slow phase and the local motion direction in most cases. However the speed of this motion was very often considerably lower than the corresponding local stimulus speed in the fovea, with an average gain ratio of 0.5 for humans and monkeys. However when flow from the entire visual field was averaged, a much higher gain was obtained.

Mestre and Masson (1997) looked at eye movements in the presence of sideways translational flow generated with a selection of depth planes. They found that such a display elicited optokinetic eye movements, and not merely active visual pursuit. In the pre-attentional phase of processing (up to 400 ms) and during steady-state OKN (with more than 10 object velocities simultaneously displayed) they found the OKN to be modulated by the average speed of motion. However when observers were instructed to pay attention to the global scene and for longer viewing times, they tended to track with a velocity

dominance tuned to the slowest velocity in the display.

OKN is inhibited in the presence of a stationary fixation object (Howard, 1982). However, this inhibition is not complete, and a small amount of eye movement still occurs (May, Flanagan, & Dobie, 2001). This is especially true of the optokinetic following reflex, which occurs 60-150 ms after the presentation of a moving field, and is almost impossible to inhibit.

On the basis of this research it appears reasonable to assume that the lamellar component of the heading displays in Section A could induce a physical eye movement.

Physiological Processing of Eye-Body Rotations

Although Section A of this thesis contains a review of the physiology believed to underlie heading estimation it is now useful to examine more closely some of the physiology associated specifically with rotation processing.

Area MST appears to be the region of the brain most likely to process rotational information, and both retinal and extra-retinal rotation signals appear to be dealt with there. For example, target motion is known to be represented in MST by both visual and efference copy signals, and a number of studies have indicated that MST cells responses are linear with log target velocity for a range of velocities consistent with smooth pursuit eye movements. This has been demonstrated for MST responses to visual motion stimuli (Kawano, Shidara, Watanabe, & Yamane, 1994; Tanaka, Sugita, Moriya, & Saito, 1993) and for efference copy signals when retinal stimulation is absent (Komatsu & Wurtz , 1988; Sakata, Shibutani, & Kawano, 1983). The data indicate that MST cells maintain a representation of target velocity. If this is true, then increasing the activity of the MST cells during smooth pursuit should increase the velocity of eye movement. Komatsu and Wurtz

(1988) verified this by introducing electrical stimulation of MSTv neurons while monkeys made smooth pursuit eye movements at different speeds. Stimulation biased pursuit velocity towards the stimulated hemisphere.

Directional selectivity has also been found in MST. Erickson and Their (1991) observed that a large quantity of MST cells responded in a direction sensitive manner to stimuli moving across their receptive fields during fixation of a stationary point. When the same retinal stimulation was obtained by moving the eye across a stationary stimulus, directional sensitivity was lost. This effect was not observed in MT. Thus MST seems to maintain an extra-retinal representation of stimulus motion or stationarity that is largely independent of retinal stimulation.

Recent studies in macaque monkeys suggest that correction for pursuit eye movements may occur in MSTd because these neurons are tuned to the retinal position of the FOE, and modify their tuning during pursuit to partially compensate for the focus shift. Wurtz and colleagues did not find any evidence of pursuit-related activity in area MT except for a small region of the fovea, but found many neurons in MSTd in which activity during pursuit continued even when the target was blanked (Wurtz, Komatsu, Dursteler, & Yamasaki, 1990b)

Further, in the lateral part of MSTd, 'pursuit' or 'visual tracking' neurons have been found (Bradley et. al., 1996; Newsome, Wurtz, & Komatsu, 1988; Page & Duffy, 1999; Wurtz, et al., 1990b). These neurons seem to have a preferred axis of rotation, and fire at a rate roughly proportional to eye velocity (Thier & Erickson, 1992a).

Although this does not rule out the possibility that eye movements might affect the input to the MST cells, within area MST itself an interaction between eye movement signals and motion-pattern sensitive cells is more likely. Rather, direct evidence has been provided for such a transformation involving eye velocity signals. Bradley et al. (1996)

examined neurons in MSTd to test how optic flow and eye velocity signals might be used to compute the direction of self-motion. The results demonstrated that MSTd neurons use a pursuit signal to effectively subtract visual-motion artefacts introduced by moving the eyes. However they found that compensation of MST tuning for ongoing head or eye movements is incomplete. Bradley et al. suggest that linear combination of the activity of cells with different preferred retinal centres of expansion and the linear weights modulated by pursuit can explain their major results. Modulation of the activity of retinal heading templates by pursuit signals provides a mechanism of arriving at a template in which the preferred heading is less sensitive to rotational flow.

Evidence for vestibular signals related to head rotation in MST has been presented by a number of researchers (Kawano, Sasaki, & Yamashita, 1984; Their & Erickson, 1992). These signals could be used as an efference signal, to maintain a representation of target velocity during head and body movements, and to nullify the resulting retinal motion of the background. The latter function has been observed in a population of cells in MSTd. Shenoy, Bradley, and Andersen, (1996) found that MSTd neurons are able to shift their tuning in a similar way whether displacement is caused by pursuit or by whole body rotation with fixed head direction and gaze – Vestibulo-occular reflex cancellation (VORC). The experiment demonstrated that many MSTd cells compensate for general gaze rotation, whether produced by eye movement or by body rotation. A simulated pursuit condition revealed that neurons compensate more given VORC or pursuit signals than for retinal signals alone. For the simulated rotation, rotational flow drives approximately 50% of complete compensation, whereas when VORC or pursuit cues are also available, the level of compensation reaches 80 and 90% respectively. This evidence suggests that most MSTd neurons use a combination of retinal and VORC or pursuit cues to compensate at least partially for the retinal effects of gaze rotation. These results also implicate MSTd in

the computation of heading. The authors suggest that MSTd may use vestibular information to create a compensated heading representation within at least a subpopulation of cells, which is accessed perceptually only when additional cues relating to active head rotations are also present.

Britten and van Wezel (2002) examined heading estimation in macaque monkeys simultaneous with microstimulation. Activation of MST frequently affected performance, usually causing heading bias. The induced biases were often large and usually concordant with the preference of the neurons being activated. The bias frequently depended on the pursuit condition. Stimulation had a greater effect with pursuit than without it. Further, pursuit in a particular direction facilitates the effects of micro-stimulation in the same direction, independent of the magnitude of the effect without pursuit. Compensation is larger and more consistent under pursuit than simulated rotation. Also, under left pursuit, monkeys made more left choices as predicted by under-compensation for the retinal effects of eye movements. This is because horizontal pursuit produces retinal image motion in a direction opposite that of the pursuit. Adding such motion shifts the FOE in the direction of pursuit (Regan & Beverley, 1982; Duffy & Wurtz, 1997), which then causes a bias in the direction of pursuit if not compensated for.

Taken as a whole, the body of research examining rotation processing in MST suggests that MSTd is the most likely site of such compensation. It appears that visual information, eye-movement signals and vestibular information are incorporated into the output of this region. MSTv also appears to have its own role to play as it is known to contain a representation of target velocity (Komatsu & Wurtz, 1988), however not so much is known about the processes involving neurons in this pathway.

Aims

As an extension to the experimental investigation into bias already completed, it was decided to investigate the possible influence of eye movements in causing the bias found in Section A. To do this, an attempt will be made to replicate the results of Experiment Ten (Chapter 11) using a heading model developed by Perrone (1992). This work is detailed in Chapter 14.

CHAPTER 15

Detecting Visual Rotation in Optical Flow Fields

The Perrone (1992) Self-motion Estimation Model

Early models of self-motion estimation were designed to recover the instantaneous direction of heading, any rotation about three axes (roll, pitch, and yaw) and the relative distances of the points in the environment from the visual motion information projected onto a 2-D image plane. Perrone (1992) presented a model of how a biological visual system could achieve this using the properties of cells in areas MT and MST of the primate brain. Briefly, 2-D motion sensors are connected into networks (templates) that recover the translational heading direction of the observer, and detect any rotation.

The basic elements of the translation detectors are the speed- and direction-tuned neurons commonly found in area MT. Directionally selective neurons respond maximally to motion across their receptive fields in one direction, and if the motion is not in this direction, their output is reduced by an amount dependent upon the 'bandwidth' of the neuron. A normalised Gaussian function is used as a model of directional tuning in the Perrone model. Neurons in MT also respond maximally when the motion across their receptive field falls within a fairly narrow band of speeds. This speed tuning is also simulated using a Gaussian function in the Perrone model.

Although the Perrone model does not require an accurate estimate of image speed at each point in the visual field, it does need at least one 2-D motion sensor at each location to respond to the motion. Therefore it is assumed that each location is sampled by a range of MT-like motion sensors each tuned to a different range of speeds and directions. The speed

and direction outputs of the sensors are computed separately, with the total output of the local 2-D motion sensor (simulating MT neurons) arising from the product of the speed and direction outputs. By combining the outputs from a number of the MT-like 2-D motion sensors that have their preferred directions radially aligned, and have their receptive field in the appropriate place, a forward translation detector (or heading template) can be generated that responds selectively to the radial expansion pattern surrounding the FOE. These detectors work like MST neurons, and sum motion information from across the whole visual field. Any motion towards the FOE is subtracted from the total activity of the detector, as it provides evidence against translation in that direction.

In order to sample the full range of possible heading directions there is a need for many heading detectors distributed across the visual field. The task of finding the FOE therefore becomes one of finding the detector with the greatest total activity. In the model these are arranged using equal, arbitrary steps of 5° steps of azimuth and elevation from –85° to +85°, thus generating a 35 x 35 array of translation detectors.

Rotation is detected in a similar manner, independent of translation, and is extracted prior to translation. This process relies on the fact that during combined translation and rotation movement of the observer, the image motion of distant points consists mostly of rotational components, and given that there are sufficient distant points in a scene (an consequently show little motion), a large part of the visual field will not register translation.

Detectors designed to pick up rotation need to sample a large area of the visual field, summing the activity from motion sensors tuned to the same direction. The speed tuning for each motion sensor making up the detector network needs to be identical for all positions in the visual field, as rotation-induced flow fields are unidirectional (at least for the central visual field) with a high level of uniformity of the image speeds. By contrast,

motion with a large proportion of translational flow tends to be multidirectional and for most scenes, exhibits a wide range of image speeds.

In order to capture a range of rotation speeds, the Perrone model uses a range of rotation detectors, each tuned to a different rotation speed. The decision on how many are required is somewhat arbitrary, but Perrone (1992) used the following range: 1.5, 3.0, 6.0, 9.0, and 12.0°s^{-1}. Detectors also need to cover a range of directions, and the model covers the full 360° of directions about the centre of the field with 5° steps between them. Each rotation detector is tuned to a different direction that represents a different combination of yaw and pitch.

Each rotation detector sums the activity from MT-like 2-D motion sensors that have their peak responses at a given speed. Such a detector was designed by Perrone to mimic the properties of a certain class of MST neurone tuned to unidirectional motion. The total output of the 2-D sensors tuned to 0° and a particular speed are summed across the whole field. The total output of sensors tuned to 180° and a particular speed are also summed and subtracted from the total 0° output to give the net output for the 0° direction rotation detector. The sensitivity of the model is improved by the subtraction of any activity from motion sensors with a preferred direction that is 180° from the primary direction of the sensors in the detector. This produces low levels of activity when the field contains motion in many directions, as is the case during translation.

The Perrone rotation detector model assumes direction- and speed-tuning curves and output mechanisms similar to those used for the heading detectors described earlier. The procedure for determining the different levels of total activity is also similar. For each direction the output for each MT-like 2-D motion sensor in the field is calculated based on the image speed relative to the optimum speed for the sensor and the difference between the preferred direction and the image-motion direction. The speed and direction outputs are

multiplied together to give the combined activity for that 2-D sensor, and the output from that sensor is summed with activity from all of the other sensors in the field to give the total output level from the rotation detector. This is repeated for the other rotation detectors, tuned to different directions and rotation rates. The rotation detectors give a measure of rotation in parallel with the operation of the translation (heading) detectors.

Method

The current work aims to investigate the idea that some of the heading stimuli used in Section 1 of this thesis contain a rotation component that could trigger an eye-movement and hence introduce the heading estimation biases that were observed in so many of the experiments. In the work that follows, a rotation detector model will be used to show that the rotation signal present in the heading stimuli is correlated with the heading bias errors that occurred in these experiments (specifically Experiment 10).

The original heading model proposed by Perrone (1992) was developed in order to better simulate a rotational component. This development was done in consultation with the original author. In the modified form use was made of an extended set of rotation detectors tuned to a wide range of speeds (0.25, 0.5, 0.75, 1.0, 1.5, 2.0, 2.5, 3.0, 3.5, 4.0, 4.5, 5.0°s^{-1}) and directions (0 - 360°, in steps of 15°).

The original model used log-Gaussian speed tuning for the MT units, but subsequent research by Perrone and Thiele (2001, 2002) has revealed more about the speed tuning of neurons in the MT region. Consequently the rotation detectors were modified to fit this new form of MT tuning. A description and plot of the new speed tuning curves can be found in Perrone and Thiele (2002, see their Figure 5).

For the new version of the rotation detector model, the net output of each of the rotation detectors is determined somewhat differently from the way it was done in the original model (Perrone, 1992). In the original rotation detectors, there was only one form of inhibition. It came from the MT-like motion sensors tuned to the opposite (180° away) direction from the optimum direction tuning of the detector. The results of our modelling efforts have revealed that this basic form of inhibition is insufficient to account for several classes of heading bias data found in Section A of this work.

In the new modified rotation detector model, inhibition is derived from MT-like units tuned to different directions and speeds. In contrast to the earlier work, the amount of inhibition at each location is weighted by an amount depending on the following rules:

Direction weight = $w1 = e^{-0.5\left(\frac{(\alpha-\vartheta+180)^2}{\sigma^2}\right)}$ where θ = the rotation detector preferred tuning direction, and α = the preferred direction of the MT-like sensor and σ is the tuning bandwidth of the direction inhibition (set at 60°).

Speed weight = ($w2$ = s1/S if s1 < S or $w2$ = S/s1 if s1 > S).

Where s1 is the speed tuning of the MT-like sensor and S is the optimum speed preference of the rotation detector.

Total weight = $w1$ x $w2$

The direction weighting process (based on a Gaussian function) provides a greater level of inhibition from MT-like 2-D sensors tuned to directions 180 deg from the optimum tuning of the rotation detector and less inhibition from directions close to the optimum tuning of the detector. It also provides inhibition from sensors that are tuned to different speeds from the optimum speed tuning of the rotation detector, with a greater amount of inhibition arising from sensors tuned to very different speeds from the optimum speed. These features of the new rotation model were added to make the rotation detectors more sensitive to visual rotation in optical flow fields. Pure visual rotation is characterised by uniform directional image motion and uniform speeds. Any evidence of multiple directions

or multiple speeds is counter to the idea that visual rotation is present and so it should inhibit the visual rotation detector.

Another feature was added to the original Perrone (1992) model by weighting the activity of the 'winning' rotation detector (the one with the maximum output) by the optimal speed tuning of the detector. In the original model, just the speed of the winning unit was passed onto the next stage of self-motion estimation processing. It was found that the activity of the units also has to be taken into account in order to fit the data from Section A.

The input to the rotation detector model is simulated using the theoretical 2-D motion vectors generated by the particular heading scenario used in the heading experiments (see Experiment Ten). The steps for determining the rotation activity being generated by the optic flow field are as follows:

1. For a particular rotation detector (R) tuned to direction θ and rate S, test each vector in the flow field against an MT-like sensor tuned to direction $\alpha = \theta$ and speed S with the direction and speed tuning properties described above. This produces a local activity level A_i.

2. For all of the flow vectors over the field (T), sum the activity from all of the different MT sensors, i.e. find $P = \sum_{i}^{T} A_i$. This is the amount of positive activity for the unit R

3. Repeat Step 1 using values for the preferred direction tuning (α) of the MT-like sensor that sample the 360° range of directions (in 15° steps) and multiply the

activity coming out of the MT sensor by the direction and speed weights given above.

4. For all of the flow vectors over the field (T), sum the weighted inhibitory activity from all of the different MT sensors, i.e., find $N=\sum_{i}^{T} I_i$. This is the amount of inhibitory activity for the unit R.

5. The total activity for the rotation detector R is then found from P/N (divisive inhibition).

6. Repeat all of the above steps for a range of rotation detectors tuned to different directions (θ_k) and speeds S_k.

7. Find the rotation detector that has the maximum activity and multiply its activity by the optimum speed tuning of the detector (S). This is the final output of the rotation detector network and it represents the hypothetical rotation signal that it is suggested drives the eye movements causing the heading bias.

(A copy of the modified model is available from Dr. J. Perrone, University of Waikato, Private Bag 3105, Hamilton, New Zealand.)

Results

In order to test the adapted rotation model, the data generated in Experiment Ten (Chapter 11), which varied speed at depths of 25 and 100 m, were used to provide the underlying data with which the model could be tested. This experiment was selected because it gave the best range of biases and thus provided a rigorous test for any model.

First, the yaw rate required to provide the observed mean heading estimate for each condition was determined from the data. This was found by incrementally adding a small amount of yaw to the pure translational flow until the heading detectors (see Perrone, 1992) responded maximally at the observed heading direction value. The final amount of yaw determined by this procedure represents the assumed amount of eye rotation that occurred (on average across all participants) during the particular heading trial. The results of this are shown below in Table 15.1.

Table 15.1

Computed yaws ($^{o}s^{-1}$) required to give estimated headings found in Experiment 10.

Condition		**15°**	**10°**	**5°**	**0°**
25 m	1 $m.s^{-1}$	0.60	0.35	0.15	0
	2 $m.s^{-1}$	0.73	0.40	0.18	0
	3$m.s^{-1}$	0.85	0.40	0.12	0
	4 $m.s^{-1}$	1.00	0.50	0.18	0
100 m	1 $m.s^{-1}$	0.20	0.15	0.08	0
	2 $m.s^{-1}$	0.26	0.12	0.15	0
	3$m.s^{-1}$	0.26	0.12	0.07	0
	4 $m.s^{-1}$	0.35	0.15	0.07	0
	5$m.s^{-1}$	0.30	0.12	0.00	0

Under the hypothesis that eye-movements during the trial are causing the heading bias, the values in the Table 15.1 represent the yaw rate of the eye that would have occurred under the different experimental conditions. The next stage of the modeling process was to compute the output of the rotation detectors (using steps 1-7 above) for each of the experimental conditions. Neuronal rotation activity was therefore computed for each of the conditions in Experiment Ten, using a set of rotation detectors tuned to a wide range of speeds (0.25, 0.5, 0.75, 1.0, 1.5, 2.0, 2.5, 3.0, 3.5, 4.0, 4.5, 5.0°s^{-1}) and directions (0 - 360°, in steps of 15°). The results (in arbitrary units) are given in Table 15.2.

Table 15.2

Net activity for the winning Rotation detectors for each of the conditions of Experiment 10

Condition		15°	10°	5°
25 m	1 $m.s^{-1}$	85	25	12
	2 $m.s^{-1}$	131	47	24
	3$m.s^{-1}$	170	67	30
	4 $m.s^{-1}$	183	85	42
100 m	1 $m.s^{-1}$	34	16	5
	2 $m.s^{-1}$	48	17	7
	3$m.s^{-1}$	49	23	11
	4 $m.s^{-1}$	75	33	11
	5$m.s^{-1}$	75	34	16

Earlier in this work it has been suggested that the heading stimuli contain certain amounts of lamellar flow and that this flow could be generating activity in rotation detectors (in the MST area of the brain). The output of the rotation detectors causes an eye-movement to occur (in the yaw direction) which affects the retinal flow occurring on the eye and this leads to heading bias. If this hypothesis is correct, there should be a positive relationship between the output of the rotation detectors (Table 15.2) and the amount of yaw alleged to produce

the bias in the heading experiments (Table 15.1). A regression analysis was carried out, and the results of this are shown in Figure 15.1 and Table 15.4 below. The exact level of gain between the level of activity and the amount of yaw predicted is not known, but the aim of this analysis is to demonstrate that the two are related in some way.

Table 15.3

Linear regression statistics for net neuronal rotation detector output against yaw rate for bias.

Slope	95% C.I.	Intercept	95% C.I.	R	p
5.091	4.449 to 5.733	0.0356	-0.008 to 0.079	0.956	<.0001

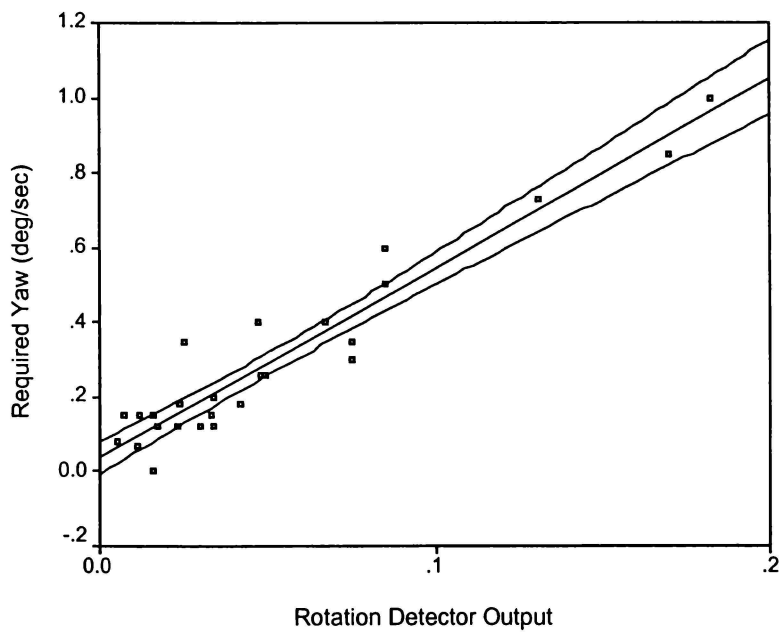

Figure 15.1. Scatterplot and regression line (± 95% C.I.) for net output of rotation detectors against computed yaw values for Experiment 10.

Table 15.4

Yaw values derived from the regression equation

Condition		15°	10°	5°	0°
25 m	1 $m.s^{-1}$	8.0	7.8	3.7	0
	2 $m.s^{-1}$	9.8	8.1	4.0	0
	3$m.s^{-1}$	10.7	8.2	4.0	0
	4 $m.s^{-1}$	11.5	8.5	4.2	0
100 m	1 $m.s^{-1}$	5.5	4.8	2.4	0
	2 $m.s^{-1}$	6.6	6.4	3.0	0
	3$m.s^{-1}$	9.9	7.5	3.4	0
	4 $m.s^{-1}$	9.3	7.5	4.0	0
	5$m.s^{-1}$	10.6	7.8	3.7	0

Using the regression equation a new set of yaw values was computed for the experimental conditions used in Experiment Ten. In order to compare the heading results predicted by these yaw values with those obtained in Experiment Ten, these yaw values were inserted into the heading model (Perrone 1992). The results of this are shown below in Figures 15.2 to 15.5

Overall there is a remarkably close correspondence between the experimentally determined pattern of heading biases and the patterns predicted when rotational movement is carefully accounted for in the modified Perrone model.

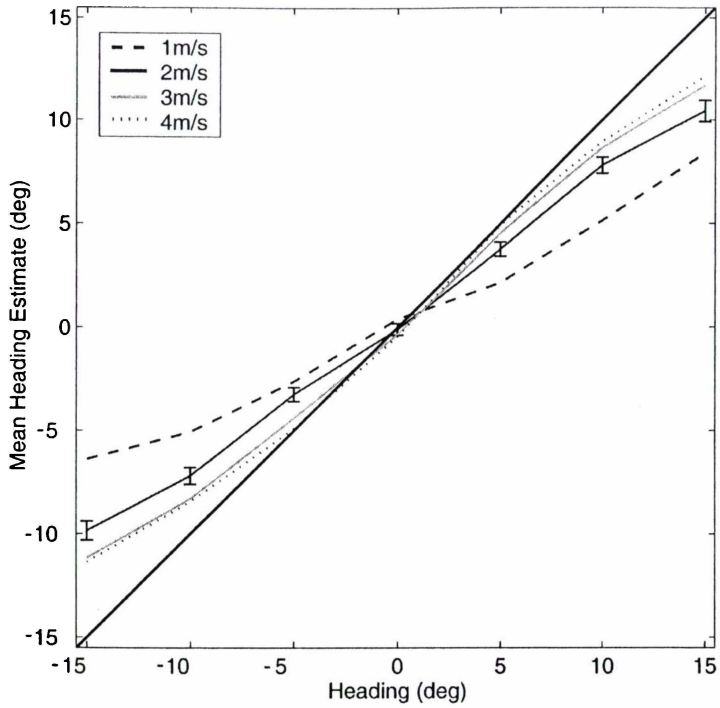

Figure 15.2. Mean Experimental Heading Estimates for speed with a depth of 25 m. Veridical performance is shown by the 45° line.

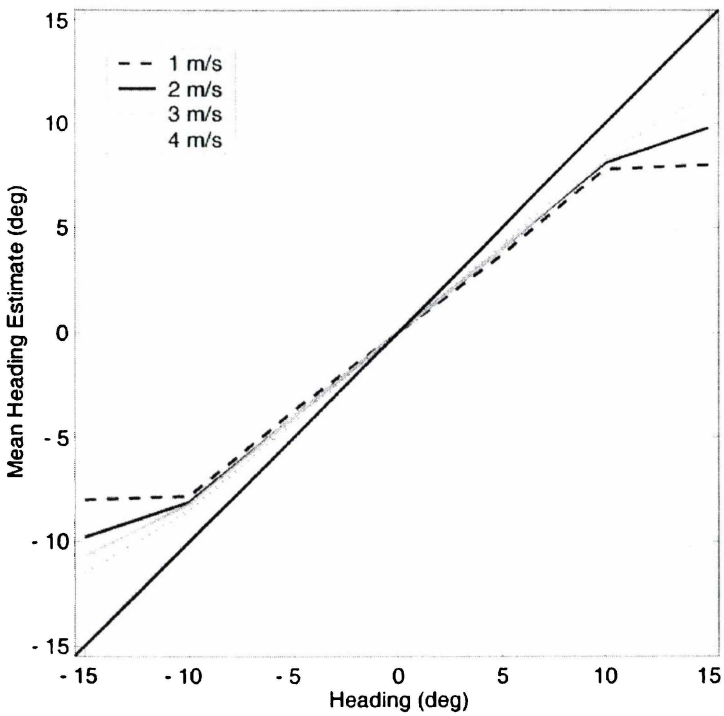

Figure 15.3. Predicted mean heading estimates for speed with a depth of 25 m. Veridical performance is shown by the 45° line.

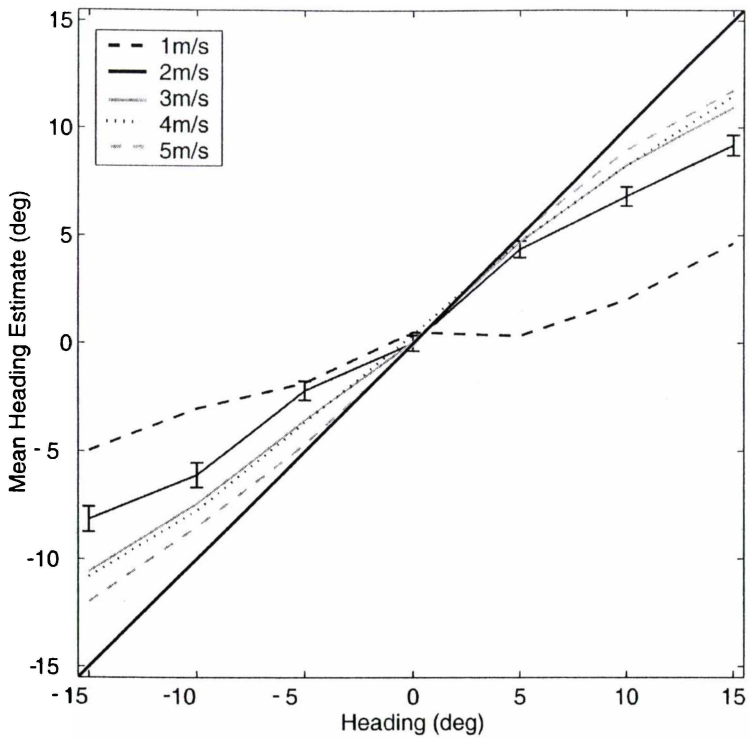

Figure 15.4. Mean Experimental Heading Estimates for speed with a depth of 100 m. Veridical performance is shown by the 45° line.

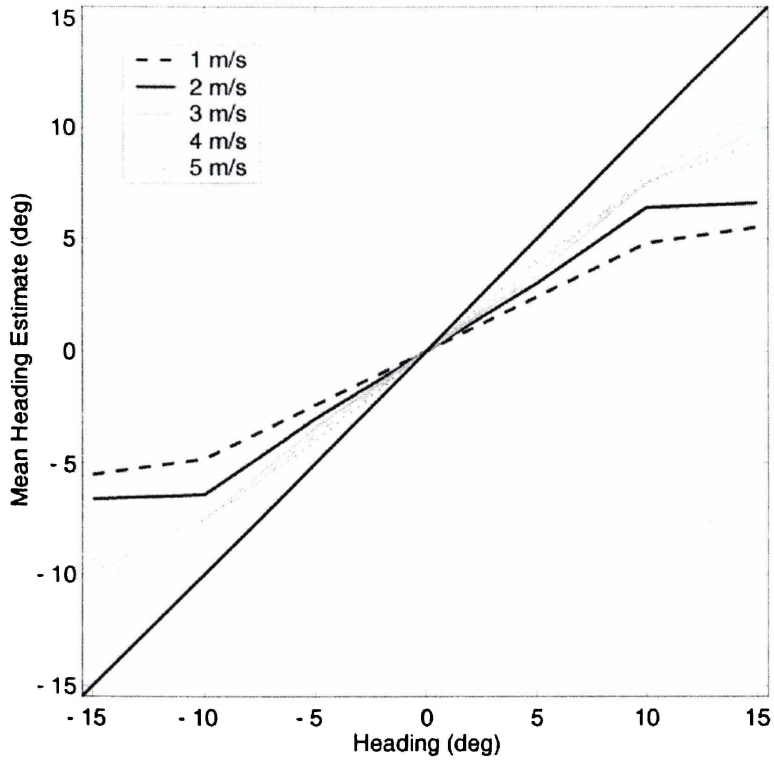

Figure 15.5. Predicted mean heading estimates for speed with a depth of 100 m. Veridical performance is shown by the 45° line.

Discussion

The work presented here is concerned with discovering the effect of rotation signals upon the accuracy of heading estimation, and the neural mechanisms that underlie this process.

In order to achieve this, the Perrone (1992) heading model was modified in such a way that rotation detectors were used to drive physical eye-movement behaviour in response to lamellar flow. When an observer fixates the centre of a screen showing simulated heading, any self-motion information shown on the screen is transformed into a 2-D retinal image showing full-field motion. The modified Perrone model incorporates that assumption that the lamellar component of the flow is detected by rotation detectors in the models, and the detectors produce a level of activity which drives an eye movement in the same direction as the dominant component of the lamellar flow. This eye movement modifies the flow field, and the heading detectors determine heading based on this altered flow, thereby biasing the perceived heading direction in the direction of the eye rotation. Thus the bias observed in these experiments is largely derived from the capacity for the visual system to confuse the lamellar component of radial flow with a full field rotation.

Using this model it was found to be possible to reproduce the pattern of central bias observed in human estimation of heading with a correlation of 0.96 being obtained between the predictions of the model and the experimental results found in Experiment 10. There are a few exceptions to the accuracy of prediction. For both the 25 m and 100 m depths, the predicted estimates for the 1 $m.s^{-1}$and 2 $m.s^{-1}$conditions were somewhat more accurate than those actually observed in the experimental data. However the difference is slight and mostly occurs with headings of 5° and 10°. For the 100 m depth there is also a reversal in accuracy between the 3 and 4 $m.s^{-1}$ conditions at the 15° mark, which is not observed in the

experimental data. However these differences are minor when the overall trend of the data is considered.

The close correspondence between experimental and modelled results adds support to the hypothesis that a large component of heading errors observed in the Motion conditions are due to the misperception of rotation in the presence of lamellar flow. The agreement between experiment and model does not constitute definitive proof of this, but it does strengthen the case substantially.

The eye movements elicited by the lamellar flow are presumed to be similar to those of an OKN movement. Although OKN is inhibited in the presence of a stationary fixation object (Howard, 1982), this inhibition is not complete, and a small amount of eye movement still occurs, especially in response to the first few milliseconds of a display (May, Flanagan, & Dobie, 2001). In the present work the amount of yaw required to cause the observed bias is extremely slow, in all cases less than $1^{o}s^{-1}$. Therefore we can be reasonably confident that such eye-movements could occur. Unfortunately, the small size of the eye-movements concerned means that they are unable to be quantified with the measurement tools currently available to me.

One possible area of dispute relating to this model concerns the use of an extra-retinal signal to perturb the flow field. Corollary discharge theory proposes that information about the observer's eye movements is provided by signals generated whenever the observer moves his or her eyes (Teuber, 1960, cited in Goldstein, 1989). These signals are of two forms, retinal (visual) and extra-retinal. According to this model, we will not see movement when both a retinal and extra-retinal signal reach the 'comparator' together, but we will if only one reaches the comparator such as is the case when the eyeball is physically moved with a finger (visual alone) or when an afterimage is pursed in the dark (extra-retinal alone).

It is generally believed that when a physical eye movement is made, the visual system is able to fully account for this motion, either by visual means or through an oculomotor efference copy, and to discount it from the resulting visual flow, meaning that, in the current case, the inferred FOE would once again accurately specify the direction of heading (Royden Crowell & Banks, 1994; W.H. Warren & Hannon, 1990). This creates a problem for the model outlined here. However there is reason to believe that extra-retinal motion is not encoded veridically, as experiments examining the Filehne illusion have consistently found a gain ratio less than 1 for extra-retinal motion (Freeman, 1999; Freeman & Banks, 1998; Freeman, Banks, & Crowell, 2000).

Although it is likely that a physical eye movement is made in response to the rotation detector activity, it is still possible that an eye movement is not made but that the visual motion changes the expansion flow field motion in some way. Duffy and Wurtz (1993) have suggested that one possible explanation is that the visual system interprets lamellar flow as a reafferent eye movement signal resulting from a horizontal eye rotation. Applied to this work, the implication is that this eye movement signal is then subtracted from the radial motion in order to compensate for the apparent eye rotation, thereby creating an error in heading estimation. The perceptual shift is different from that predicted by vector summation, which would predict a shift in the opposite direction to the lamellar flow. Similarly, Post and colleagues (e.g. Post, Shupert, & Leibowitz, 1984) have suggested that observation of a translating pattern in combination with stable fixation would evoke mis-registration of an eye movement in the opposite direction to the flow due to a suppression of optokinetic nystagmus, which could potentially be induced if there were no fixation. This proposition is supported by the studies using simulated and actual eye-movements in heading estimation. When physical eye movement information was not available, the perceived direction of heading was biased in the direction of the simulated

eye movement (Regan & Beverley, 1982). In the absence of any firm evidence for a physical eye movement having occurred in response to the experimental stimuli in the current work, the possibility of such a process being at work has to be considered.

Another possibility, suggested by Perrone (1992), is that preferred directions of the heading detectors may be modified in response to the lamellar flow. There is some evidence for the modification of MT neurons based on full-field stimulation of the field (Allman, Miezin, & McGuinness, 1985), however, it is not entirely clear how such a system may work physiologically.

Although the ratio of eye-movement speed to neural activity in the new model was chosen to give us the closest match to the average data for the group of observers, individual performance differs in heading estimation, and the model is also able to account for this. It is likely that people have different gain mechanisms at work. For example a larger net output for the rotation detectors would give a larger yaw eye movement, which would in turn bias the perceived heading further away from the true direction. This response would explain the results found in earlier experiments for those individuals whose responses were inverted relative to the true heading direction. It would be interesting to expose such a group of individuals to various OKN inducing stimuli in order to quantify their responses to various speeds of motion when compared to a 'normal' population. A smaller eye movement response would give an increased level of accuracy relative to the mean. Such individuals would be better able to stabilise their eye against these small movements. Given the difference that the present work found between those with considerable computer experience and those without, it is likely that such stabilisation techniques can be learned over time.

CHAPTER 16

Final Discussion and Conclusions

Overview

A number of experiments have been carried out in the field of self-motion perception to examine heading estimation, including those in section A of this thesis (see summary chapter 13, 150). Although the computer-based experimental paradigm used in this research has become very pervasive and is still being used extensively, the type of visual optical flow used in these displays is relatively uncommon, as humans do not generally fixate in a forward direction whilst moving off to the side in everyday navigation. In such a situation when the eye is fixated on the centre of the screen, various amounts of lamellar flow move across the foveal region, and rotational signals would grow increasingly strong with heading eccentricity. It is proposed therefore, that a significant component of the heading bias observed in this and previous work in this area is largely a result of the particular experimental stimuli being used to test heading perception.

In order to avoid having rotational flow moving across the static eye, the visual system probably incorporates a mechanism whereby the viewer's eyes actively pursue some point in the world, or continually re-fixate their gaze upon the current direction of heading (Cutting et al., 1992; Land & Lee, 1994; Solomon and Cohen, 1992a, 1992b; Wagner, Baird, & Barbaresi, 1981). The exact method of gaze stabilization will depend upon the type of observer motion being undertaken.

Modelling Results

Using a model developed from that of Perrone (1992), in which rotation detectors were used to process the lamellar component of the flow, it was possible to accurately reproduce the pattern of central bias observed in human estimation of heading, with a correlation of 0.96 ($p<.0001$) being obtained between the predictions of the model and the experimental results found in Experiment 10. The heading bias found in each of a critical set of experimental conditions can be accounted for by hypothesising that a particular rate of eye-movement occurs during the heading trial. By further hypothesising that the rotation detectors drive an eye-movement at a yaw rate proportional to their output, it was possible to account for the heading bias that occurred under the different experimental conditions. The net activity of the maximum responding rotation detector (determined by its optimal speed tuning and rate of firing) was proportional to the size of the eye-movement yaw rates associated with the heading bias.

Although it is suggested that the rotation detectors in this model generate actual physical eye movements, it is possible that retinal rotation signals could also be generated by the rotation detectors, and that these may operate alone or in conjunction with the eye movements.

Applying the Model to other Experimental Results

Although the model was tested using the yaw values required for the mean heading estimates of Experiment 10, the results of the other experiments in section A are also able to be explained by the model. Overall, eye movements being induced by the lamellar flow component of observer translation can explain the central bias seen in these experiments. Lamellar flow increases with heading eccentricity, and thus an increasingly large eye

movement will be seen as the heading direction becomes more distant from fixation. The lack of effect found for different object shape and size (Experiment 4), dots remaining or not (Experiment 5), having the head on an angle or not (Experiment 7) the number of dots (Experiment 8) and Time (Experiment 11) can be explained by these factors not impacting upon the size of the lamellar flow and therefore the eye movements. The results of other experiments have implications for the heading model, and these will be discussed in turn.

In Experiment 2, I crossed black and grey response screens with motion and static dot displays, and found that motion displays led to far more bias than did static. This initially appears counterintuitive, as motion displays contain both motion and static components. However, this result makes sense in light of the model as the motion displays contained a lamellar flow component, which would have caused a yaw eye movement to occur, with heading bias being the result. Very little or no eye movement would have occurred with the static display.

Experiment 3 provides more of a challenge for the model, as the participants were asked to find the location of a yellow spot placed at the 'FOE' of static and motion displays. They were able to do so with a high degree of accuracy, and in this case motion and static estimates were made with equal accuracy. The question that arises is why the eye movement did not occur with this experiment if it had in Experiment 2, which was otherwise identical. One possible explanation of this difference is that the participants were able to disregard the activity of the heading detectors due to the yellow spot being fixed in position and somehow anchoring the eyes. Another possible explanation involves attentional factors, as participants may be able to selectively attend to various components of the flow field (e.g. concentrating on the yellow spot and ignoring the flow).

Experiment 5 examined the role of fixation direction upon heading estimation and found that the perceived direction of heading was towards the centre of the screen rather

than towards fixation, although estimates were somewhat more accurate when the true direction of heading lay close to the fixation direction. Two aspects of this experiment are worth noting as they demonstrate the ability of the model to explain previously challenging results. The first involves the situation when the observer is looking at an eccentric fixation point, and the actual heading direction lies to the outside of this. In this case, the estimated heading direction lay to the inside of fixation. This was unexpected, because the actual heading direction lay close to fixation and a high level of accuracy would be expected. However this result is easily explained by the model as the direction of flow would have generated a yaw eye movement, biasing the perceived FOE towards the centre of the screen.

The second aspect is, on the surface, harder to explain, and involves the case when the observer is looking at an eccentric fixation point, and the actual direction of heading lies between the screen centre and the fixation point. In this case the flow across the fovea should be towards the outside of the screen, and should in theory lead to an overestimation of heading with the perceived FOE being moved outwards. However this is true only in the foveal region, and when the overall flow in the visual field is taken into account, the global pattern of flow will be in the opposite direction and bias will be towards the centre of the screen as before.

Depth was found to be an important factor for improving the accuracy of estimates, with less depth leading to less heading bias. In terms of the rotation model, although decreasing depth does increase the size of the lamellar component of flow (i.e., makes it more uniform in speed), and thus the size of the yaw eye movement, it also increases the size of the radial flow components indicating the FOE, and therefore makes the direction of heading more robust against any yaw eye movement. That is, although the eye movement is made, it does not affect the accuracy of heading estimates to such an extent as when depth

is large. The impact of the eye movement will depend both on the size of the eye movement and the strength of the heading signal.

An important aspect of the predictions of the model is the way in which it can explain the increase in heading error found with approaches to fronto-parallel planes (e.g. Rieger & Toet, 1985; W.H. Warren, 1986; W.H. Warren & Hannon, 1988, 1990). In theory, the FOE should be easily discernable in these conditions, and so the heading direction should be accurately estimated. However, people have been found to make more heading errors in this case than with displays depicting a variety of object depths. In the past, this result has been used as support for differential motion models (e.g. Crowell, Banks and Royden 1989; Hildreth, 1992; Longuet-Higgins & Pradzny, 1980; Reiger & Lawton, 1985; Royden, Banks, & Crowell, 1992; Royden, 1997) because a fronto-parallel plane lacks differential motion and hence heading performance should be poor. However the rotation model can also explain this counterintuitive result. When an approach is made to a fronto-parallel plane, a large amount of lamellar flow will be seen as a consequence of the lack of depth. This flow will have a small range of image speeds and will appear more uniform in its speed distribution. Because the model incorporates an inhibitory component that is determined by the range of image speeds present in the flow, the fronto-parallel plane situation will generate less inhibition in the rotation detectors. This will in turn drive a eye movement in the direction of the lamellar flow causing more heading error.

Section A led to two other findings that can be explained by the rotation model. One group of participants is particularly interesting in relation to the predictions of the model: these are the people who consistently inverted their estimates of heading. These inversions represent a serious performance deficit in that an actual heading of 10° to the right was perceived as being some 5-10° to the left, and so on. Such a strong heading error can be simulated by adding a relatively large amount of yaw eye-rotation to the heading

stimuli. The model could help to explain these results if we consider the idea that in these individuals, the 'gain' controlling the amount of eye-movement generated by a particular rotation detector output may be higher than in the average observer. The size of the eye-movements driven by the lamellar flow in the heading stimuli could be higher than normal, and so their perceived heading direction is biased more strongly away from the true position. For example, for a heading of +10, a yaw rate of 0.55 would explain the results of the inverse responders, while, for the normal population, a yaw rate of 0.13 is needed (note that both of these rates are very small). This suggests that a range of rotation gain levels could exist within a normal population, with some people being more or less sensitive to lamellar flow.

Another group of participants of interest are those who were able to estimate their direction of heading with little or no bias under a wide range of conditions. These people were normally highly experienced computer users, and had presumably learned to control their eye movements. This suggests that the rotation gain level may be modified through exposure to various stimuli.

Recommendations for Future Research

The results of the experimental and modelling sections of this thesis have suggested some interesting possibilities regarding future research directions. These recommendations will be discussed in the following section.

- The most essential research involves investigating the existence and size of eye movements generated by lamellar flow stimuli. This should be carried out in two ways, firstly using purely lamellar flow to determine the nature of the relationship between the stimulus and the induced eye movements. Secondly, a series of

experiments similar to those carried out in this thesis should be run to determine the size of eye movements induced by the various experimental stimuli. Note however that because the size and rate of the eye-movements tend to be very small (see Table 15.1), this would require a fairly high resolution eye-movement measuring system. Such a system of experimentation would allow a systematic examination of the nature of the eye movements and allow a much more accurate prediction of human heading estimation performance.

- It would be of interest to run experiments involving different amounts of combined observer translation and rotation (e.g. motion along curvilinear paths). The model needs to be further developed to allow for these more complex inputs.
- In this work I assumed a physical eye movement was elicited by the lamellar flow, but it is also possible that the visual system perceived an eye movement to have occurred on the basis of visual information. It would be extremely valuable if these two possibilities could be isolated from one another, and the relationship between them explored. This would permit a greater understanding of the nature of the processing of rotational flow in the brain.
- The rotation model could also be applied to results of research in aviation research. For example, Kim, (2000) examined estimations of aim-point during simulated aircraft landings. The aim-point was consistently underestimated (i.e. made closer to the near end of the runway than was the actual heading direction), and the underestimation increased as the aim-point got further from the threshold. The scenario in aircraft landings is basically an oblique approach to a fronto-parallel plane, with estimates being made in an elevational direction rather than azimuthal (as in the majority of experiments reported in this thesis), and therefore does not

directly correspond to the 3-D cloud display used in this work. However when the aim-point was further down the runway than the fixation point, the downwards flow would induce a vertical pitching eye movement increasing in size as the aim-point got further from the fixation point. Such horizontal pitch movements are known to occur in response to moving stimuli (Howard, 1982). Again, as in Experiment 6 (Fixation), although the direction of flow in the foveal region may be against the observed bias, the overall direction of flow across the visual field leads to a pitch eye movement in the predicted direction. Research in this area should focus upon the relationship between the stimuli and eye movement behaviours, and the aim-point estimations made. It would also be valuable to investigate the way in which pilots could train to overcome such problems when landing aircraft. In this way specific recommendations could be developed (e.g. regarding fixation strategies) which would assist in reducing the risk of major accidents, especially in small aircraft that do not have instrument landing capabilities.

- The model also has implications in automobile driving, in that it suggests that errors in heading will be created when a driver is faced with flow containing large amounts of lamellar components. One possible example of such a situation is when a car drives around a tight corner on a mountain road, during which a large vertical surface may fall along the line of sight. While the observer is likely to move the eyes to track a point or to focus upon the direction of heading itself, the potential remains for errors in heading estimation to be made in response to such stimuli, and these could have disastrous consequences. Research should concentrate upon understanding drivers' responses to such stimuli, and in developing strategies to

overcome any problems (for a discussion of the use of optic flow in cornering behaviour see Wann & Land, 2000).

Conclusion

Section A of this thesis involved a systematic examination of the possible factors involved in heading bias observed using classic experimental approaches. A significant amount of heading bias was found, and this lay towards the centre of the screen, with the amount of bias increasing as the eccentricity of heading direction increased. The main experimental factors influencing heading were found to be observer speed and scene depth, with more speed and less depth leading to more accurate estimates of heading, although some bias was found to occur even with optimal levels of each. Viewing time and the number of dots had some effect, however these were minor factors, and provided sufficient viewing time (> 400 ms) and dots ($\leq$400 dots) were given, bias did not increase.

As a result of Section A, it was proposed that the bias arose because of an eye movement driven by the lamellar component of the flow field. Section B involved the development of a rotation model based on the Perrone (1992) model of heading, in which eye movements were driven by the output of rotation detectors. A correlation of 0.96 ($p<.0001$) was found between the predictions of the model and the results of Experiment 10. Many of the results from other experiments in the thesis could also be accounted for using the mechanisms outlined in the model. The model needs further refining but, even in its current state it is able to account for many of the deficits in performance of human participants in heading experiments involving pure translation.

References

Adiv, G. (1985). Determining three-dimensional motion and structure from optical flow generated by several moving objects. *IEEE Transactions on Pattern Analysis and Machine Intelligence, PAMI-7*, 384-401.

Albright, T. D. (1984). Direction and orientation selectivity of neurons in visual area MT of the macaque. *Journal of Neurophysiology, 52*, 1106-1130.

Albright, T. D. (1992). Form-cue invariant motion processing in primate visual cortex. *Science, 255*, 1141-1143.

Albright, T.D.,& Desimone, R. (1987). Local precision of visuotopic organization in the middle temporal area (MT) of the macaque. *Experimental Brain Research, 65*, 582-592.

Alfano, P. L., & Michel, G.F. (1990). Restricting the field of view: Perceptual and performance effects. *Perceptual and Motor Skills, 70*, 35-45

Allman, J., Miezin, F., & McGuinness, E. (1985). Direction and velocity specific responses from beyond the classical receptive field in the middle temporal visual area. *Perception, 14*, 105-126.

Andersen, G. J., & Saidpour, A. (2002). Necessity of spatial pooling for the perception of heading in nonrigid environments. *Journal of Experimental Psychology: Human perception and performance, 28* (5), 1192-1201.

Atchley P. A., & Andersen, G. J. (1999). The discrimination of heading from optic flow is not retinally invariant. *Perception & Psychophysics, 61* (3), 387-396.

D'Avossa, G., & Kersten, D. (1996). Evidence in human subjects for independent coding of azimuth and elevation for direction of heading from optic flow. *Vision Research, 18*, 2915-1924.

Ballard, D. H., & Kimball, O. A. (1983). Rigid body motion from depth and optical flow. *Computer Vision Graphics Image Processing, 22*, 95-115.

Bavelier, D., & Green, S. (2003). Action video game modifies visual selective attention. *Nature, 423*, 534 – 537.

Beintema, J. A., & van den Berg, A. V. (1998a). Heading detection using motion templates and eye velocity gain fields. *Vision Research, 38* (14), 2155-2179.

Beintema, J. A., & van den Berg, A. V. (1998b). Effect of torsional flow on heading percept. *Investigative Ophthalmology and Visual Science, 39* (4) (Suppl.), 5020 (Abstract).

Beintema, J. A., & van den Berg, A. V. (2000). Perceived heading during simulated torsional eye movements. *Vision Research, 40*, 549-566.

Beintema, J. A., & van den Berg, A. V. (2001). Pursuit affects precision of perceived heading for small viewing apertures. *Vision Research, 41*, 2375-2391.

van den Berg, A. V. (1992). Robustness of perception of heading from optic flow. *Vision Research, 32* (7), 1285-1296.

van den Berg, A. V. (1999). Predicting the present direction of heading. *Vision Research, 39*, 3608-3620.

van den Berg, A. V., & Beintema, J. A. (1997). Motion templates with eye velocity gain fields for transformation of retinal to head-centric flow. *Neuroreport, 8*, 835-840.

van den Berg, A. V., & Brenner, E. (1994). Humans combine the optic flow with static depth cues for robust perception of heading. *Vision Research, 34* (16), 2153-2167.

Beusmans, J. M. H. (1998). Perceived object shape affects the perceived direction of self-movement. *Perception, 27* (9), 1079 - 1085

Bradley, D. C., Maxwell, M., Andersen, R. A., Banks, M. S., and Shenoy, K. V. (1996) Mechanisms of heading perception in primate visual cortex. *Science, 273*, 1544-1547.

Britten, K. J. & van Wezel, R. J. (1998). Electrical microstimulation of cortical area MST biases heading perception in monkeys. *Nature Neuroscience, 1*, 59-63.

Britten, K. H., and van Wezel, R. J. A. (2002). Area MST and heading perception in macaque monkeys. *Cerebral Cortex. 12*, 692-701.

Bruss, A. R., & Horn, B. K. P. (1983). Passive navigation. *Computer Vision, Graphics and Image Processing, 21*, 3-20.

Burr, D.C., Morrone, M. C., & Vaina, L. M. (1998). Large receptive fields for optic flow detection in humans. *Vision Research, 38*, 1731-1743.

Busettini, C., Miles, F. A., Schwarz, Y. & Carl, J. (1994). Human ocular responses to the translation of the observer and the scene: Dependence on viewing distance. *Experimental Brain Research, 100*, 484-494.

Cheng, K., Hasegawa, T., Saleem, K. S., & Tanaka, K. (1994). Comparison of neuronal selectivity for stimulus speed, length and contrast in the prestriate visual cortical areas V4 and MT of the macaque monkey. *Journal of Neurophysiology, 71*, 2269-2280.

Crowell, J. A. & Banks. M. S. (1993). Perceiving heading with different retinal regions and types of optic flow. *Vision Research, 37*, 1653-1671.

Crowell, J. A., & Banks, M. S. (1996). Ideal observer for heading judgments. *Vision Research, 36*, 471-190.

Crowell, J.A., Banks, M.S. and Royden, C.S. (1989). A physiologically plausible model of optic flow perception. *Annual Meeting Abstract Issue, Association for Research. in Vision and Ophthalmology, 30*, 427.

Crowell, J. A., Banks, M. S., Shenoy, K. V., & Andersen, R. A. (1997). Visual self-motion perception during head turns. *Nature Neuroscience, 1*, 732-737.

Crowell, J. A., Royden, C. S., Banks, M. S., Swenson, K. H., & Sekuler, A. B. (1990). Optic flow and heading judgments. *Investigative Ophthalmology and Visual Science Supplement, 31*, 522.

Cutting, J.E. (1986). *Perception with an eye for motion*. Cambridge, MA: MIT Press.

Cutting, J. E., Vishton, P. M., Fluckiger, M., Baumberger, B., & Gerndt, J. (1997). Heading and path information from retinal flow in naturalistic environments. *Perception & Psychophysics, 59*, 426-441.

Dobkins, K.R. & Albright, T.D. (1994). What happens if it changes color when it moves?: The nature of chromatic input to macaque visual area MT. *Journal of Neuroscience, 14* (8), 4854-4870.

Dubner, R., & Zeki, S. M. (1971). Response properties and receptive fields of cells in an anatomically defined region of the superior temporal sulcus in the monkey. *Brain Research, 35*, 528-532.

Dubois, M. F. W., & Colleqijn, H. (1979). Optokinetic reactions in man elicited by localized retinal motion stimuli. *Vision Research, 19*, 1105-1115.

Duffy, C. J., & Wurtz, R. H. (1991a). Sensitivity of MST neurons to optic flow stimuli. I: A continuum of response selectivity to large-field stimuli. *Journal of Neurophysiology, 65*, 1329-1345.

Duffy, C. J., & Wurtz, R. H. (1991b). Sensitivity of MST neurons to optic flow stimuli. II: Mechanisms of response selectivity revealed by small-field stimuli. *Journal of Neurophysiology, 65*, 1346-1359.

Duffy, C. J., & Wurtz, R. H. (1993). MSTd neuronal responses to the center-of-motion in optic flow fields. *Society for Neuroscience Abstracts, 19*, 1283.

Duffy, C. J., & Wurtz, R. H. (1995a). Response of Monkey MST neurons to optic flow stimuli with shifted centres of motion. *Journal of Neuroscience, 15*, 5192-5208.

Duffy, C.J. and Wurtz, R.H. (1995b). Medial superior temporal area neurons respond to speed patterns in optic flow. *Journal of Neuroscience, 17*, 2839-2851

Duffy, C. J., & Wurtz, R. H. (1997). Planar directional contributions to optic flow responses in MST neurons. *Journal of Neurophysiology, 77*, 782-796.

Eckert, M.P, & Buchsbaum, G. (1993). Effect of tracking strategies on the velocity structure of two-dimensional image sequences. *Journal of the Optical Society of America A. 10*, 1993-1996.

Ehrlich, S. M., Beck, D. M., Crowell, J. A., Freeman, T. C., & Banks. M. S. (1998). Depth information and perceived self-motion during simulated gaze rotations. *Vision Research, 38*, 3129-3145.

Eriksson, E. S. (1974). Movement parallax during locomotion. *Perception & Psychophysics, 16*, 197-200.

Erickson, R. G., & Their, P. (1991). A neuronal correlate of spatial stability during periods of self-induced visual motion. *Experimental Brain Research, 86*, 608-616.

Freeman, T. C. A. (1999). Path perception and Filehne illusion compared: model and data. *Vision Research, 39*, 2659-2667.

Freeman, T. C. A., & Banks, M. S. (1998). Rapid Communication: perceived head-centric speed is affected by both extra-retinal and retinal errors. *Vision Research, 38* (7), 941-945.

Freeman, T. C., Banks, M. S., & Crowell, J. A. (2000). Extraretinal and retinal amplitude and phase errors during Filehne illusion and path perception. *Perception & Psychophysics, 62* (5), 900-909.

Frey, B. F., & Owen, D. H. (1999). The utility of motion parallax information for the perception and control of heading. *Journal of Experimental Psychology: Human Perception and Performance, 25*, 445-460.

Gibson, J. J. (1947). *Motion picture testing and research.* (AAF Aviation Psychology Research Report No, 7). Washington, DC: U.S. Government Printing Office.

Gibson, J. J. (1950). *The Perception of the Visual World.* Boston: Houghton Mifflin.

Gibson, J. J. (1966). *The Senses Considered as Perceptual Systems.* Boston: Houghton Mifflin.

Gibson, J. J., Olum, P., & Rosenblatt, F. (1955). Parallax and perspective during aircraft landings. *American Journal of Psychology, 68*, 372-385.

Glünder, H. (1990). Correlative velocity estimation: Visual motion analysis, independent of object form, in arrays of velocity-tuned bilocal detectors. *Journal of the Optical Society of America A, 7*, 255-263.

Gnadt, J. W., Bracewell, R. M., & Andersen, R. A. (1991). Sensorimotor transformations during eye movements to remembered visual targets. *Vision Research, 31*, 693-715.

Goldstein, E. B. (1989). *Sensation and perception* (3rd. ed). Pacific Grove, CA: Brooks/ Cole Publishing Group.

Graziano, M. S. A., Andersen, R. A., & Snowden, R. J. (1994). Tuning of MST neurons to spiral motions. *Journal of Neuroscience, 14*, 54-67.

Grigo, A., & Lappe, M. (1998). Interaction of stereo vision and optic flow processing revealed by an illusory stimulus. *Vision Research, 38* (2), 281-290.

Grossman, G. E., & Leigh, R. J. (1990). Instability of gaze during locomotion in patients with deficient vestibular function. *Annals of Neurology, 27*, 528-532.

Hanada, M., & Ejima, Y. (2000a). A method for recovery of heading from motion. *Journal of the Optical Society of America A, 17*, 966-973,

Hanada, M., & Ejima, Y. (2000b). Effects of roll and pitch components in retinal flow on heading judgement, *Vision Research, 40* (14), 1827-1838.

Hatsopoulos, N, G., & Warren, W. H. (1991). Visual navigation with a neural network. *Neural Networks, 4*, 303-317.

Heeger, D. J., & Jepson, A. D. (1992). Subspace methods for recovering rigid motion 1: Algorithm and implementation. *International Journal of Computer Vision, 7*, 95-117.

Hildreth, E. C. (1992). Recovering heading for visually guided navigation. *Vision Research, 32*, 1177-1192.

Hildreth, E. C., & Royden, C. S. (1998). Computing observer motion from optical flow. In T. Watanable (Ed.), *High-level motion processing computational, neurobiological and psychophysical perspectives*. Cambridge, MA: MIT Press

Honrubia, V., Downey, W. L., Mitchell, D. P., & Ward, P. H. (1968). Experimental studies of optokinetic nystagmus. II. Normal Humans, *Acta Oto-laryngol, 37*, 65-73.

Howard, I. P. (1982). *Human visual orientation*. New York: Wiley.

Johnston, I. R., White, G. R., & Cumming, R. W. (1973). The role of optical expansion patterns in locomotor control. *American Journal of Psychology, 86* (2), 311-324.

Kaufman, L. (1964). *Research in visual perception for carrier landing: Supp. 2. Studies on the perception of the impact point based on shadowgraph techniques* (Report SDG-5265-0031). Great Neck, N.Y.: Sperry Rand Corp.

Kawano, K., Sasaki, M., & Yamashita, M. (1984). Response properties of neurons in posterior parietal cortex of monkey during visual-vestibular stimulation. I. Visual tracking neurons. *Journal of Neurophysiology, 51*, 340-351.

Kawano, K., Shidara, M., Watanabe, Y., & Yamane, S. (1994). Neural activity in cortical area MST of alert monkey during ocular following responses. *Journal of Neurophysiology, 71*, 2305-2324.

Kim, R.S. (2000). Estimates of approach-angle and aim-point during computer simulated landing approaches. Unpublished Masters Thesis, Waikato University.

Koenderink, J. J. (1986). Optic flow. *Vision Research, 26*, 161-180.

Koenderink, J. J., & van Doorn, A. J. (1975). Invariant properties of the motion parallax field due to the movement of rigid bodies relative to an observer. *Optica Acta, 22*, 773-791.

Koenderink, J. J., & van Doorn, A. J. (1976). Local structure of movement parallax of the plane. *Journal of the Optical Society of America A, 66*, 717-723.

Koenderink, J. J., & van Doorn, A. J. (1987). Facts on optic flow. *Biological Cybernetics, 56*, 247-354.

Komatsu, H., & Wurtz, R. H. (1988). Relation of cortical areas MT and MST to pursuit eye movements. I. Location and visual properties of neurons. *Journal of Neurophysiology, 60*, 580-603.

Lagae, S., Raiguel, S., & Orban, G. A. (1993). Speed and direction selectivity of macaque middle temporal neurons. *Journal of Neurophysiology, 69*. 19-39.

Land, M. F., & Lee, D. N. (1994). Where we look when we steer. *Nature, 369*, 742-744.

Lappe, M., Bremmer, F., Pekel, M., Thiele, A, & Hoffmann, K. –P. (1996). Optic flow processing in monkey STS: a theoretical and experimental approach. *Journal of Neuroscience, 16*, 6265-6285.

Lappe, M., & Duffy, C. J. (1999). Optic flow illusion and single neuron behaviour reconciled by a population model. *European Journal of Neuroscience, 11* (7), 2323-2331.

Lappe, M., Pekel, M., & Hoffmann, K. -P. (1998). Optokinetic eye movements elicited by radial optic flow in the macaque monkey. *Journal of Neurophysiology, 79*, 1461-14801.

Lappe, M., Pekel, M., & Hoffmann, K. -P. (1999). Properties of saccades during optokinetic responses to radial optic flow in monkeys. In W. Becker, H. Deubel, & T. Mergner (Eds.), *Current Oculomotor Research: Physiological and Psychological Aspects* (pp. 45-52). New York: Plenum.

Lappe, M., & Rauschecker, J. P. (1993). A neural network for the processing of optic flow from egomotion in man and higher mammals. *Neural Computation, 5*, 374-391.

Lappe, M., & Rauschecker, J. P. (1994). On heading detection from optic flow. *Nature, 369*, 712-713.

Lee, D. N. (1980). The optic flow field: The foundation of vision. *Philosophical Transactions of the Royal Society of London, Series B, 290*, 169-179.

Lisberger, S. G., & Movshon, J. A. (1999). Visual motion analysis for pursuit eye movements in area MT of macaque monkeys. *Journal of Neuroscience, 19*, 2224-2246.

Llewellyn, K. R. (1971). Visual guidance of locomotion. *Journal of Experimental Psychology, 91*, 194-196.

Longuet-Higgins, H. C., & Prazdny, K. (1980). The interpretation of a moving retinal image. *Proceedings of the Royal Society of London, B, 208*, 385-397.

Longuet-Higgins, H. C. (1981). A computer algorithm for reconstructing a scene from two projections. *Nature, 293*, 133-135.

Loomis, J. M. & Beall, A. C. (1998). Visually-controlled locomotion: Its dependence on optic flow, 3-D space perception, and cognition. *Ecological Psychology, 10*, 271-285.

MATLAB version 12 [Computer program]. (2002). Natick, Massachusetts, The MathWorks, Inc.

Maunsell, J. H. R., & van Essen, D. C. (1983a). The connections of the middle temporal area (MT) and their relationship to cortical hierarchy in the macaque monkey. *Journal of Neuroscience, 3*, 2563-2568.

Maunsell, J. H. R., & van Essen, D. C. (1983b). Functional properties of neurons in middle temporal visual area of the Macaque monkey: II. Binocular interactions and sensitivity to binocular disparity. *Journal of Neurophysiology, 49*, 1148-1167.

Maunsell, J. H. R., & Newsome, W. T. (1987). Visual processing in monkey extrastriate cortex. *Annual Review of Neuroscience, 10*, 363-401.

May, J. G., Flanagan, M. B., and Dobie, T. G. (2001). *OKN, Ego Vection, and Motion Sickness*. Poster presented at the Vision Sciences Society Conference, Sarasota, Florida, May 6.

Mestre, D. R., & Masson, G. S. (1997). Ocular responses to motion parallax stimuli: the role of perceptual and attentional factors. *Vision Research, 37* (12), 1627-1641.

Miles, F. A. (1994). Stimulus specificity in the primate optokinetic system. In J. M. Delgado-Garcia, E. Godeux, and P. –P. Vidal (Eds.), *Information Processing Underlying Gaze Control* (pp. 251-259). Oxford: Pergamon.

Morrone, M. C., Burr, D. C., DiPietro, S., & Stefanelli, M. A. (1999). Cardinal directions for visual optic flow. *Current Biology, 9*, 763-766.

Nagel, H. (1981). On the derivation of 3-D rigid point configurations from image sequences. *IEEE Conference on Pattern Recognition and Image Processing*, 103-108. New York: IEEE Computer Society Press.

Nakayama, K., & Loomis, J. M. (1974). Optical velocity patterns, velocity sensitive neurons, and space perception: a hypothesis. *Perception, 3*, 63-80.

Newsome, W. T., Wurtz, R. H., Dursteler, M. R., & Mikami, A. (1985). Deficits in visual motion processing following ibotenic acid lesions of the middle-temporal visual area of the macaque monkey. *Journal of Neuroscience, 5*, 825-840.

Newsome, W. T., Wurtz, R. H., & Komatsu, H. (1988). Relation of cortical areas MT and MST to pursuit eye movements. II. Differentiation of retinal from extraretinal inputs. *Journal of Neurophysiology, 49*, 1148-1167.

Niemann, T., Lappe, M., Büscher, A., & Hoffmann, K. –P. (1999). Ocular responses to radial optic flow and single accelerated targets. *Vision Research, 39*, 1359-1371.

Orban, G. A., Lagae, L., Verri, A., Raiguel, S., Xiao, D., Maes, H., & Torre, V. (1992). First-order analysis of optical flow in monkey brain. *Proceedings of the National Academy of Sciences, USA, 89*, 2595-2599.

Pack, C., & Mingolla, E. (1998). Global induced motion and visual stability in an optic flow illusion. *Vision Research, 38*, 3083-3093.

Page, W. K., Duffy, C. J. (1999). MST neuronal responses to heading direction during pursuit eye movements. *Journal of Neurophysiology, 81*, 596-610.

Perrone, J. A. (1987). Extracting 3-D egomotion from a 2-D flow field: A biological solution? *Optical Society of America Technical Digest Series, 22*, 47.

Perrone, J. A. (1992). Model for the computation of self-motion in biological systems. *Journal of the Optical Society of America A, 9*, 177-194.

Perrone, J. A. (2001). A closer look at the visual input to self-motion estimation. In J. M. Zanker & J. Zeil (Eds.), Motion Vision. Computational, Neural, and Ecological Constraints (pp. 169-179). Heidelberg: Springer-Verlag.

Perrone, J. A., & Stone, L. S. (1994). A model of self-motion estimation within primate extrastriate visual cortex. *Vision Research, 34*, 2917-1938.

Perrone, J. A., & Stone, L. S. (1997). Emulating the visual receptive-field properties of MST neurons with a template model of heading estimation. *Journal of Neuroscience, 18* (15), 5958-5975.

Perrone, J. A., & Thiele, A. (2001). Speed skills: measuring the visual speed analysing properties of primate MT neurons. *Nature Neuroscience, 4* (5), 526-532.

Perrone, J. A., & Thiele, A. (2002). A model of speed tuning in MT neurons. *Vision Research, 42*, 1035-1051.

Poggio, T., Verre, A., & Torre, V. (1991). *Green Theorems and Qualitative Properties of the Optical Flow.* Artificial Intelligence Lab memo no. 1289. Cambridge: MIT Press.

Post, R. B., Shupert, C. L., & Leibowitz, H. W. (1984). Implications of OKN suppression by smooth pursuit for induced motion. *Perception & Psychophysics, 36*, 493-498.

Regan, D., & Beverly, K. I. (1979). Visually guided locomotion: Psychophysical evidence for a neural mechanism sensitive to flow patterns. *Science, 205*, 311-313.

Regan, D., & Beverly, K. I. (1982). How do we avoid confounding the direction we are looking and the direction we are moving? *Science, 215*, 194-196.

Rieger, J. H., & Lawton, D. T. (1985). Processing differential image motion. *Journal of the Optical Society of America A, 215*, 354-360.

Rieger, J. H., & Toet, L. (1985). Human visual navigation in the presence of 3-D rotations. *Biological Cybernetics, 52*, 377-381.

Royden, C. S. (1994). Analysis of misperceived observer motion during simulated eye rotations. *Vision Research, 34*, 3215-3222.

Royden, C. S. (1997). Mathematical analysis of motion-opponent mechanisms used in the determination of heading and depth. *Journal of the Optical Society of America A, 14* (9), 2128-2143.

Royden, C. S., Banks, M. S., & Crowell, J. A. (1992). The perception of heading during eye movements. *Nature, 360*, 583-585.

Royden, C. S., Crowell, J. A., & Banks, M. S. (1994). Estimating heading during eye movements. *Vision Research, 34*, 3197-3214.

Royden, C. S., & Hildreth, E. C. (1994). The effect of moving objects on heading perception. *Investigative Ophthalmology and Visual Science, Suppl, 35*, 1999.

Royden, C. S., & Hildreth, E. C. (1995a). The effect of attention on judgment of heading and 3-D object motion. *Investigative Ophthalmology and Visual Science, Suppl, 36*, 3830.

Royden, C. S., & Hildreth, E. C. (1995b),Factors affecting the judgment of heading and 3-D object motion. *Society for Neuroscience Abstracts. 21*, 124.

Royden, C. S., & Hildreth, E. C. (1996). Human heading judgments in the presence of moving objects. *Perception and Psychophysics, 58*, 836-856.

Saito, H., Yukie, M., Tanaka, K., Hikosaka, K., Fukada, Y., & Iwai, E. (1986). Integration of direction signals of image motion in the superior temporal sulcus of the macaque monkey. *Journal of Neuroscience, 6*, 145-157.

Saito, H., Tanaka, K., Isono, H., Yasuda, M., & Mikami, A. (1989). Directionally selective response of cells in the middle temporal area (MT) of the macaque monkey to the movement of equiluminous opponent color stimuli. *Experimental Brain Research, 75*, 1-14.

Sakata, H., Shibutani, H., & Kawano, K. (1983). Functional properties of visual tracking neurons in posterior parietal association cortex of the monkey. *Journal of Neurophysiology, 49*, 1364-1380.

Shenoy, K. V., Bradley, D. C., & Andersen, R. A. (1996). Heading computation during head movements in macaque cortical area MSTd. *Society of Neuroscience Abstracts, 20*, 1278.

Sheth B. R., Shimojo S. (2001). Compression of space in visual memory. *Vision Research, 41*, 329-341

Snowden, R. J., & Milne, A. B. (1996). The effect of adapting to complex motions: position invariance and tuning to spiral motions. *Journal of Cognitive Neuroscience, 8* (5), 435-452.

Solomon, D., & Cohen, B. (1992a). Stabilization of gaze during circular motion in light I. Compensatory head and eye nystagmus in the running monkey. *Journal of Neurophysiology, 67* (5), 1146-1157.

Solomon, D., & Cohen, B. (1992b). Stabilization of gaze during circular motion in darkness II. Contribution of velocity storage to compensatory head and eye nystagmus in the running monkey. *Journal of Neurophysiology, 67 (*5), 1158-1170.

SPSS version 10 [Computer Software]. (1992) Chicago, Illinois: SPSS inc.

Steinmetz, M. A., Motter, B. C., Duffy, C. J., & Mountcastle, V. B. (1987). Functional properties of parietal visual neurons: Radial organization of directionalities within the visual field. *Journal of Neuroscience, 7*, 177-191.

Stone, L. S., & Perrone, J. A. (1997). Human heading estimation during visually simulated curvilinear motion. *Vision Research, 37* (5), 573-590.

Stoner, G. R., and T. D. Albright. (1996). The interpretation of visual motion: Evidence for surface segmentation mechanisms. *Vision Research 36*, 1291-1310.

Subbarao, M., & Waxman, A. M. (1986). Closed form solutions to image flow equations for planar surfaces in motion. *Computer Vision, Graphics, and Image Processing, 36*, 208-228.

Tanaka, K. (1998). Representation of visual motion in the extrastriate visual cortex. In T. Watanable (Ed.), *High-level motion processing computational, neurobiological and psychophysical perspectives.* Cambridge, MA: MIT Press

Tanaka, K., Hikosaka, K., Saito, H., Yukie, M., Fukada, Y., & Iwai, E. (1986). Analysis of local and wide-field movements in the superior temporal visual areas of the macaque monkey. Journal of Neurophysiology, 69, 128-142.

Tanaka, K., Fukada, Y., & Saito, H. (1989). Underlying mechanisms of the response specificity of expansion/contraction and rotation cells in the dorsal part of the medial superior temporal area of the macaque monkey. *Journal of Neurophysiology, 62*, 642-656.

Tanaka, K., & Saito, H. (1989). Analysis of motion of the visual field by direction, expansion/contraction, and rotation cells clustered in the dorsal part of the medial superior temporal area of the macaque monkey. *Journal of Neurophysiology, 62*, 626-641.

Tanaka, K., Sugita, Y., Moriya, M., & Saito, H. (1993). Analysis of object motion in the ventral part of the medial superior temporal area of the macaque visual cortex. *Journal of Neurophysiology, 69*, 128-142.

Telford, L. and Howard, I.P. (1996). Role of optical flow field asymmetry in the perception of heading during linear motion. *Perception and Psychophysics , 58*, 283-288.

Thier, P. & Erickson, R. G. (1992a). Responses of visual-tracking neurons from cortical area MST1 to visual, eye, and head motion. *European Journal of Neuroscience, 4*, 539-553.

Tsai, R. Y., & Huang, T. S. (1981). Estimating three-dimensional motion parameters of a rigid planar patch. *IEEE Transactions of Acoustics, Speech, and Signal Processing, ASSP-29*, 1147-1152.

Tsai, R. Y., & Huang, T. S. (1982). Estimating three-dimensional motion parameters of a rigid planar patch. II: Singular value decomposition. *IEEE Transactions of Acoustics, Speech, and Signal Processing, ASSP-30*, 525-534.

Tsai, R. Y., & Huang, T. S. (1984a). Estimating three-dimensional motion parameters of a rigid planar patch. III: Finite point correspondence and the three-view problem. *IEEE Transactions of Acoustics, Speech, and Signal Processing, ASSP-32*, 213-220.

Tsai, R. Y., & Huang, T. S. (1984b). Uniqueness and estimation of three-dimensional motion parameters of rigid objects with curved surfaces. *IEEE Transactions on Pattern Analysis of Machine Intelligence, PAMI-6*, 13-27.

Turano, K., & Wang, X. (1994). Visual discrimination between a curved and straight path of self-motion: effects of forward speed. *Vision Research, 34*, 107-114.

Ungerleider, L., & Desimone, R. (1986). Cortical connections of area MT in the Macaque. *Journal of Comparative Neurology, 248*, 190-222.

Verri, A., Girosi, F., & Torre, V. (1989). Mathematical properties of the two-dimensional motion field: From singular point to motion parameters. *Journal of the Optical Society of America, A 6*, 698-712.

Vishton, P. M., & Cutting, J. E. (1995). Wayfinding, displacements, and mental maps: velocity fields are not typically used to determine one's aimpoint. *Journal of Experimental Psychology: Human Perception and Performance, 215*, 978-995.

Wagner, M., Baird, J. C., & Barbaresi, W. (1981). The locus of environmental attention. *Journal of Environmental Psychology, 1*, 195-206.

Wann, J., & Land, M. (2000). Steering with or without the flow: is the retrieval of heading necessary? *Trends in Cognitive Science, 4* (8), 319-324.

Warren, R. (1976). The perception of egomotion. *Journal of Experimental Psychology: Human Perception and Performance, 2*, 448-456.

Warren, W. H. (1995). Self-motion: visual perception and visual control. In W. Epstein, and S. Rogers, (Eds.), *Perception of Space and Motion* (pp. 263-325). San Diego: Academic Press.

Warren, W. H., Blackwell, A. W., Kurtz, K. J., Hatsopoulos, N. G., & Kalish, M. (1991). On the sufficiency of the velocity field for perception of heading. *Biological Cybernetics, 65*, 311-320.

Warren, W. H., & Hannon, D. J. (1988). Direction of self motion is perceived from optical flow. *Nature, 336*, 162-163.

Warren, W. H., & Hannon, D. J. (1990). Eye movements and optical flow. *Journal of the Optical Society of America A, 7*, 160-169.

Warren, W. H., & Kurtz, K. J. (1992). The role of central and peripheral vision in perceiving the direction of self-motion. *Perception and Psychophysics, 51*, 443-454.

Warren, W. H., Mestre, D. R., Blackwell, A. W., & Morris, M. W. (1991). Perception of circular heading from optical flow. *Journal of Experimental Psychology: Human Perception and Performance, 17*, 28-43.

Warren, W. H., Morris, M. W., & Kalish, M. (1988). Perception of translational heading from optical flow. *Journal of Experimental Psychology: Human Perception and Performance, 14*, 646-660.

Warren, W. H., & Saunders, J. A. (1995a). Perception of heading in the presence of moving objects. *Perception, 24*, 315-331.

Warren, W. H., & Saunders, J. A. (1995b). Perceived heading depends on the direction of local object motion. *Investigative Ophthalmology and Visual Science, Suppl. 36*, S829.

Waxman, A. M., & Ullman, S. (1985). Surface structure and 3-D motion from image flow: A kinematic analysis. *International Journal of Robotics Research, 4*, 72-94.

Waxman, A. M., & Wohn, K. (1988). Image flow theory: a framework for 3d inference from time-varying imagery. *Advances in Computer Vision*, 166-224.

Weng, J., Huang, T. S., & Ahuja, N. (1989). Motion and structure from two perspective views: Algorithms, error analysis, and error estimation. *IEEE Transactions on Pattern Analysis and Machine Intelligence, 11*, 451-476.

Wurtz, R.H., Komatsu, H., Yamasaki, D.S.G. and Dursteler, M.R. (1990a). Cortical visual motion processing for oculomotor control. In B. Cohen and I. Bodis-Woller (Eds.),*Vision and the Brain* (pp.211-231). New York: Raven Press

Wurtz, R., Komatsu, H., Dursteler, M., & Yamasaki, D. (1990b). Motion to movements. Cerebral cortex visual processing for pursuit eye movements. In G. Edelman & W. M. Cowen (Eds.) *Signal and sense. Local and global order in perceptual maps.* New York: Wiley.

Zacharias, G. L., Caglayan, A. K., & Sinacori, J. B. (1985). A visual model for terrain-following applications. *Journal of Guidance, 8* (2), 201-207.

Zeki, S. M. (1974). Cells responding to changing image size and disparity in the cortex of Rhesus monkey. *Journal of Physiology, 242*, 827-841.

Appendix A

Participant information provided on departmental notice board.

Participants Wanted

I am running experiments to find out how well people can tell their direction of motion from the movement of dots on a computer screen. The results of these experiments are very important in the design of safety features for planes and cars, and they also help us to understand how the brain deals with visual information.

To do these experiments, you just need to sit in front of a computer screen and use a computer mouse. You will see a lot of dots moving towards you – just like the space screen savers. All of the dots will be coming from a certain direction (this is different for each trial). You just move the mouse to show the direction that the dots were coming from. This is the same thing, visually, as your direction of motion.

The experiment will take under 1 hour 10 minutes (normally about 40 minutes) and **2%** course credit will be given. Sign up on the board for a time that suits you.

Any questions? Come and see Ruth in K1.06, or Dr. Perrone in K1.08.

Procedure for Experiments as Read to Participants

About the Experiments

These experiments use computer displays to examine the question of how well people can tell the direction they are moving in. This is known as the problem of 'heading estimation'. From previous research we know that people are usually fairly accurate at heading estimation. However, it is not properly understood exactly how heading estimates are made, and how errors can occur. I aim to examine these issues in more detail.

These experiments are computer based, and will require you to sit in front of a computer screen with your head supported by a chin rest. An eye patch will cover your left eye, because we want to keep the experiment as straight forward as possible, and binocular vision is believed to affect estimates of heading. The room will be darkened during the experimental session, which will take under an hour to complete.

In the centre of the screen you will see a red cross. This will remain on-screen at all times. It is very important that you fixate on this cross during the trials and while responding, because any movement of your eye will interfere with your ability to do the task properly.

Each trial will show motion in a straight line through a cloud of small white dots (like the space screen-savers you may have seen). The motion will last for a brief time, after which the dots will disappear and a white response cross will appear in the centre of the screen. Move the white cross across the screen, using the computer mouse, until it is located in the direction you felt yourself to be moving. Once you are satisfied, a left click of the mouse will start the next trial.

There will be a small practice session of 10 trials before the experiment begins so that you can become familiar with the requirements of this experiment.

Consent form signed by each participant

University of Waikato
Psychology Department

CONSENT FORM

PARTICIPANT'S COPY

Research Project:____

Name of Researcher:____

Name of Supervisor (if applicable):________________________________

I have received an information sheet about this research project or the researcher has explained the study to me. I have had the chance to ask any questions and discuss my participation with other people. Any questions have been answered to my satisfaction.

I agree to participate in this research projects and I understand that I may withdraw at any time. If I have any concerns about this project, I may contact the convenor of the Research and Ethics Committee,

Participant's Name: Signature: Date:

✂ =

RESEARCHER'S COPY

Research Project:____

Name of Researcher:____

Name of Supervisor (if applicable):________________________________

I have received an information sheet about this research project or the researcher has explained the study to me. I have had the chance to ask any questions and discuss my participation with other people. Any questions have been answered to my satisfaction.

I agree to participate in this research projects and I understand that I may withdraw at any time. If I have any concerns about this project, I may contact the convenor of the Research and Ethics Committee,
Participant's Name:____________________Signature:__________________Date:______

Appendix B

Mean Azimuthal and Elemental Components of Heading Estimates

Table B.1

Mean azimuthal and elevational components of heading estimates for the Black-motion condition.

Azimuth	Elevation	Mean Azimuth	Mean Elevation
-10	-10	-3.02	-2.23
-10	-5	-2.23	-1.21
-10	0	-3.40	-0.21
-10	5	-2.97	0.55
-10	10	-3.20	2.19
-5	-10	-1.57	-2.43
-5	-5	-2.27	-1.56
-5	0	-1.63	-0.87
-5	5	-1.57	0.57
-5	10	-2.01	3.077
0	-10	0.16	-2.35
0	-5	-0.23	-1.12
0	0	0.26	0.01
0	5	0.34	0.14
0	10	0.07	2.84
5	-10	1.18	-1.80
5	-5	1.21	-1.17
5	0	1.82	-0.56
5	5	2.13	1.12
5	10	1.85	3.52
10	-10	3.19	-3.1
10	-5	3.06	-1.5
10	0	2.92	-0.15
10	5	3.13	0.49
10	10	4.01	2.65

Table B.2

Mean azimuthal and elevational components of heading estimates for the black-line condition.

Azimuth	Elevation	Mean Azimuth	Mean Elevation
-10	-10	-6.47	-5.74
-10	-5	-6.47	-3.91
-10	0	-6.53	-0.43
-10	5	-6.38	2.87
-10	10	-5.63	4.82
-5	-10	-4.28	-6.14
-5	-5	-4.29	-3.57
-5	0	-4.45	0.10
-5	5	-4.45	3.42
-5	10	-3.48	4.47
0	-10	-0.32	-6.00
0	-5	0.31	-4.28
0	0	0.32	0.10
0	5	0.19	2.82
0	10	0.48	5.47
5	-10	3.67	-5.85
5	-5	3.35	-3.49
5	0	4.81	-1.00
5	5	4.92	4.11
5	10	4.64	6.67
10	-10	5.80	-5.55
10	-5	6.46	-3.09
10	0	6.91	-0.58
10	5	7.16	3.02
10	10	6.02	5.34

Table B.3

Mean azimuthal and elevational components of heading estimates for the grey-motion condition.

Azimuth	Elevation	Mean Azimuth	Mean Elevation
-10	-10	-4.54	-3.77
-10	-5	-3.69	-2.19
-10	0	-4.49	-0.95
-10	5	-4.31	1.20
-10	10	-4.39	3.10
-5	-10	-2.06	-3.54
-5	-5	-2.19	-2.42
-5	0	-1.55	-0.71
-5	5	-3.00	0.66
-5	10	-2.66	3.38
0	-10	-0.11	-2.98
0	-5	0.27	-1.75
0	0	0.05	-0.17
0	5	-0.29	0.70
0	10	-0.39	3.19
5	-10	1.84	-2.91
5	-5	1.55	-1.84
5	0	1.67	-0.74
5	5	2.17	0.99
5	10	1.74	3.20
10	-10	3.91	-4.15
10	-5	3.89	-2.08
10	0	4.14	-0.38
10	5	3.86	0.79
10	10	4.46	2.99

Table B.4

Mean azimuthal and elevational components of heading estimates for the grey-line condition.

Azimuth	Elevation	Mean Azimuth	Mean Elevation
-10	-10	-7.18	-6.55
-10	-5	-7.64	-4.57
-10	0	-7.94	-0.76
-10	5	-7.74	3.36
-10	10	-6.81	5.98
-5	-10	-4.44	-6.67
-5	-5	-4.62	-4.11
-5	0	-4.56	0.12
-5	5	-5.39	4.10
-5	10	-4.22	5.68
0	-10	-0.53	-6.87
0	-5	0.13	-3.76
0	0	0.23	-0.09
0	5	0.37	2.95
0	10	0.53	5.97
5	-10	3.95	-6.84
5	-5	3.78	-4.37
5	0	4.78	-0.71
5	5	4.85	3.88
5	10	4.97	7.06
10	-10	6.71	-6.30
10	-5	7.62	-4.22
10	0	7.37	-0.58
10	5	7.57	3.645
10	10	6.49	5.97

Appendix C

Azimuthal and Elevational Components of Estimates

Table C.1

Mean azimuthal and elevational components of heading estimates for the dots of fixed size condition.

Azimuth	Elevation	Mean Azimuth	Mean Elevation
-10	-10	-3.35	-1.78
-10	-5	-3.92	-1.94
-10	0	-3.30	-0.42
-10	5	-4.00	0.67
-10	10	-3.98	1.39
-5	-10	-2.25	-3.69
-5	-5	-2.09	-2.01
-5	0	-1.78	-0.66
-5	5	-3.32	0.69
-5	10	-2.80	1.08
0	-10	0.12	-2.40
0	-5	-0.12	-0.82
0	0	-0.65	-0.10
0	5	-0.45	0.47
0	10	-0.41	2.50
5	-10	2.29	-2.96
5	-5	2.15	-2.20
5	0	2.12	-0.50
5	5	1.89	0.94
5	10	2.47	2.54
10	-10	3.15	-2.76
10	-5	3.45	-1.67
10	0	3.68	0.42
10	5	3.99	1.44
10	10	3.95	3.27

Table C.2

Mean azimuthal and elevational components of heading estimates for the growing dots condition.

Azimuth	Elevation	Mean Azimuth	Mean Elevation
-10	-10	-4.19	-2.94
-10	-5	-3.89	-1.84
-10	0	-3.96	-0.15
-10	5	-3.83	1.26
-10	10	-3.76	1.75
-5	-10	-1.59	-2.86
-5	-5	-2.36	-1.46
-5	0	-2.483	0.12
-5	5	-2.63	1.54
-5	10	-3.20	2.14
0	-10	-0.02	-2.53
0	-5	-1.18	-1.44
0	0	-0.04	-1.17
0	5	-0.23	1.04
0	10	0.30	2.18
5	-10	1.23	-3.39
5	-5	2.22	-1.68
5	0	1.36	-0.74
5	5	1.81	1.49
5	10	1.83	2.85
10	-10	3.57	-2.67
10	-5	3.73	-0.92
10	0	3.79	-0.59
10	5	3.83	1.06
10	10	4.27	2.61

Table C.3

Mean azimuthal and elevational components of heading estimates for the growing cubes condition.

Azimuth	Elevation	Mean Azimuth	Mean Elevation
-10	-10	-3.93	-2.79
-10	-5	-2.93	-1.29
-10	0	-4.16	-0.62
-10	5	-3.59	0.84
-10	10	-3.76	1.335
-5	-10	-2.37	-3.60
-5	-5	-2.57	-2.31
-5	0	-2.21	0.22
-5	5	-1.90	-0.07
-5	10	-2.24	2.45
0	-10	-0.16	-2.16
0	-5	0.09	-1.35
0	0	0.41	0.04
0	5	-0.12	0.36
0	10	-0.34	2.56
5	-10	2.32	-2.27
5	-5	1.68	-1.60
5	0	2.11	-0.46
5	5	2.52	1.02
5	10	1.95	2.80
10	-10	4.05	-3.34
10	-5	3.40	-1.33
10	0	3.57	-0.12
10	5	4.06	1.58
10	10	3.45	2.55

Appendix D

Azimuthal and Elevation Components of Estimates

Table D.1

Mean azimuthal and elevational components of heading estimates for the dots not remaining condition.

Azimuth	Elevation	Mean Azimuth	Mean Elevation
-10	-10	-3.05	-3.28
-10	-5	-3.49	-2.89
-10	0	-3.71	-0.84
-10	5	-3.50	1.06
-10	10	-3.75	3.19
-5	-10	-1.23	-2.94
-5	-5	-1.93	-1.35
-5	0	-0.96	-0.10
-5	5	-1.88	1.86
-5	10	-2.11	3.36
0	-10	-0.07	-3.70
0	-5	0.53	-1.45
0	0	-0.28	-0.19
0	5	-0.08	1.97
0	10	0.50	4.09
5	-10	1.50	-2.66
5	-5	2.63	-2.33
5	0	2.82	-0.58
5	5	3.61	1.24
5	10	2.77	3.06
10	-10	3.78	-3.54
10	-5	4.07	-2.01
10	0	4.30	-0.18
10	5	3.42	1.09
10	10	4.34	3.08

Table D.2

Mean azimuthal and elevational components of heading estimates for the dots remaining condition.

Azimuth	Elevation	Mean Azimuth	Mean Elevation
-10	-10	-3.95	-3.18
-10	-5	-4.60	-3.04
-10	-5	-4.49	-0.53
-10	5	-4.21	1.67
-10	10	-4.80	3.45
-5	-10	-2.63	-3.46
-5	-5	-3.49	-2.01
-5	0	-2.48	-0.86
-5	5	-3.09	1.66
-5	10	-2.27	3.63
0	-10	-0.49	-4.08
0	-5	0.41	-1.62
0	0	-0.67	-0.76
0	5	-0.18	0.89
0	10	0.54	3.61
5	-10	2.15	-3.46
5	-5	2.93	-2.88
5	0	3.23	-0.87
5	5	3.44	0.737
5	10	3.83	3.62
10	-10	3.90	-4.03
10	-5	4.13	-3.19
10	0	4.31	-0.45
10	5	4.41	1.09
10	10	4.42	4.07

Appendix E

Table E.1

Mean azimuthal and elevational components of heading estimates for the left fixation condition.

Azimuth	Elevation	Mean Azimuth	Mean Elevation
-10	-10	-6.36	-5.39
-10	-5	-6.37	-3.45
-10	0	-6.07	-0.76
-10	5	-6.46	1.81
-10	10	-6.37	4.23
-5	-10	-3.75	-4.39
-5	-5	-2.31	-2.51
-5	0	-3.14	-0.89
-5	5	-4.37	1.86
-5	10	-3.50	4.82
0	-10	0.01	-4.02
0	-5	-1.04	-2.64
0	0	0.24	-0.96
0	5	-0.46	1.49
0	10	-0.41	4.28
5	-10	2.18	-4.42
5	-5	1.77	-2.19
5	0	2.20	-0.39
5	5	1.64	1.88
5	10	1.67	4.12
10	-10	4.26	-4.06
10	-5	4.30	-2.48
10	0	4.14	-1.01
10	5	5.14	2.45
10	10	4.55	4.68

Table E.2

Mean azimuthal and elevational components of heading estimates for the right fixation condition.

Azimuth	Elevation	Mean Azimuth	Mean Elevation
-10	-10	-3.48	-5.00
-10	-5	-4.10	-3.88
-10	0	-3.82	-0.87
-10	5	-4.16	1.23
-10	10	-3.95	4.61
-5	-10	-2.43	-4.18
-5	-5	-1.98	-3.19
-5	0	-2.59	-1.38
-5	5	-3.00	1.66
-5	10	-2.14	4.99
0	-10	0.16	-4.51
0	-5	1.11	-1.73
0	0	0.22	-0.54
0	5	0.06	2.81
0	10	0.53	4.11
5	-10	3.21	-5.01
5	-5	4.02	-2.90
5	0	2.47	-0.38
5	5	2.75	1.47
5	10	2.69	3.80
10	-10	6.15	-4.29
10	-5	5.70	-2.16
10	0	5.59	-1.50
10	5	6.95	2.84
10	10	6.93	4.31

Table E.3

Mean azimuthal and elevational components of heading estimates for the upwards fixation condition.

Azimuth	Elevation	Mean Azimuth	Mean Elevation
-10	-10	-4.88	-3.00
-10	-5	-4.40	-2.25
-10	0	-4.11	0.93
-10	5	-5.84	3.04
-10	10	-5.19	5.70
-5	-10	-2.36	-3.62
-5	-5	-2.40	-1.77
-5	0	-2.41	-0.02
-5	5	-2.52	3.32
-5	10	-2.97	6.12
0	-10	0.42	-2.57
0	-5	-0.28	-0.84
0	0	0.37	0.31
0	5	0.76	2.03
0	10	-0.15	4.92
5	-10	2.97	-2.28
5	-5	2.35	-1.10
5	0	2.41	1.13
5	5	2.80	2.04
5	10	2.66	4.74
10	-10	5.01	-3.39
10	-5	5.49	-1.81
10	0	4.74	0.59
10	5	6.01	3.45
10	10	5.91	5.44

Table E.4

Mean azimuthal and elevational components of heading estimates for the for downwards fixation condition.

Azimuth	Elevation	Mean Azimuth	Mean Elevation
-10	-10	-4.70	-7.02
-10	-5	-6.09	-4.74
-10	0	-5.56	-1.68
-10	5	-4.97	1.19
-10	10	-5.19	3.23
-5	-10	-2.437	-6.40
-5	-5	-2.65	-3.85
-5	0	-2.87	-0.96
-5	5	-3.46	0.99
-5	10	-3.34	3.84
0	-10	-0.22	-6.52
0	-5	0.55	-3.84
0	0	0.52	-0.48
0	5	-0.35	2.26
0	10	-0.13	3.12
5	-10	3.52	-7.88
5	-5	2.51	-5.14
5	0	2.38	-0.73
5	5	3.16	1.31
5	10	2.67	3.38
10	-10	5.04	-6.68
10	-5	5.92	-4.82
10	0	5.58	-1.52
10	5	5.23	1.42
10	10	4.87	3.06

Table E.5

Mean azimuthal and elevational components of heading estimates for the for central fixation condition.

Azimuth	Elevation	Mean Azimuth	Mean Elevation
-10	-10	-3.72	-2.69
-10	-5	-3.14	-2.47
-10	0	-3.16	-0.93
-10	5	-3.75	0.85
-10	10	-3.26	1.56
-5	-10	-1.77	-3.40
-5	-5	-1.61	-1.71
-5	0	-1.25	-0.73
-5	5	-1.24	1.13
-5	10	-2.60	2.85
0	-10	-0.55	-2.43
0	-5	-0.16	-0.40
0	0	-0.21	-0.59
0	5	-0.09	1.08
0	10	-0.11	2.82
5	-10	1.48	-2.47
5	-5	1.77	-1.61
5	0	2.22	-0.39
5	5	0.91	0.30
5	10	1.69	1.58
10	-10	3.21	-2.96
10	-5	2.40	-2.41
10	0	3.50	-0.77
10	5	3.39	0.70
10	10	3.70	1.72